The

Geophysical Journal

of the

Royal Astronomical Society

incorporating

the Geophysical Supplement to the Monthly Notices of the R. A. S.

Volume 5 No. 1 May 1961

Published and Sold by the

Royal Astronomical Society

Burlington House, London, W.1, England

Price £1; (US$ 3) *Annual Subscription £3; (US$ 9)*

The Geophysical Journal

of the Royal Astronomical Society

Editors

A. H. Cook, M.A., Ph.D., F.R.A.S., F.G.S. (*Geophysical Secretary*), National Physical Laboratory, Teddington.

T. F. Gaskell, M.A., Ph.D., F.R.A.S. British Petroleum Company, London.

The following papers have been accepted for publication:

N. KAWAI, Mountain-building movement in Japan and its vicinity.

K. HELBIG and H. I. S. THIRLAWAY, New gravity measurements in West Pakistan.

L. J. B. LACOSTE and J. C. HARRISON, Some theoretical considerations in the measurement of gravity at sea.

W. M. KAULA, Analysis of gravitational and geometric aspects of geodetic utilization of satellites.

N. S. HEAPS, Seiches in a narrow lake, uniformly stratified in three layers.

C. LOMNITZ, On thermodynamics of planets.

T. HATHERTON, Note on the seismicity of the Ross Sea region.

R. W. GIRDLER, Some preliminary measurements of anisotropy of magnetic susceptibility of rocks.

M. H. P. BOTT, The granitic layer.

N. KAWAI, H. ITO and S. KUME, Formation of the Japanese arc inferred from rock magnetism.

R. L. DUBOIS, Remanent magnetism of carboniferous limestone.

I. ABUBAKAR, Dispersive properties of liquid overlying an aeolotropic half-space, Part I.

J. A. HUDSON, Dispersive properties of liquid overlying an aeolotropic half-space, Part II.

K. F. BOWDEN and P. HUGHES, The flow of water through the Irish Sea and its relation to wind.

A. I. REES, The effect of currents on the magnetic remanence and anisotropy of susceptibility of some sediments.

A. R. RITSEMA, Some 1951 earthquake mechanisms based on *P* and *PKP* data.

N. A. OSTENSO, Note of the paper of F. F. EVISON, C. E. INGHAM, R. H. ORR and J. H. LEFORT, "Thickness of the Earth's crust in Antarctica and the surrounding oceans".

K. AKI and F. PRESS, Upper mantle structure under oceans and continents from Rayleigh waves.

B. H. BRIGGS, The correlation of radio star scintillations with geomagnetic disturbances.

The Editors apologise to contributors and subscribers for the delay in publishing this issue of the *Geophysical Journal* and hope that Part 2 of Volume 5 will appear in July.

The Geophysical Journal

of the

ROYAL ASTRONOMICAL SOCIETY

Vol. 5 No. 1 May 1961

The Effect of the Ocean on Rapid Geomagnetic Changes

T. Rikitake

(Received 1960 July 16)

Summary

With the aid of two-dimensional experiments and mathematical theory, the electromagnetic induction in a conductor covered by a conducting sheet is studied. Applying the results to the effect of the ocean on rapid geomagnetic changes, it turns out that the previous estimate of the ocean effect based on the induction in a single sheet is an overestimate.

C. S. Cox's model, by which he explained the anomaly of geomagnetic variations in Japan as the effect of the ocean at its margin, is also criticized. The writer is of the opinion, contrary to Cox, that the anomaly is likely to be caused by the induced electric currents at some depth in the Earth's interior beneath Japan.

1. Introduction

Many authors (Chapman & Whitehead 1922, Lahiri & Price 1939, Price 1949, de Wet 1949, Ashour 1950, Rikitake 1950, 1959, 1960, Rikitake & Yokoyama 1955) have studied the possible influence of seas and oceans on transient geomagnetic variations. All through these studies the importance of self-induction has become well recognized. In some cases it has also become clear that the electric currents induced in an ocean produce anomalous magnetic fields around the land–sea boundaries, though only the induction within a thin sheet has been treated in these studies.

Cox (1960) has recently pointed out, however, that the conducting part of the mantle, the existence of which has been established through the application of the theory of electromagnetic induction to the observational results of geomagnetic variations, should be taken into account in studying the local anomalous field at the margins of an ocean. Since the depth of the conducting region has been estimated as only about 400 km, less than 10 per cent of the Earth's radius, the electric currents induced by a rapid magnetic change on its surface produce magnetic fields which would not differ much from those produced by the induced currents

The Geophysical Journal

of the Royal Astronomical Society

Editors

A. H. Cook, M.A., Ph.D., F.R.A.S., F.G.S. (*Geophysical Secretary*), National Physical Laboratory, Teddington.

T. F. Gaskell, M.A., Ph.D., F.R.A.S. British Petroleum Company, London.

The following papers have been accepted for publication:

N. Kawai, Mountain-building movement in Japan and its vicinity.

K. Helbig and H. I. S. Thirlaway, New gravity measurements in West Pakistan.

L. J. B. Lacoste and J. C. Harrison, Some theoretical considerations in the measurement of gravity at sea.

W. M. Kaula, Analysis of gravitational and geometric aspects of geodetic utilization of satellites.

N. S. Heaps, Seiches in a narrow lake, uniformly stratified in three layers.

C. Lomnitz, On thermodynamics of planets.

T. Hatherton, Note on the seismicity of the Ross Sea region.

R. W. Girdler, Some preliminary measurements of anisotropy of magnetic susceptibility of rocks.

M. H. P. Bott, The granitic layer.

N. Kawai, H. Ito and S. Kume, Formation of the Japanese arc inferred from rock magnetism.

R. L. Dubois, Remanent magnetism of carboniferous limestone.

I. Abubakar, Dispersive properties of liquid overlying an aeolotropic half-space, Part I.

J. A. Hudson, Dispersive properties of liquid overlying an aeolotropic half-space, Part II.

K. F. Bowden and P. Hughes, The flow of water through the Irish Sea and its relation to wind.

A. I. Rees, The effect of currents on the magnetic remanence and anisotropy of susceptibility of some sediments.

A. R. Ritsema, Some 1951 earthquake mechanisms based on *P* and *PKP* data.

N. A. Ostenso, Note of the paper of F. F. Evison, C. E. Ingham, R. H. Orr and J. H. LeFort, "Thickness of the Earth's crust in Antarctica and the surrounding oceans".

K. Aki and F. Press, Upper mantle structure under oceans and continents from Rayleigh waves.

B. H. Briggs, The correlation of radio star scintillations with geomagnetic disturbances.

The Editors apologise to contributors and subscribers for the delay in publishing this issue of the *Geophysical Journal* and hope that Part 2 of Volume 5 will appear in July.

The Geophysical Journal

of the

ROYAL ASTRONOMICAL SOCIETY

Vol. 5 No. 1 May 1961

The Effect of the Ocean on Rapid Geomagnetic Changes

T. Rikitake

(Received 1960 July 16)

Summary

With the aid of two-dimensional experiments and mathematical theory, the electromagnetic induction in a conductor covered by a conducting sheet is studied. Applying the results to the effect of the ocean on rapid geomagnetic changes, it turns out that the previous estimate of the ocean effect based on the induction in a single sheet is an overestimate.

C. S. Cox's model, by which he explained the anomaly of geomagnetic variations in Japan as the effect of the ocean at its margin, is also criticized. The writer is of the opinion, contrary to Cox, that the anomaly is likely to be caused by the induced electric currents at some depth in the Earth's interior beneath Japan.

1. Introduction

Many authors (Chapman & Whitehead 1922, Lahiri & Price 1939, Price 1949, de Wet 1949, Ashour 1950, Rikitake 1950, 1959, 1960, Rikitake & Yokoyama 1955) have studied the possible influence of seas and oceans on transient geomagnetic variations. All through these studies the importance of self-induction has become well recognized. In some cases it has also become clear that the electric currents induced in an ocean produce anomalous magnetic fields around the land–sea boundaries, though only the induction within a thin sheet has been treated in these studies.

Cox (1960) has recently pointed out, however, that the conducting part of the mantle, the existence of which has been established through the application of the theory of electromagnetic induction to the observational results of geomagnetic variations, should be taken into account in studying the local anomalous field at the margins of an ocean. Since the depth of the conducting region has been estimated as only about 400 km, less than 10 per cent of the Earth's radius, the electric currents induced by a rapid magnetic change on its surface produce magnetic fields which would not differ much from those produced by the induced currents

in a large conducting sheet supposed at the Earth's surface. If this is true, the influence of the ocean on geomagnetic variations that has been estimated on the basis of the induction in a single conducting sheet seems to be an overestimate.

It is intended in this paper to estimate the induction of electric currents in a conducting sheet, which is regarded as an ocean, without neglecting the electromagnetic coupling between the sheet and the conducting mantle. In order to get an idea of the distribution of the magnetic field, preliminary experiments based on two-dimensional models are first made as can be seen in Section 2. Experiments of this sort are sometimes useful for examining complicated fields. In Section 3, a theory of induction in a spherical sheet covered by a concentric hemispherical sheet is advanced. From the result, the possible influence of a large ocean like the Pacific may be studied. Some comments on Cox's view that the anomalous behaviour of geomagnetic variations found in Japan is caused by the effect of the ocean are also attempted in Section 4.

2. Preliminary experiments

In discussing problems of electromagnetic induction in a conductor, we take magnetic potential W outside the conductor which satisfies

$$\nabla^2 W = 0. \tag{1}$$

The boundary conditions for a perfect conductor are

$$\frac{\partial W}{\partial n} = 0 \tag{2}$$

at the surface of the conductor, where n is the normal to the boundary surface, and the magnetic field at a large distance from the conductor is given by the inducing one.

Let us next consider problems of steady electric currents flowing around a perfect insulator. The potential of the electric field should satisfy

$$\nabla^2 \phi = 0. \tag{3}$$

At the boundary surface, we have

$$\frac{\partial \phi}{\partial n} = 0. \tag{4}$$

We therefore see that, as long as the distribution of the electric field at a large distance from the insulator is identical with that of the inducing magnetic field considered above, the distribution of ϕ becomes identical to that of W. If we can solve a steady current problem somehow, the corresponding electromagnetic induction problem can be immediately solved.

For a two-dimensional case, the equipotentials can be easily obtained by a model experiment (Kasahara 1959, Rikitake 1959). We make use of a sheet of facsimile paper. Corresponding to the insulator, part of the sheet is cut off in the shape wanted. The paper is covered by fine carbon film on which a very thin screen of wax is spread. As the carbon layer is fairly uniform, the paper is suitable for an experiment of two-dimensional steady electric currents.

Taking a rectangular sheet of 35 cm × 25·3 cm, two brass electrodes are placed on the 25 cm sides. The electric contact between the paper and the electrodes

is made by putting carbon powder on the paper with a pencil. The central part of the sheet is cut according to the shape of the insulator to be tested as can be seen in Figure 1. Applying 100 V between the two electrodes, the equipotentials are traced by means of null method with a valve voltmeter. Since the input impedance of the meter is very high, the equipotentials obtained are highly reliable.

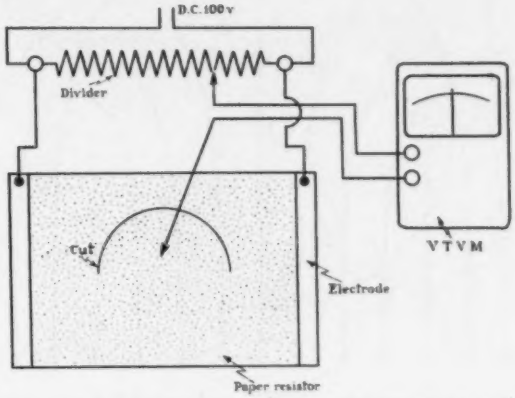

FIG. 1.—The arrangement for the experiment.

Let us first examine a semicircular cut. This model corresponds to a perfectly conducting semi-cylindrical sheet placed in a rapidly varying magnetic field. When the inducing magnetic field is directed to the direction connecting the ends of the semicircle, the equipotentials are obtained as can be seen in Figure 2. We see that the magnetic fields along the conductor have no components normal to the boundary. It is noticeable, however, that some normal component should appear nearby the edge points. The distribution of the magnetic fields on the non-conducting semicircle differs very much from that on the conducting one.

The next experiment is made for a model in which we added a circular conductor of a little smaller radius to the former conducting sheet. From the equipotentials in Figure 3, we see that the distribution of the magnetic field is fairly symmetric in spite of the presence of the semi-cylindrical sheet. Marked asymmetry can be seen only in the neighbourhood of the edge of the sheet.

If it is permissible to regard the sheet and the circle as the ocean and the surface of the conducting part of the mantle respectively, the above experiments suggest that the effect of the conducting mantle is so large that, if only the effect of the sheet is taken into account, we will overestimate the effect of the ocean on rapid magnetic changes.

3. Electromagnetic induction in a spherical sheet covered by a concentric hemispherical sheet

Although a rough idea of the electromagnetic induction in a conductor covered by a thin sheet is given by the two-dimensional experiments in the last section, more accurate research is needed for investigating quantitatively the possible effect of the ocean on the Earth's magnetic field.

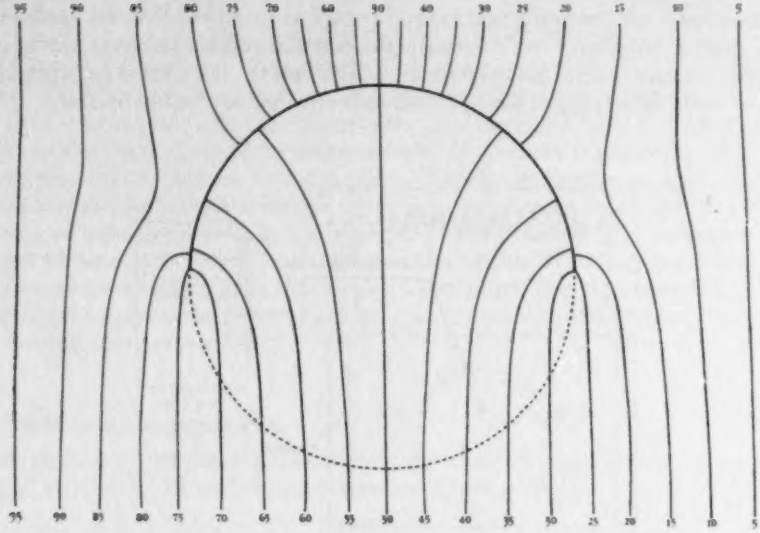

FIG. 2.—The equipotentials around a semi-cylindrical conducting sheet when the inducing field is applied from left to right.

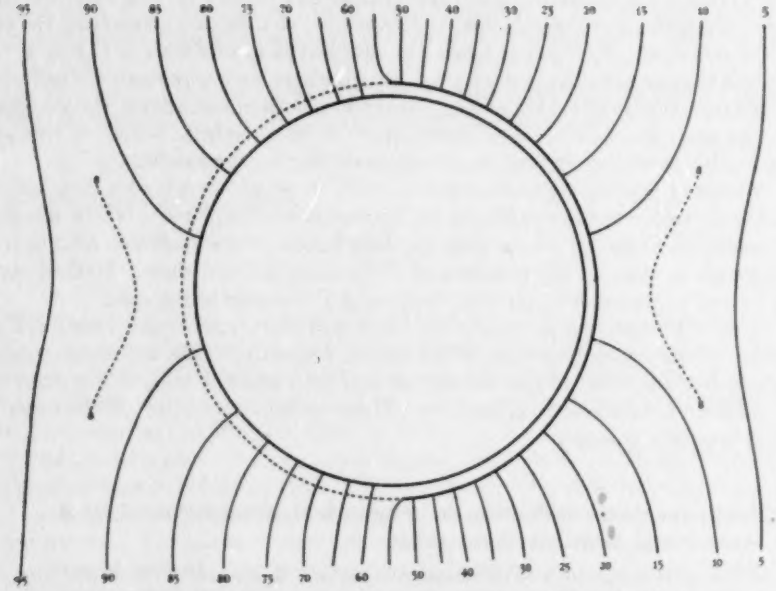

FIG. 3.—The equipotentials in the presence of a semi-cylindrical sheet and a circle both conducting, when the inducing field is applied from left to right.

In this section, a theory of electromagnetic induction in a spherical sheet covered by a concentric hemispherical sheet will be developed. Let us study the system of conductors as shown in Figure 4. The magnetic potential of the inducing field is given as

$$We = -rHP_1^1(\cos\theta)\cos\phi, \tag{5}$$

where

$$P_n^1(\cos\theta) = -\sqrt{\left[\frac{2}{n(n+1)}\right]}\frac{dP_n(\cos\theta)}{d\theta}. \tag{6}$$

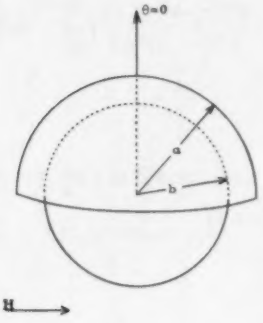

FIG. 4.

The current functions that are induced on the surfaces of the conductors are to be of the form such as

$$\Phi_a = \sum_n a_n P_n^1 \cos\phi \qquad \text{on } r = a, \tag{7}$$

$$\Phi_b = \sum_n b_n P_n^1 \cos\phi \qquad \text{on } r = b. \tag{8}$$

(7) is effective not only on the conducting part of the sheet but also on the whole spherical surface defined by $r = a$.

Either for a sudden change of the inducing field or for perfect conductors, the induced currents flow only on the surfaces of the conductors. In such a case, from (5), (7) and (8) the total magnetic potential becomes

$$\left.\begin{aligned} W = {} & -rHP_1^1\cos\phi + \\ & + 4\pi\sum_n \frac{n}{2n+1}a_n\left(\frac{a}{r}\right)^{n+1}P_n^1\cos\phi + 4\pi\sum_n \frac{n}{2n+1}b_n\left(\frac{b}{r}\right)^{n+1}P_n^1\cos\phi \\ & \qquad \text{for } r > a, \\ W = {} & -rHP_1^1\cos\phi - \\ & - 4\pi\sum_n \frac{n+1}{2n+1}a_n\left(\frac{r}{a}\right)^{n}P_n^1\cos\phi + 4\pi\sum_n \frac{n}{2n+1}b_n\left(\frac{b}{r}\right)^{n+1}P_n^1\cos\phi \\ & \qquad \text{for } a > r > b. \end{aligned}\right\} \tag{9}$$

The boundary conditions are that the normal components of the magnetic field should vanish at the surfaces of the conductors. For a conductor of the Earth's size having a conductivity of sea water, the conditions are a good approximation as long as changes having a period not exceeding a few minutes are concerned.

We therefore obtain

$$b_1 = -\frac{3}{2}\frac{bH}{4\pi} - \frac{b}{a}a_1, \qquad b_n = -\left(\frac{b}{a}\right)^n a_n \qquad (n \neq 1), \quad (10)$$

from the condition on $r = b$, while, on $r = a$, the condition becomes

$$\left.\begin{aligned} &HP_1^1 + \frac{4\pi}{a}\sum_n \frac{n(n+1)}{2n+1}a_n P_n^1 + \frac{4\pi}{b}\sum_n \frac{n(n+1)}{2n+1}\left(\frac{b}{a}\right)^{n+2} b_n P_n^1 = 0 \quad \text{for } 0 < \theta < \frac{\pi}{2}, \\ &\sum_n a_n P_n^1 = 0 \qquad\qquad \text{for } \frac{\pi}{2} < \theta < \pi \end{aligned}\right\} \quad (11)$$

Eliminating b_n from (11) with the aid of (10), we obtain

$$\left.\begin{aligned} &\frac{a}{4\pi}(1-\nu^3)HP_1^1 + \sum_n \frac{n(n+1)}{2n+1}(1-\nu^{2n+1})a_n P_n^1 = 0 \qquad \text{for } 0 < \theta < \frac{\pi}{2}, \\ &\sum_n a_n P_n^1 = 0 \qquad\qquad \text{for } \frac{\pi}{2} < \theta < \pi, \end{aligned}\right\} \quad (12)$$

where

$$\nu = \frac{b}{a}. \quad (13)$$

(12) can be utilized to determine a_n's in a way similar to that which was adopted in the writer's previous paper (Rikitake T. & Yokoyama I. 1955). (12) can be also rewritten as

$$\left.\begin{aligned} &\sum_n a_n P_n^1 = -\sum_n \left[\frac{n(n+1)}{2n+1}(1-\nu^{2n+1}) - 1\right] a_n P_n^1 - \frac{aH}{4\pi}(1-\nu^3)P_1^1 \\ &\qquad\qquad\qquad\qquad\qquad\qquad\qquad\qquad\qquad\qquad \text{for } 0 < \theta < \frac{\pi}{2}, \\ &\sum_n a_n P_n^1 = 0 \qquad\qquad\qquad\qquad\qquad\qquad\qquad\qquad\qquad\qquad \text{for } \frac{\pi}{2} < \theta < \pi. \end{aligned}\right\} \quad (14)$$

After multiplying by $P_N^1 \sin\theta$, we shall integrate (14) with respect to θ from $\theta = 0$ to $\theta = \pi$. The integral should be divided into two parts, from $\theta = 0$ to $\theta = \pi/2$ and from $\theta = \pi/2$ to $\theta = \pi$. We then obtain

$$2a_N R_{NN} + \sum_n \left[\frac{n(n+1)}{2n+1}(1-\nu^{2n+1}) - 1\right] a_n R_{nN} = -\frac{aH}{4\pi}R_{1N}(1-\nu^3), \quad (15)$$

where

$$R_{nN} = \int_0^{\pi/2} P_n^1 P_N^1 \sin\theta \, d\theta. \quad (16)$$

Table 1

The coefficients and the right-hand members of simultaneous equations (15)

1	2	3	4	5	6	7	8	9	10	11	12	Right-hand member*
1	−0·39725	0	0·00908	0	0·07580	0	−0·11094	0	0·12799	0	−0·13641	0·15222
−0·72785	1	−0·13312	0	−0·02294	0	0·03413	0	−0·03261	0	0·02913	0	0·13901
0	−0·26279	1	−0·02026	0	−0·10028	0	0·12843	0	−0·13996	0	0·14476	0
0·26987	0	−0·16658	1	0·09185	0	−0·07908	0	0·06529	0	−0·05468	0	−0·05154
0	0·05574	0	−0·01375	1	0·21273	0	−0·15568	0	0·14548	0	−0·14037	0
−0·14822	0	0·05421	0	0·09342	1	0·24819	0	−0·11621	0	0·08305	0	0·02831
0	−0·02244	0	0·00320	0	0·15294	1	0·27226	0	−0·18076	0	0·14835	0
0·09410	0	−0·03012	0	−0·02965	0	0·19166	1	0·34431	0	−0·13848	0	−0·01797
0	0·01144	0	−0·00141	0	−0·03821	0	0·20697	1	0·41807	0	−0·19253	0
−0·06545	0	0·01978	0	0·01671	0	−0·07672	0	0·33254	1	0·40509	0	0·01250
0	−0·00669	0	0·00077	0	0·01788	0	−0·06870	0	0·33351	1	0·46462	0
0·05047	0	−0·01481	0	−0·01166	0	0·04556	0	−0·11081	0	0·40834	1	−0·00964

* The right-hand members should be multiplied by $-\frac{aH}{4\pi}$.

R_{nN}'s have been already calculated for $n = 1, 2, \ldots, 12$ in the 1955 paper. (15) can be regarded as the simultaneous equations for $a_1, a_2, \ldots, a_{12}$. The coefficients of a_n's and the right-hand members of the simultaneous equations for $\nu = 0{\cdot}94$ are given in Table 1. Since the coefficients of the diagonal terms are relatively large, we can easily solve the equations though no account is taken of the rigorous proof of convergency. The solutions that are solved by making use of the relaxation method are given in Table 2.

Table 2

The solution of (15) *in units of* $-(aH/4\pi)$

a_1	a_2	a_3	a_4	a_5	a_6
0·2760	0·3526	0·1106	−0·1010	−0·0493	0·0619
a_7	a_8	a_9	a_{10}	a_{11}	a_{12}
0·0203	−0·0429	−0·0098	0·0350	−0·0023	−0·0236

b_n's are immediately obtained from (10) as given in Table 3.

Table 3

b_n's in units of $-(aH/4\pi)$

b_1	b_2	b_3	b_4	b_5	b_6
1·1506	−0·3116	−0·0919	0·0789	0·0362	−0·0427
b_7	b_8	b_9	b_{10}	b_{11}	b_{12}
−0·0132	0·0262	0·0056	−0·0189	0·0012	0·0112

With the coefficients given in Tables 2 and 3, the current functions on $r = a$ and $r = b$ are easily obtained. Their distributions along $\phi = 0$ are shown in Figure 5. We see that the condition of no current for $\pi/2 < \theta < \pi$ on $r = a$ is approximately satisfied. The curve drawn by a chain line shows the current function which we would have either on $r = a$ if the sheet were to be extended over the whole spherical surface or on $r = b$ if the sheet were absent. It is also seen that the induced currents on $r = b$ are not affected very much on the side which is not covered by the sheet.

The magnetic fields produced by the induced currents can be readily calculated. The normal component on $r = a$ along $\phi = 0$ is shown in Figure 6. The contributions of the currents on $r = a$ and $r = b$ are also separately shown there with dotted curves a and b. The curves A and B show respectively the normal components which we would have if the whole surface of $r = a$ were conducting and if the sheet were absent. We see that the normal component of the magnetic field on the conducting part of $r = a$ agrees fairly well with curve A, while curves b and B coincide with one another for $120° < \theta < 180°$. These results are physically acceptable.

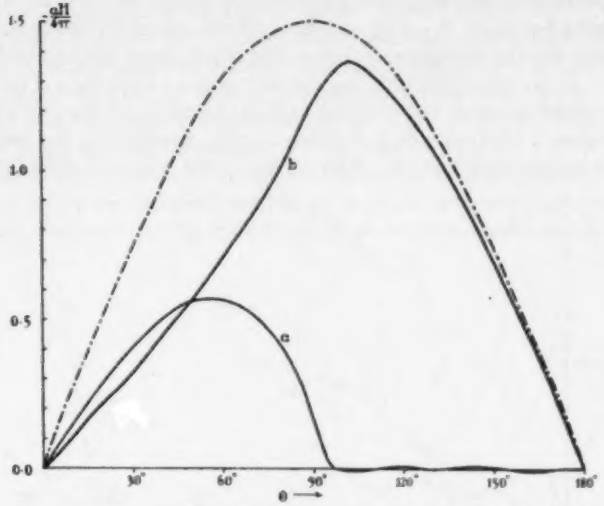

FIG. 5.—Curves a and b denote respectively the current functions on $r = a$ and $r = b$ along $\phi = 0$. The chain line shows the current function which we would have either on $r = a$ if the sheet were to be extended over the whole spherical surface or on $r = b$ if the sheet were absent.

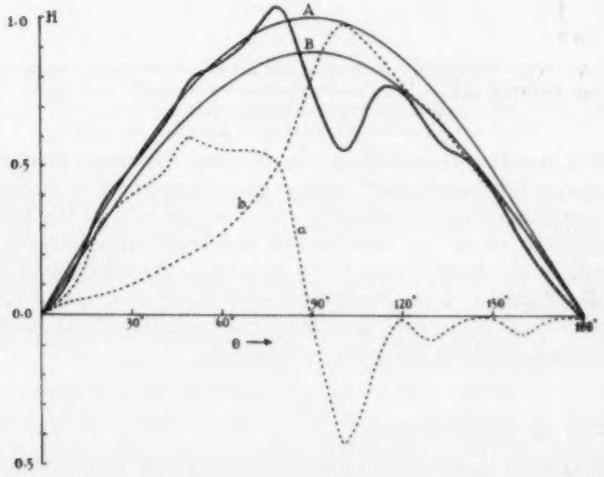

FIG. 6.—The distributions of the normal component on $r = a$ along $\phi = 0$. a and b are produced by the induced currents respectively on $r = a$ and $r = b$. The curve shown by a thick line is the sum of a and b. Curves A and B show respectively the normal components which we would have if the whole surface of $r = a$ were conducting and if the sheet were absent.

R_{nN}'s have been already calculated for $n = 1, 2, \ldots, 12$ in the 1955 paper. (15) can be regarded as the simultaneous equations for $a_1, a_2, \ldots, a_{12}$. The coefficients of a_n's and the right-hand members of the simultaneous equations for $\nu = 0{\cdot}94$ are given in Table 1. Since the coefficients of the diagonal terms are relatively large, we can easily solve the equations though no account is taken of the rigorous proof of convergency. The solutions that are solved by making use of the relaxation method are given in Table 2.

Table 2

The solution of (15) *in units of* $-(aH/4\pi)$

a_1	a_2	a_3	a_4	a_5	a_6
0·2760	0·3526	0·1106	−0·1010	−0·0493	0·0619
a_7	a_8	a_9	a_{10}	a_{11}	a_{12}
0·0203	−0·0429	−0·0098	0·0350	−0·0023	−0·0236

b_n's are immediately obtained from (10) as given in Table 3.

Table 3

b_n's in units of $-(aH/4\pi)$

b_1	b_2	b_3	b_4	b_5	b_6
1·1506	−0·3116	−0·0919	0·0789	0·0362	−0·0427
b_7	b_8	b_9	b_{10}	b_{11}	b_{12}
−0·0132	0·0262	0·0056	−0·0189	0·0012	0·0112

With the coefficients given in Tables 2 and 3, the current functions on $r = a$ and $r = b$ are easily obtained. Their distributions along $\phi = 0$ are shown in Figure 5. We see that the condition of no current for $\pi/2 < 0 < \pi$ on $r = a$ is approximately satisfied. The curve drawn by a chain line shows the current function which we would have either on $r = a$ if the sheet were to be extended over the whole spherical surface or on $r = b$ if the sheet were absent. It is also seen that the induced currents on $r = b$ are not affected very much on the side which is not covered by the sheet.

The magnetic fields produced by the induced currents can be readily calculated. The normal component on $r = a$ along $\phi = 0$ is shown in Figure 6. The contributions of the currents on $r = a$ and $r = b$ are also separately shown there with dotted curves a and b. The curves A and B show respectively the normal components which we would have if the whole surface of $r = a$ were conducting and if the sheet were absent. We see that the normal component of the magnetic field on the conducting part of $r = a$ agrees fairly well with curve A, while curves b and B coincide with one another for $120° < \theta < 180°$. These results are physically acceptable.

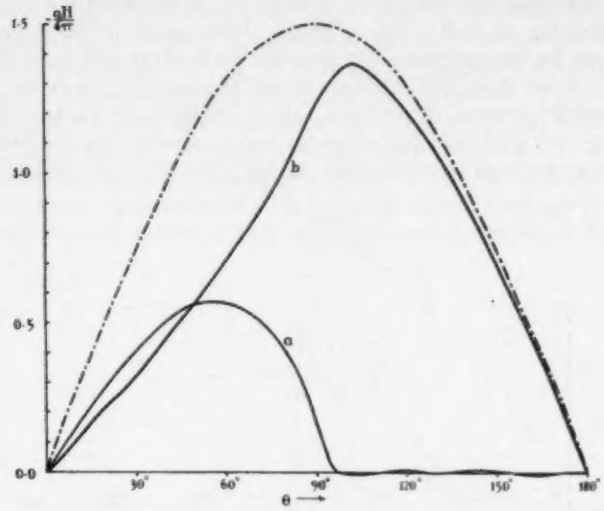

FIG. 5.—Curves a and b denote respectively the current functions on $r = a$ and $r = b$ along $\phi = 0$. The chain line shows the current function which we would have either on $r = a$ if the sheet were to be extended over the whole spherical surface or on $r = b$ if the sheet were absent.

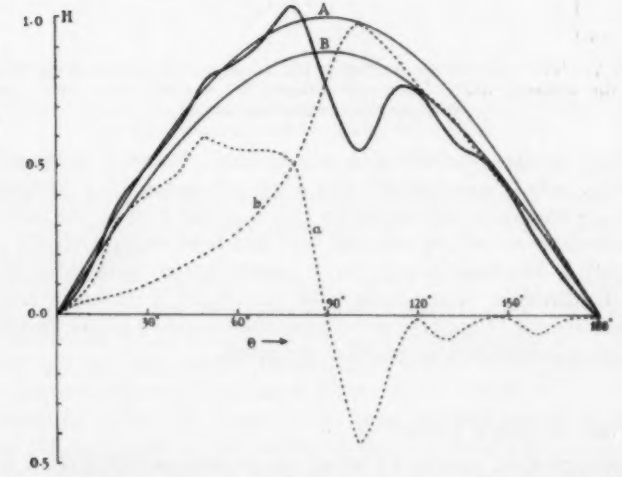

FIG. 6.—The distributions of the normal component on $r = a$ along $\phi = 0$. a and b are produced by the induced currents respectively on $r = a$ and $r = b$. The curve shown by a thick line is the sum of a and b. Curves A and B show respectively the normal components which we would have if the whole surface of $r = a$ were conducting and if the sheet were absent.

If there were only the conducting mantle, we should observe an induced field which is shown by curve B. The influence of the ocean on the induced field is therefore given by the difference between the thick curve and curve B as shown in Figure 7. If we disregard the mantle and assume that the ocean is a hemispherical conducting sheet, the induced field is known to be the one which is also shown in Figure 7 (Rikitake & Yokoyama 1955). Comparing the two curves in the figure, it is observed that the effect of the ocean which is estimated ignoring

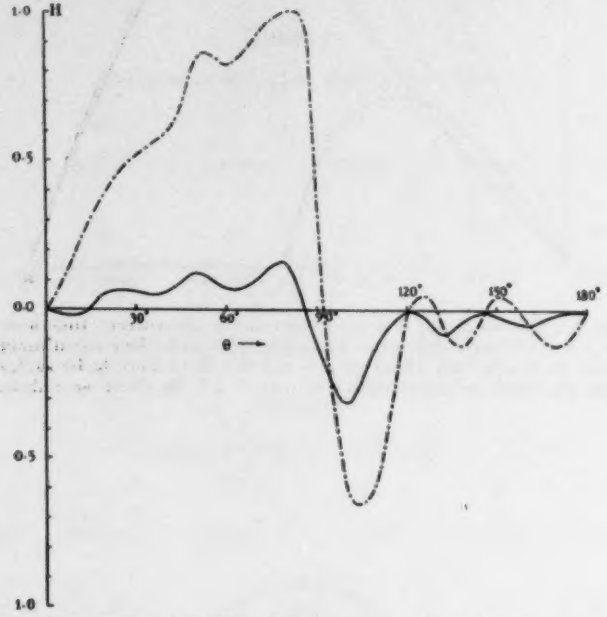

FIG. 7.—The effect of the hemispherical ocean on the normal component of the induced field. The curve shown by a chain line shows that without the conducting mantle.

the conducting mantle is definitely an overestimate. However, there still remains what the writer called "coast effect", that is the enhancement of the inducing field at the land–sea boundary amounting to about 40 per cent of the inducing field. Such an enchancement of the external field has been experimentally proved by Nagata, Oguti & Maekawa (1955) for a hemispherical conducting sheet. The anomalous distributions of magnetic field over Japan at times of s.s.c. or geomagnetic bays are not of the type in so far as the boundary of the Pacific Ocean is regarded to be running from the north to the south.

4. Comments on Cox's model

Cox (1960) proposed a model by which the anomalous distribution of geomagnetic variations of short period (Rikitake & others 1952, 1953, 1958, 1959, Rikitake & Yokoyama 1953, 1954, 1955) might be explained. The model consists of a perfectly conducting half-plane (ocean) over a non-conductor and underlain by a perfectly conducting infinite plane (surface of the conducting part of the mantle). He

solved an electromagnetic induction problem in such a system, by applying a conformal transformation. He further showed that the ratio of the vertical component (ΔZ) to the horizontal one (ΔH) varies in a way similar to the results actually observed as the distance from the ocean boundary increases. In his study it is assumed that the inducing field changes in the north direction while the Pacific coast-line of Japan is assumed to run from the west to the east.

Experiments appropriate to test Cox's model are also undertaken here. The equipotentials when the inducing field is perpendicular to the plane including the two edge lines of a semi-circular cylindrical sheet are shown in Figure 8, while those

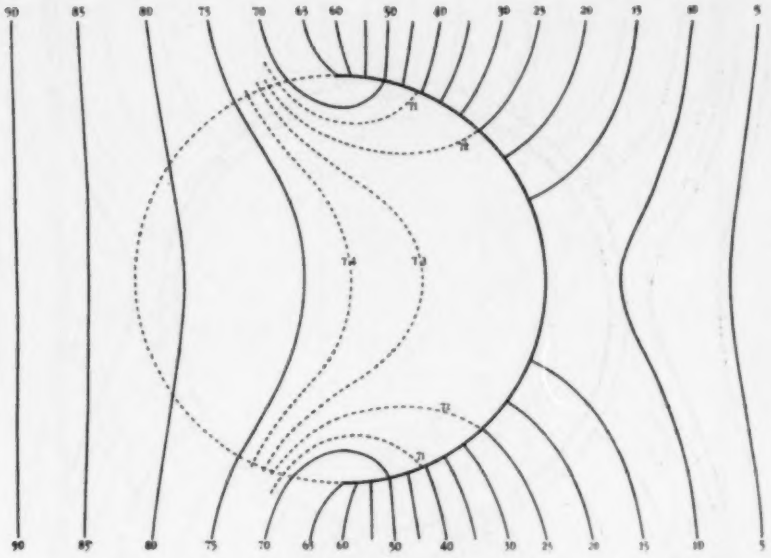

FIG. 8.—The equipotentials around a semi-cylindrical conducting sheet when the inducing field is applied from left to right.

for the case when we add a circular conductor are also shown in Figure 9. Examining these figures, we see that the relation between ΔZ and ΔH as obtained by Cox seems to be quite right.

The writer is of the opinion, however, that Cox's model will present some difficulties. First of all, the writer would like to point out the fact that ΔZ is very small on the islands like Hachijo-shima and Aoga-shima Islands, a few hundred kilometres south of Tokyo, as can be seen in Figure 10 which is reproduced from the writer's previous paper (Rikitake & others 1959). According to Cox's model, this smallness of ΔZ would suggest that these islands should be regarded as situated on the ocean-side in his model, so that ΔH should be much larger there than on the land-side. But the observation proved that ΔH are almost of the same magnitude throughout Japan.

Irregularities of an ocean of small dimension would not affect rapid geomagnetic variations so much because of the smallness of their self-inductance, as pointed out by Cox himself. For instance, the Japan Sea would have a free decay

period of only a few minutes. Taking these circumstances into account, it seems to the writer that the boundary of the Pacific Ocean may be thought to be running roughly parallel to a meridian, unlike Cox's model.

Cox has also criticized the induction effect of a periodic distribution of land and sea as studied by the writer and Yokoyama (1955). He pointed out that such a model is not adequate as a model in the vicinity of Japan because the horizontal scales of magnetic field are too limited. Since small scale irregularities of oceans like the Japan Sea can be disregarded, however, the writer thinks that it is possible

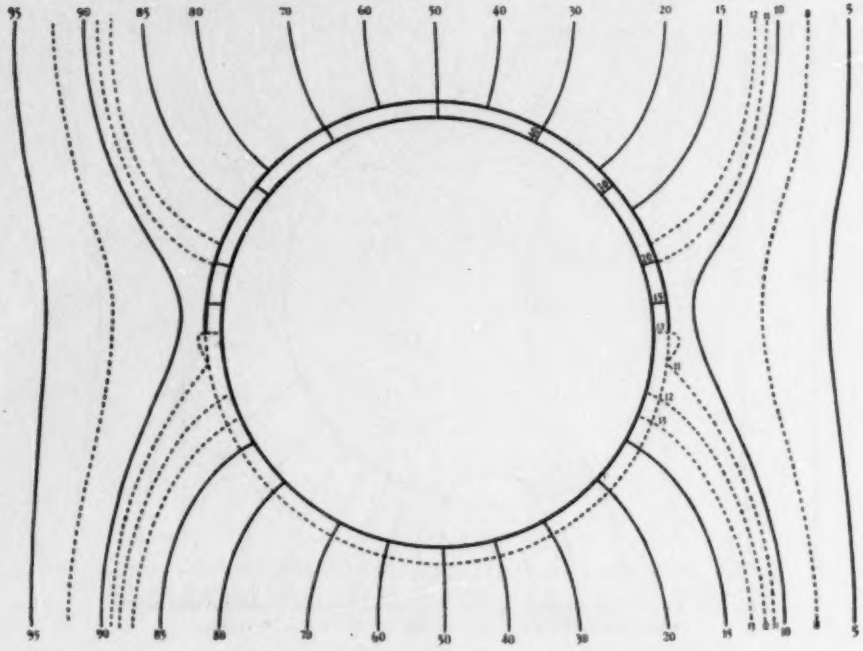

FIG. 9.—The equipotentials in the presence of a semi-cylindrical sheet and a circle, both conducting, when the inducing field is applied from left to right.

to take the period of both the distribution of land and sea and the magnetic field as large as one likes. In that case, the model could be used for estimating the field only as far as the vicinity of the ocean boundary is concerned.

As the anomaly of geomagnetic variations localized in the central part of Japan seems to have a tendency that we observe it more clearly at times of geomagnetic bays having 1 or 2 hour periods than at times of s.s.c. of a few minutes duration, the writer is still inclined to believe that the anomaly may be caused by some agency at some depths in the Earth's interior, though nothing definite can be said from observation of the actual effect of the ocean on rapid geomagnetic changes in Japan.

5. Concluding remarks

Electromagnetic induction by a rapid magnetic change in a conductor, a part of which is covered by a conducting sheet is studied both experimentally and theoretically. Applying the study to the Earth, it turns out that the effect of an ocean

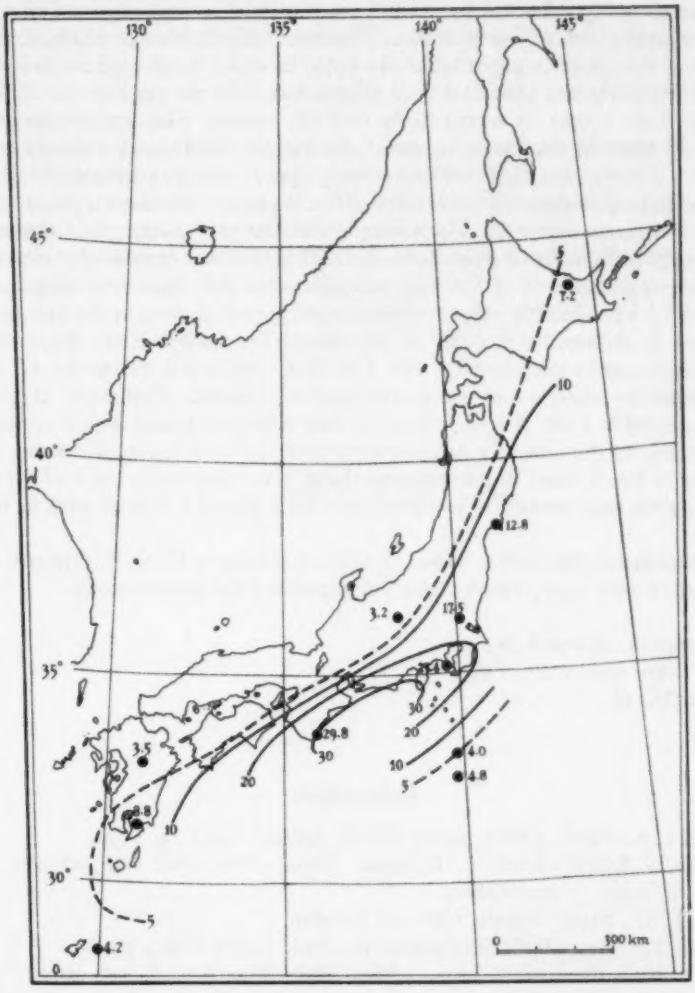

FIG. 10.—The distribution of ΔZ in units of gamma for the maximum stage of the bay on 1958 April 18.

on geomagnetic changes, which has been estimated on the basis of a model neglecting the conductivity inside the Earth, is an overestimate. But there still arises a localized distribution of induced field near the ocean boundary. If the inside conductor could be assumed to be found at a shallower depth, the anomaly would

become very small, so that there might be a possibility that the ocean-effect is not so large as has been supposed.

The mathematical theory in this paper is made only for a limited configuration of conductors. If we want to develop a theory of electromagnetic induction by a magnetic field parallel to the $\theta = 0$ axis in Figure 4, it seems hardly possible to get at an accurate distribution of induced currents and associated magnetic fields because so many spherical harmonics are required for that purpose that such a calculation is practically impossible. The writer regrets that he has reported false results in the previous paper (Rikitake 1959) in which he treated the induction of electric currents in a spherical shell with a hole. At the edge of the conducting shell in such a case, it seems likely that the current function changes discontinuously from its maximum to zero. If we approximate such a function with a number of harmonics, there will necessarily appear electric currents which flow in the direction opposite to the actual ones. The magnetic field there is greatly affected by the erroneous currents. The writer would like to announce that the result in the 1959 paper should be cancelled. According to a two-dimensional experiment, the vertical component of the magnetic field over the non-conducting part surrounded by a conducting sheet is weakened very much as long as the non-conducting area is defined by $\theta < 20°$ or so, though no mathematical study of three dimensions can be performed. The fact that very small variations of vertical component are observed in the central part of Australia (Parkinson 1959) seems then acceptable from the view that the Australian continent is non-conducting.

Turning to the anomaly of geomagnetic variation in Japan, the writer thinks, contrary to Cox's view, that it has something to do with the interior of the Earth. A few points that cannot be explained by Cox's model are dealt with in the last section.

In conclusion, the writer wishes to express thanks to Dr C. S. Cox and Mr T. Teramoto whose unpublished paper has stimulated the present study.

Earthquake Research Institute,
Tokyo University, Tokyo:
1960 *March*

References

Ashour, A. A., 1950. *Quart. Journ. Mech. Applied Math.*, **3**, 119.
Chapman, S. & Whitehead, T. T., 1922. *Trans. Camb. Phil. Soc.*, **22**, 463.
Cox, C. S., 1960. Unpublished.
de Wet, J. M., 1949. Thesis, Univ. of London.
Kasahara, K., 1959. *Bull. Earthquake Res. Inst. Tokyo Univ.*, **37**, 39.
Lahiri, B. N. & Price, A. T., 1939. *Phil. Trans. Roy. Soc. A*, **237**, 509.
Nagata, T., Oguti, T. & Maekawa, H., 1955. *Bull. Earthquake Res. Inst. Tokyo Univ.*, **33**, 561.
Parkinson, W. D., 1959. *Geophys. J.*, **2**, 1.
Price, A. T., 1949. *Quart. Journ. Mech. Applied Math.*, **2**, 283.
Rikitake, T., 1950. *Bull. Earthquake Res. Inst. Tokyo Univ.*, **28**, 45.
Rikitake, T., 1959. *Bull. Earthquake Res. Inst. Tokyo Univ.*, **37**, 545.
Rikitake, T., 1960. *J. Geomagn. Geoelectr.*, **11**, 65.
Rikitake, T. & Yokoyama, I., 1953. *J. Geomagn. Geoelectr.*, **5**, 59.

Rikitake, T. & Yokoyama, I., 1954. *Naturwiss.*, **18**, 420.
Rikitake, T. & Yokoyama, I., 1955. *Bull. Earthquake Res. Inst. Tokyo Univ.*, **33**, 297.
Rikitake, T., Yokoyama, I. & Hishiyama, Y., 1952. *Bull. Earthquake Res. Inst. Tokyo Univ.*, **30**, 207.
Rikitake, T., Yokoyama, I. & Hishiyama, Y., 1953a. *Bull. Earthquake Res. Inst. Tokyo Univ.*, **31**, 19.
Rikitake, T., Yokoyama, I. & Hishiyama, Y., 1953b. *Bull. Earthquake Res. Inst. Tokyo Univ.*, **31**, 89.
Rikitake, T., Yokoyama, I. & Hishiyama, Y., 1953c. *Bull. Earthquake Res. Inst. Tokyo Univ.*, **31**, 101.
Rikitake, T., Yokoyama, I. & Hishiyama, Y., 1953d. *Bull. Earthquake Res. Inst. Tokyo Univ.*, **31**, 119.
Rikitake, T., Yokoyama, I., Uyeda, S., Yukutake, T. & Nakagawa, E., 1958. *Bull. Earthquake Res. Inst. Tokyo Univ.*, **36**, 1.
Rikitake, T., Uyeda, S., Yukutake, T., Tanaoka, I. & Nakagawa, E., 1959. *Bull. Earthquake Res. Inst. Tokyo Univ.*, **37**, 1.

Superparamagnetism in Red Sandstones

K. M. Creer

(Received 1960 July 21)

Summary

Susceptibility measurements down to liquid hydrogen temperatures have been made on rocks with (a) unstable and (b) stable natural remanent magnetization. The former follow a Curie Law and this indicates that most of the magnetic content is apparently paramagnetic. Measurements in different fields fail to reveal the weak ferromagnetism responsible for the natural remanence. The latter measurements suggest that an apparent paramagnetic component is present together with a component having a susceptibility independent of temperature. In both cases the magnetization–applied field relationship at liquid helium temperature in fields up to 20 000 oersteds is not linear and this probably indicates that both rocks contain ferromagnetic material in a superparamagnetic state, the particle size of which is calculated to be of the order of 20 Å. The material is thought to be hydrous alpha ferric oxide of which the cement is made. Viscous magnetization of about the same strength as the weak fossil remanence has previously been observed in the unstable rock but is not noticeable in low fields in the stable one. The remanent magnetization of red rocks is thought to be due in part to grains of the red cement larger than those responsible for viscous magnetization and superparamagnetism and in part to black haematite grains. These are sparsely distributed in the unstable rock but are more abundant in the stable one.

Magnetization of the cement might occur soon after formation, or during a sintering process during burial at depth, or in some cases in geologically recent times due to tropical weathering.

The calculated grain size of about 20 Å for the superparamagnetic particles differs appreciably from that of about 1 000 Å previously estimated for the viscous particles. Experiments are being made on artificially produced haematite of known particle size to attempt to resolve this anomaly.

1. Introduction

The origin of the remanent magnetization of red rocks is not yet understood although many measurements of this property have been made in recent years. The bulk of the now considerable palaeomagnetic evidence supporting the theory of continental drift is derived from studies made on red rocks from several

continents from various geological periods and hence it is important that the mode and time of origin of their natural remanence be understood.

The work described here attempts to reveal some of the magnetic properties of the magnetic material present in these rocks. Chemical analysis, X-ray techniques and ore microscopy all indicate that the magnetic material contained in such rocks is mainly haematite, except where local reduction has occurred. But identification of magnetic minerals and estimation of their grain size is sometimes better attempted by measurement of magnetic properties as functions of applied field strength and of temperature. In this respect, work on sediments at elevated temperatures is complicated by the possibility of chemical or mineralogical changes, such as that of maghemite ($Fe_2O_3\gamma$) to haematite ($Fe_2O_3\alpha$) at about 500 °K. Also, reduction of haematite to magnetite can be particularly serious because of the stronger magnetization of the latter. Measurements at low temperatures are free from these objections and may be used to determine grain size and also possibly for identification of minerals by observing transition temperatures such as that known to occur at about 250 °K in some haematites and that at 118 °K in magnetite. An attempt to estimate grain size is made here. The measurements were made at Institut Fourier by kind permission of Professor L. Néel.

2. Apparatus

2.1. *The translation balance for low temperature work.*—Cohen (1958) has described this fully. The specimen is mounted at the end of a thin constantan rod rigidly held at the top by a tetrahedral balsa wood framework which is suspended by five fibres so as to allow only a horizontal translational movement in the direction of the field gradient. The force $F_x = \chi H(dH/dx)$ on a specimen of susceptibility χ due to a field H and field gradient dH/dx is measured by a null method. A double walled Dewar vessel may be placed round the sample the temperature of which is measured with a platinum resistance thermometer.

2.2. *For measurement of magnetization: applied field relationship, at low temperatures.*—The pole pieces of a large electromagnet contain a hole running axially through them and the specimen, surrounded by a Dewar vessel, is placed in the pole gap through this hole. Its magnetization is measured by an induction method. Dr R. Pauthenet kindly made the measurements with this apparatus.

3. Measurements on the rock with unstable remanent magnetization

3.1. *Susceptibility-temperature measurements.*—In Figure 1 the susceptibility is seen to be inversely proportional to the temperature according to the Curie law. The measurements shown were made in a field of 10 000 oersteds. Measurements in other fields (7 000 and 8 500 oersteds) showed no measurable ferromagnetism to be present.

3.2. *Brief description of rock.*—The specimen is of a red mudstone from the Keuper Marl. It consists of a fine silt with an admixture of clay minerals and comes from a well stratified bed, probably deposited in a temporary lake. It is bound together by a red cement, probably of hydrous haematite. A minute amount of black ferromagnetic has been separated out and X-ray powder analysis indicates that this is haematite.

It possesses a weak fossil magnetization and acquires a viscous magnetization (Creer 1957a) of about equal strength by application of fields of a few oersteds for a few hours. The susceptibility at room temperature of the sample studied here was $7{\cdot}9 \times 10^{-6}$ e.m.u./g and this is several times higher than one would expect if the haematite had a specific susceptibility of 20×10^{-6} e.m.u./g (Chevallier 1951) for chemical analysis indicates the presence of 5 per cent Fe and so of about 7 per cent Fe_2O_3 (if all the iron is present as haematite).

It may be that magnetite or maghemite, in amounts too small to be detected by X-rays is present in the black material which shows evidence in reflected light of being an oxidization product of a former magnetite host (Phillips 1954). A possible explanation of the rather high susceptibility is given below where it is shown that the temperature variation of susceptibility is consistent with the existence of very finely divided material.

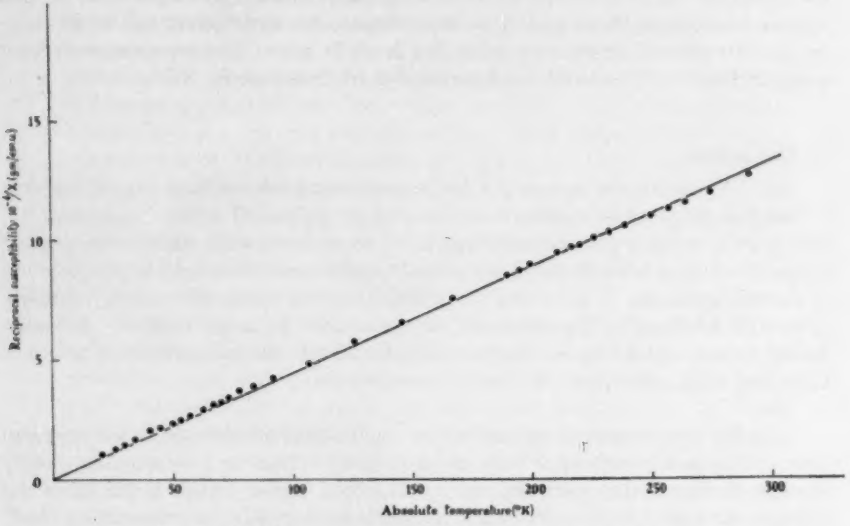

FIG. 1.—Variation of reciprocal susceptibility with temperature of a sample of Keuper Marl. The remanent magnetization of this rock at room temperature is unstable.

3·3. *Apparent paramagnetism or superparamagnetism.*—W. C. Elmore (1938) has investigated the magnetization of certain ferromagnetic colloids. Magnetization curves for colloidal magnetite and maghemite in fields up to 400 oersteds were experimentally obtained, as were theoretical curves based on the assumptions that each colloid particle was single domained and that it behaved like a molecule of a classical paramagnetic gas. A correction was made to take into account that the magnetic moments of the particles are not identical. A modified Langevin curve was shown to fit his data well, and the average moment per particle μ was estimated. Since this is equal to the product of the saturation magnetization I_s and the particle volume v, grain size can be deduced if I_s is assumed to be the same as that of the material in bulk.

Néel (1949a, b, 1953) has since pointed out that single domained particles, if small enough, can be provoked by thermal fluctuations to undergo a sort of magnetic Brownian movement of spontaneous fluctuation of their magnetization (Bean & Jacobs 1956) and that the theoretical magnetization curve of such an assemblage of particles is very similar to Elmore's, thus removing the restriction of magnetic granulometry to liquid suspensions.

The barrier between the minimum energy positions of the magnetization vector of a single domain particle is proportional to the particle moment and to the coercive force of the stable single domained particle aligned with the measuring field (Néel 1949a). For small values of v/T, the relaxation time of particles of volume v at temperature T is sufficiently short to allow the magnetization of an assemblage to attain equilibrium with the imposed conditions in a time short with the duration of an experiment. For nearly spherical particles of radius r having a dominant uniaxial anisotropy energy constant K, the criterion that the particles should behave superparamagnetically (Bean & Jacobs 1956) is $kT/r^3K > 0{\cdot}2$, where k is Boltzmann's constant. For instance, iron particles must be smaller than about 120 Å at 300°K and smaller than 80 Å at 77°K.

The expression for the initial slope of the magnetization curve of a dilute assembly of randomly orientated superparamagnetic particles is (Bean & Jacobs 1956)

$$I/H = 4\pi I_s^2 r^3/9kT. \tag{1}$$

In high external fields the approach to saturation is best given by

$$I/I_s = 1 - 3kT/4\pi I_s r^3 H \tag{2}$$

where I and I_s are referred to unit volume.

If there is a distribution of particle sizes equation (1) favours the larger particles whose moments are more easily aligned and equation (2) is more influenced by the smaller particles.

A distinction between true paramagnetic substances and ferromagnetics in a superparamagnetic state can be made by observing the form of their magnetization curves at low temperatures. The Langevin function $L(a) = \coth a - 1/a$ is linear with a only when $a = \mu H/kT$ is small. The molecular magnetic moment of a paramagnetic is given by $\mu = Jg\beta$ where J is the total quantum number, g the Landé spin factor and β the Bohr magneton. If we take $J = \frac{1}{2}$, $g = 2$ (the case of a single spin) we obtain $a = 7 \times 10^{-5}(H/T)$, and the magnetization curves of certain paramagnetic substances in Figure 2 show I to be linear with H/T for values of H/T up to several thousands of oersteds/deg. Since superparamagnetic particles consist of a very large number of atoms, μ and a will be much greater than for true paramagnetics and they will tend to saturation in lower values of H/T.

3·4. *Estimation of particle size of superparamagnetic material.*—Figures 3 and 4 show the magnetization–applied field relationship for this rock. They are demagnetization curves. Remanence and coercivity are small and remanent magnetization of the pole pieces of the electromagnetic makes reliable measurement of them impractical.

If ρ is the density and c the concentration of haematite, the following equation may be derived from equation (1),

$$r = \{9k\rho cm_1/4\pi\sigma_s^2\}^{\frac{1}{3}}. \tag{3}$$

Saturation did not occur but a rough estimate of σ_s, the specific saturation magnetization of the rock was made by linear extrapolation in Figure 4. m_1 is the initial slope of Figure 3.

From equation (2) we get

$$r = \{3kpc/4\pi m_2\}^{\frac{1}{2}} \tag{4}$$

where m_2 is the slope given by the first three points of Figure 4.

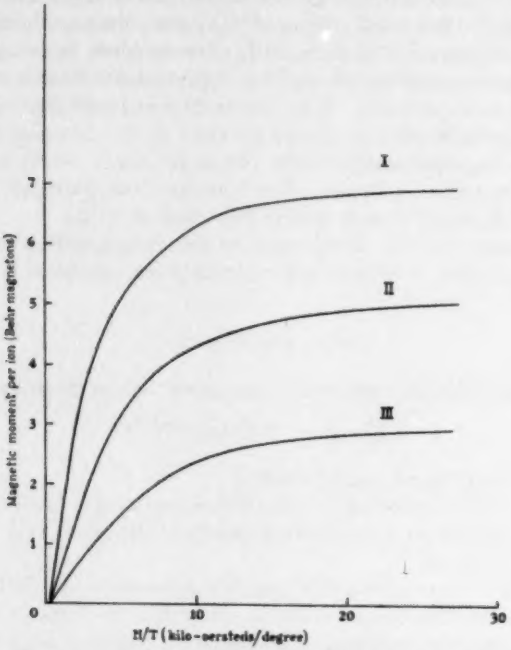

FIG. 2.—Plot of average magnetic moment per ion against H/T for paramagnetic substances, (I) potassium chrome alum, (II) iron ammonium alum and (III) gadolinium sulphate octahydrate.

Equations (3) and (4) respectively give diameters ($2r$) of 20 Å and 19 Å, taking $\rho = 5{\cdot}2$ gm/cm^3, $c = 0{\cdot}17$ and $\sigma_s = 8{\cdot}0$ e.m.u./g. The magnetic granulometry method is usually applied to iron and cobalt powders in the range of particle sizes from about 20 Å to 100 Å. It is desirable to check that it is valid for haematite and experiments with this object in view are planned.

3·5. *Viscous magnetization.*—Using the relationship given by Néel (1949a) for the time of relaxation τ of a single domained grain

$$\ln\tau = HIv/2kT - \ln[3\lambda He/m(2G/\pi k)^{\frac{1}{2}}] - 0{\cdot}5\ln v/T \tag{5}$$

and taking H (coercive force) = 1 000 oersteds, I (spontaneous magnetization/cm^3) = 2 gauss, e/m (ratio, charge to mass of electron) = $1{\cdot}76 \times 10^7$ e.m.u./gm,

k (Boltzmann's constant) $= 1{\cdot}38 \times 10^{-16}$ ergs/deg C), G (shear modulus) $= 10^{12}$ dyn cm^{-2} and λ (longitudinal magnetostriction) $= 10^{-6}$ we get

$$\log_{10}\tau = 3{\cdot}16 \times 10^{18} v/T - 18{\cdot}55 - 0{\cdot}5 \log_{10} v/T. \quad (6)$$

The values taken for G and λ are of the order of those found for ferrites (Smit & Wijn 1959) as no record of measurements of these quantities for haematite was

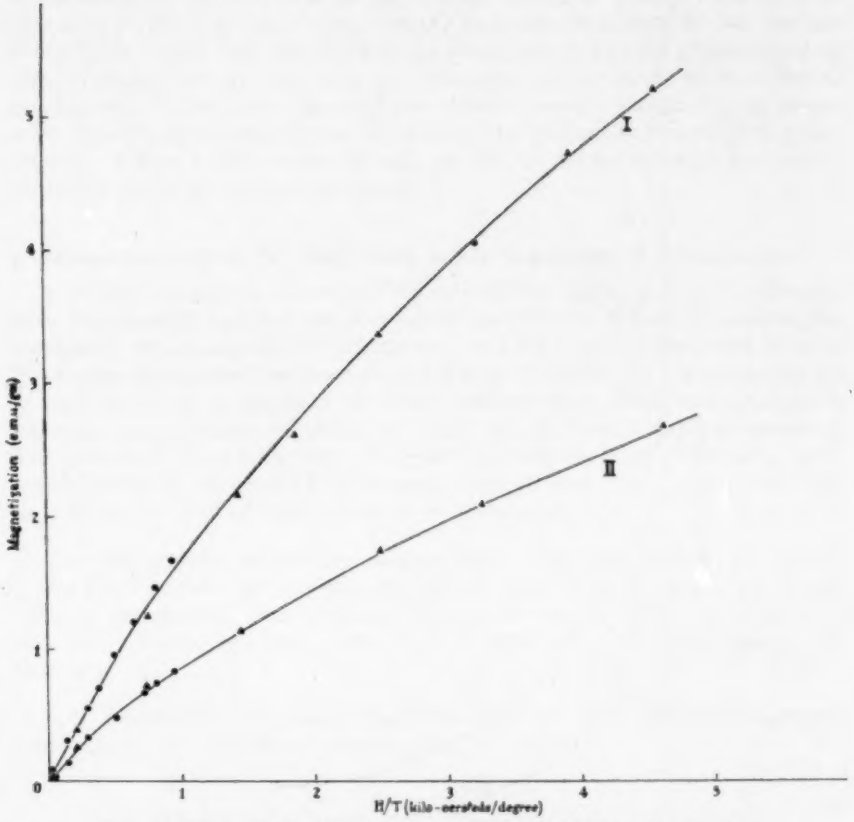

FIG. 3.—Magnetization as a function of applied field divided by absolute temperature for decreasing field. ●, observations at liquid hydrogen temperature; ▲, observations at liquid helium temperature. Curve I, unstable rock; curve II, stable rock.

found. Time constants at room temperature (290 °K) corresponding to various grain sizes have been calculated and values are given in Table 1, from which it is seen that only those grains whose diameters d fall within the range 1 200 Å $< d <$ 1 600 Å are responsible for viscous magnetization. As previously reported, this rock (Creer 1957a) was found to have (a) a fossil magnetization P, (b) a viscous magnetization S built up in the Earth's field since the latter acquired its present polarity and (c) a viscous magnetization T built up in the laboratory over times normally taken for experiments. (The viscous magnetization is probably produced

by grains with a wide spectrum of time constants, but separation into components S and T though somewhat arbitrary, is convenient.)

Table 1

d(Å)	1 200	1 300	1 400	1 500	1 600	1 700
τ	0·9 s	7·6 min	4·32 d	44·4 yr	$8{\cdot}2 \times 10^5$ yr	$2{\cdot}18 \times 10^{10}$ yr

FIG. 4.—Magnetization as a function of absolute temperature divided by applied field. These curves are constructed from the same observations as Figure 3.

The magnitudes of these components are as follows:

$P = 10{\cdot}5 \times 10^{-6}$ e.m.u./g of rock
$S = 8{\cdot}9 \times 10^{-6}$ " " "
$T = 3{\cdot}4 \times 10^{-6}$ " " "

the rock having a density of 2·25 g/cm³.

3.6. *Conclusions for unstable rock.*—Chevallier (1951) finds that the remanence of haematite powders decreases as the grain size is reduced. The remanence is about 0·1 e.m.u./g for grains of diameter in the region of 70 000 Å, and below this he finds that it decreases to about 0·01 for particles of diameter 10 000 Å. These are the smallest sizes he measured whereas it appears that those in this rock are much smaller. Remembering that the rock contains 7 per cent haematite and taking the larger value of specific remanence, it results that about 0·15 per cent of the haematite contents exist as grains large enough to possess a stable magnetization P, 0·12 per cent as grains having long time constants (the last reversal of the Earth's main field appears from palaeomagnetic evidence to have been at the end of the Tertiary), and 0·05 per cent with time constants of the order of hours to days. Thus about 99·7 per cent should possess no remanence in agreement with the predominantly superparamagnetic properties described in paragraph 4. Taking a value of 0·01 for the specific remanence about 97 per cent of the grains should be superparamagnetic.

4. Measurements on the rock with stable remanent magnetization

4.1. *Brief description of rock.*—This rock (Creer 1957b) is from the Brownstone formation in the lower Old Red Sandstone of South Wales. It consists predominantly of quartz grains bound together by a red to purple haematite cement. Black haematite grains have been separated from this rock and though scarce are at least ten times as abundant as in the unstable rock. This rock possesses a remanent magnetization of about 10^{-4} e.m.u./g and chemical analysis reveals an iron content of about 3 per cent. Viscous magnetization is not observed in weak applied fields of the order of 10 oersteds although such magnetization becomes predominant in applied fields of 100 oersteds or more.

4.2. *Susceptibility-temperature measurements.*—The results are shown in Figure 5, the three curves corresponding to applied fields of 7000, 8500 and 10000 oersteds respectively. Susceptibility tends to an infinite value at absolute zero and there is a measurable ferromagnetic component. The Curie law is not followed.

4.3. *Interpretation of results.*—Susceptibilities have been calculated assuming no ferromagnetic component present using the formula

$$F = \chi' H \frac{dH}{dx}. \tag{7}$$

However, when the magnetization is part paramagnetic and part ferromagnetic,

$$F = \chi H \frac{dH}{dx} + \sigma \frac{dH}{dx} \tag{8}$$

where χ is the reversible susceptibility and σ the ferromagnetic component. So when ferromagnetism is noticeably present, the value of χ' calculated from equation (7), varies according to the strength of the field in which the measurements are made. This is the case of Figure 5. χ and σ could be calculated as functions of temperature from the data of Figure 5 if the fields H had been sufficiently large to saturate the ferromagnetic component. Unfortunately this was not the case.

To explain the general shape of the curves, suppose that the magnetic content of the rock is of two types, the susceptibility χ_0 of one of concentration a, being independent of temperature, and that of the other, of concentration b, following a Curie law.

$$\chi = a\chi_0 + bC/T. \tag{9}$$

The first substance might be haematite in particles too large to be affected by thermal fluctuations and its susceptibility is taken to be the antiferromagnetic susceptibility of about 20×10^{-6} e.m.u./g, changing only slightly with temperature (see Figure 6), and the second might be fine-grained superparamagnetic haematite.

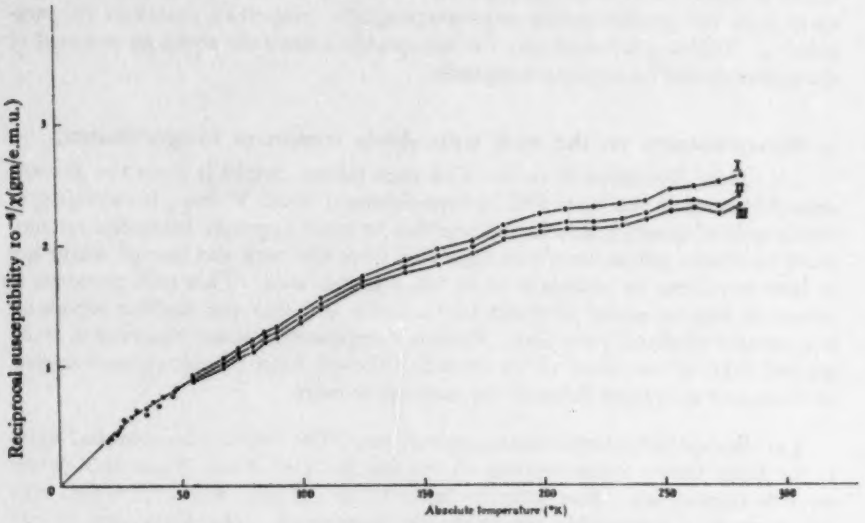

FIG. 5.—Variation of reciprocal susceptibility with temperature of a sample of Devonian Brownstone. The remanent magnetization of this rock at room temperature is stable. Measurements made in $H = 10\,000$ oersteds (curve I); $H = 8\,500$ oersteds (curve II); $H = 7\,000$ oersteds (curve III).

Taking a rock containing 3 per cent haematite and taking $C = 2{\cdot}2 \times 10^{-3}$ e.m.u. deg from Figure 1, curves (Figure 7) have been calculated for the inverse of the specific susceptibility as a function of temperature for $a = \frac{1}{3}$ and $b = \frac{2}{3}$; $a = \frac{1}{2}$ and $b = \frac{1}{2}$ and $a = \frac{2}{3}$ and $b = \frac{1}{3}$. The first is almost a straight line, the second is curved and the third more strongly curved. The shape of the experimental curves in Figure 5 may qualitatively be explained on the above assumptions.

4.4. *Magnetization-applied field measurements and estimation of particle size.*—There is the suggestion of a small remanence in the measurements from which the demagnetizing curves (II) of Figures 3 and 4 were compiled, and of a coercivity of rather less than 500 oersteds. Saturation was not possible in an applied field of 20 000 oersteds at 4·2°K but was estimated to be about 4·4 e.m.u./g of rock.

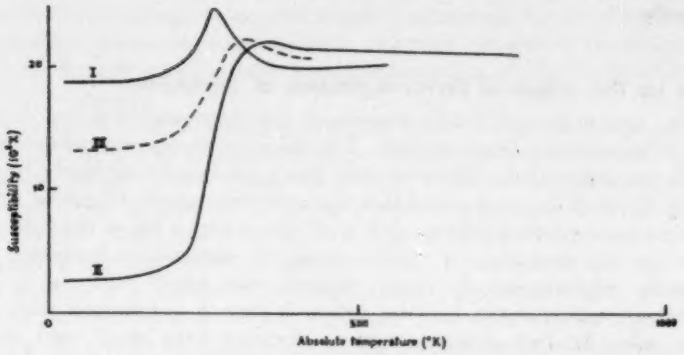

FIG. 6.—Variation of susceptibility with temperature of haematite (after Pauthenet):
(I) in basal plane, (II) along *c* axis, (III) for powder.

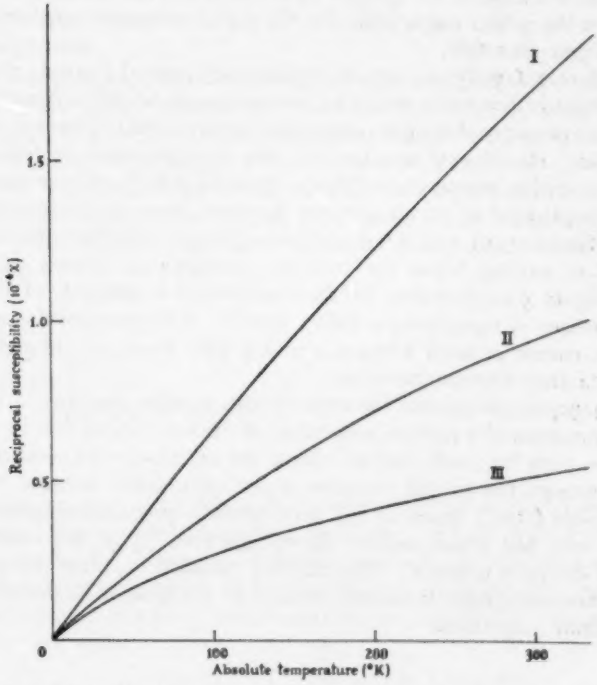

FIG. 7.—Calculated variation of reciprocal susceptibility with temperature for mixture of superparamagnetic and antiferromagnetic material in different proportions.
Curve I, $a = \frac{1}{3}$ $b = \frac{2}{3}$; curve II, $a = b = \frac{1}{2}$; curve III, $a = \frac{2}{3}$ $b = \frac{1}{3}$.

Application of equations (3) and (4) yield particle diameters of 14 Å and 16 Å respectively.

5. Note on the origin of ferromagnetism of haematite

In the application of Néel's theories it has been assumed that haematite behaves as an ordinary ferromagnetic. The origin of its ferromagnetism is, however, not yet understood. There are two kinds, an anisotropic kind (Townsend Smith 1916) which does not exist below the antiferromagnetic transition temperature and an isotropic kind which exists at all temperatures below the Néel point.

Although the formation of antiferromagnetic domains in haematite is not energetically advantageous, Li (1956) suggests they might exist due to crystal imperfections, and that the ferromagnetism is due to unbalanced spins in the domain walls. In fact antiferromagnetic domains have since been observed (William, Sherwood & Remaika 1958) in haematite. The grain size of about 20 Å estimated by the magnetic granulometry method might then refer to the thickness of the domain walls and not to the physical grain size of the magnetic material in the rocks studied. However, the estimate of about 1 500 Å for the diameter of the grains responsible for the observed viscous magnetization is more difficult to explain on this basis as the domain walls would not be expected to be so thick. Furthermore the grains responsible for the stable remanent magnetization must be rather bigger than this.

Dzyaloshinsky (1958) has argued on thermodynamical grounds that the weak ferromagnetism in haematite might be a consequence of the magnetic symmetry and that it is a property of the pure crystalline material and not due to lattice defects or impurities. His theory accounts for the disappearance of ferromagnetism below the transition temperature (Morin 1950, Néel & Pauthenet 1952).

The isotropic kind of ferromagnetism has been observed in haematite crystals (Townsend Smith 1916), and in red sandstones (Haigh 1957) the natural remanence is retained on cooling below the transition temperature (about 250°K). The curves of Figure 5 suggest that the ferromagnetism is probably of the isotropic kind as it exists at temperatures below 250°K. The reciprocal susceptibility-temperature curves in both Figures 1 and 5 pass smoothly through the antiferromagnetic transition temperatures.

Néel (1949c) suggested that the weak ferromagnetism observed in haematite is due to the presence of a minute proportion of ferrous iron so that in a haematite crystal there may be small centres where the chemical composition is that of magnetite, though the crystal structure is not quite cubic because of the small size. Chevallier (1951), however, has very carefully prepared samples containing no ferrous iron but which exhibit ferromagnetism. This, he concludes, is a property of the pure material. The effective magnetic moment per gram ion of ferric iron, calculated from the Curie constant of the Keuper Marl rock (Figure 1) is about 4 Bohr magnetons.

6. Note on the origin of the remanent magnetization of red beds

Part of the magnetization possibly originated in these rocks when the red haematite or hydrous haematite cement was formed, probably as a dehydration product of goethite. It is suggested that the haematite grains at first were so small that they were superparamagnetic, many of them growing no larger than this. A

small proportion of them grew large enough to pass through the viscous stage and then finally large enough to acquire a stable remanence in the direction of the then contemporaneous geomagnetic field. Part may be due to the black detrital grains, which might possibly have been magnetized as the oxidation of the magnetite host proceeded.

The time when these processes occurred has to be deduced from geological evidence. It can usually be inferred whether the red staining in a rock is of primary or secondary origin. Stability tests of the type introduced by Graham (1949), in those cases where application is possible, provide a younger limit to the age of magnetization. Unfortunately it appears that the time of origin of the natural remanence of red beds cannot be deduced nearly so precisely as that of lavas or of those sediments in which the magnetization is of a depositional kind. Consistency of results from red beds of different ages, and agreement with directions of magnetization revealed by igneous rocks which certainly acquire their thermoremanence at the time of formation, however, give us confidence in the reliability of the geological evidence that most of the red beds studied by us acquired their red cement soon after their formation. Furthermore, palaeoclimatological evidence suggests a strongly oxidizing environment at the time of formation of those red beds collected for palaeomagnetic studies from the British Isles and the U.S.A.

Acknowledgments

The measurements at low temperatures were made by kind permission of Professor L. Néel in the Laboratoire d'Electrostatique et de Physique du Metal, Institut Fourier, University of Grenoble, during the tenure of an O.E.E.C. Senior Visiting Fellowship. The author wishes to record his thanks to O.E.E.C. and to Professor Néel for the excellent facilities placed at his disposal and for valuable discussions concerning his experiments. Thanks are also expressed to Dr J. Cohen and Dr R. Pauthenet for their kind help and interest and for the use of their apparatus.

University of Durham,
Physics Department,
King's College,
Newcastle-upon-Tyne:
1960 *July.*

Note added in proof.—More recent experiments, the results of which will be reported soon, have shown haematite of grain size 100 Å to 500 Å to have a spontaneous magnetization. The 100 Å grains are not quite superparamagnetic at room temperature and grains having such properties must be smaller than this, supporting the estimate of a grain size of 20 Å for the material in the red sandstones described in this paper.

References

Bean, C. P. & Jacobs, I. S., 1956. *J. Appl. Phys.*, **27**, 1448.
Chevallier, R., 1951. *J. Phys. et Rad.*, **12**, 172.
Cohen, J., 1958. *C.R. Acad. Sci.* (*Paris*), **246**, 3425–3427.

Application of equations (3) and (4) yield particle diameters of 14 Å and 16 Å respectively.

5. Note on the origin of ferromagnetism of haematite

In the application of Néel's theories it has been assumed that haematite behaves as an ordinary ferromagnetic. The origin of its ferromagnetism is, however, not yet understood. There are two kinds, an anisotropic kind (Townsend Smith 1916) which does not exist below the antiferromagnetic transition temperature and an isotropic kind which exists at all temperatures below the Néel point.

Although the formation of antiferromagnetic domains in haematite is not energetically advantageous, Li (1956) suggests they might exist due to crystal imperfections, and that the ferromagnetism is due to unbalanced spins in the domain walls. In fact antiferromagnetic domains have since been observed (William, Sherwood & Remaika 1958) in haematite. The grain size of about 20 Å estimated by the magnetic granulometry method might then refer to the thickness of the domain walls and not to the physical grain size of the magnetic material in the rocks studied. However, the estimate of about 1 500 Å for the diameter of the grains responsible for the observed viscous magnetization is more difficult to explain on this basis as the domain walls would not be expected to be so thick. Furthermore the grains responsible for the stable remanent magnetization must be rather bigger than this.

Dzyaloshinsky (1958) has argued on thermodynamical grounds that the weak ferromagnetism in haematite might be a consequence of the magnetic symmetry and that it is a property of the pure crystalline material and not due to lattice defects or impurities. His theory accounts for the disappearance of ferromagnetism below the transition temperature (Morin 1950, Néel & Pauthenet 1952).

The isotropic kind of ferromagnetism has been observed in haematite crystals (Townsend Smith 1916), and in red sandstones (Haigh 1957) the natural remanence is retained on cooling below the transition temperature (about 250°K). The curves of Figure 5 suggest that the ferromagnetism is probably of the isotropic kind as it exists at temperatures below 250°K. The reciprocal susceptibility-temperature curves in both Figures 1 and 5 pass smoothly through the antiferromagnetic transition temperatures.

Néel (1949c) suggested that the weak ferromagnetism observed in haematite is due to the presence of a minute proportion of ferrous iron so that in a haematite crystal there may be small centres where the chemical composition is that of magnetite, though the crystal structure is not quite cubic because of the small size. Chevallier (1951), however, has very carefully prepared samples containing no ferrous iron but which exhibit ferromagnetism. This, he concludes, is a property of the pure material. The effective magnetic moment per gram ion of ferric iron, calculated from the Curie constant of the Keuper Marl rock (Figure 1) is about 4 Bohr magnetons.

6. Note on the origin of the remanent magnetization of red beds

Part of the magnetization possibly originated in these rocks when the red haematite or hydrous haematite cement was formed, probably as a dehydration product of goethite. It is suggested that the haematite grains at first were so small that they were superparamagnetic, many of them growing no larger than this. A

small proportion of them grew large enough to pass through the viscous stage and then finally large enough to acquire a stable remanence in the direction of the then contemporaneous geomagnetic field. Part may be due to the black detrital grains, which might possibly have been magnetized as the oxidation of the magnetite host proceeded.

The time when these processes occurred has to be deduced from geological evidence. It can usually be inferred whether the red staining in a rock is of primary or secondary origin. Stability tests of the type introduced by Graham (1949), in those cases where application is possible, provide a younger limit to the age of magnetization. Unfortunately it appears that the time of origin of the natural remanence of red beds cannot be deduced nearly so precisely as that of lavas or of those sediments in which the magnetization is of a depositional kind. Consistency of results from red beds of different ages, and agreement with directions of magnetization revealed by igneous rocks which certainly acquire their thermoremanence at the time of formation, however, give us confidence in the reliability of the geological evidence that most of the red beds studied by us acquired their red cement soon after their formation. Furthermore, palaeoclimatological evidence suggests a strongly oxidizing environment at the time of formation of those red beds collected for palaeomagnetic studies from the British Isles and the U.S.A.

Acknowledgments

The measurements at low temperatures were made by kind permission of Professor L. Néel in the Laboratoire d'Electrostatique et de Physique du Metal, Institut Fourier, University of Grenoble, during the tenure of an O.E.E.C. Senior Visiting Fellowship. The author wishes to record his thanks to O.E.E.C. and to Professor Néel for the excellent facilities placed at his disposal and for valuable discussions concerning his experiments. Thanks are also expressed to Dr J. Cohen and Dr R. Pauthenet for their kind help and interest and for the use of their apparatus.

University of Durham,
Physics Department,
King's College,
Newcastle-upon-Tyne:
1960 *July.*

Note added in proof.—More recent experiments, the results of which will be reported soon, have shown haematite of grain size 100 Å to 500 Å to have a spontaneous magnetization. The 100 Å grains are not quite superparamagnetic at room temperature and grains having such properties must be smaller than this, supporting the estimate of a grain size of 20 Å for the material in the red sandstones described in this paper.

References

Bean, C. P. & Jacobs, I. S., 1956. *J. Appl. Phys.*, **27**, 1448.
Chevallier, R., 1951. *J. Phys. et Rad.*, **12**, 172.
Cohen, J., 1958. *C.R. Acad. Sci.* (*Paris*), **246**, 3425–3427.

Creer, K. M., 1957a. *Phil. Trans. Roy. Soc. A*, **974**, 130.
Creer, K. M., 1957b. *Phil. Trans. Roy. Soc. A*, **974**, 111.
Dzyaloshinsky, I., 1958. *J. Phys. Chem. Solids*, **4**, 241.
Elmore, W. C., 1938. *Phys. Rev.*, **54**, 1092–1095.
Graham, J. W., 1949. *J. Geophys. Res.*, **54**, 31.
Haigh, G., 1957. *Phil. Mag.*, **2**, 877.
Li, Y. Y., 1956. *Phys. Rev.*, **101**, 1450.
Morin, J., 1950. *Phys. Rev.*, **78**, 819.
Néel, L., 1949a. *Ann. Geophys.*, **5**, 99.
Néel, L., 1949b. *C.R. Acad. Sci.* (*Paris*), **228**, 664.
Néel, L., 1949c. *Ann. Phys.*, **4**, 249.
Néel, L., 1953. *Rev. Mod. Phys.*, **25**, 293.
Néel, L. & Pauthenet, R., 1952. *C.R. Acad. Sci.* (*Paris*), **234**, 2172.
Phillips, R., 1954. Private communication.
Smit, J. & Wijn, H. P. J., 1959. *Ferrites* (Phillips Technical Library).
Smith Townsend, T., 1916. *Phys. Rev.*, **8**, 721.
William, H. J., Sherwood, R. C. & Remaika, J. P., 1958. *J. Appl. Phys.*, **29**, 1772.

The Comparison of the Earth's Gravitational Potential derived from Satellite Observations with Gravity Observations on the Surface

A. H. Cook

(Received 1960 August 17)

Summary

Instead of regarding gravity as a function of height above sea-level and angular co-ordinates, it may be regarded as a function of geopotential and angular co-ordinates. Since the operations of spirit levelling give differences of geopotential directly, observed values of gravity on the surface of the Earth are obtained as functions of geopotential, while gravity as a function of geopotential may be calculated from the expression for the potential derived from satellite observations. Comparing these two functions, we obtain differences between observed and calculated gravity at the same values of geopotential, the most direct possible comparison between the two sets of observational data.

1. Introduction

One of the outstanding problems of the theory of the Earth's external gravity field that has been revived by the impact of the highly accurate estimates of potential derived from observations of artificial satellites is the theoretical basis on which these estimates may be compared with surface gravity measurements. I am not concerned here with the uncertainties due to the imperfect distribution of gravity observations over the surface; the question is how to deal with the fact that observations of gravity are made on the surface of the Earth at varying heights.

2. Principles

Many discussions of this problem have, in the past, been in terms of equipotential surfaces, either of the actual Earth or of various models, at points within the topography and therefore at places where Laplace's equation is not obeyed and where, accordingly, very intricate problems arise especially when considering isostatic anomalies or models. With some models, also, it has not been shown that the external field of the model agrees at all external points (and not just on the surface) with that of the actual Earth—in dealing with artificial satellites this is a fundamental consideration. The ideas I use in this paper derive to a large extent from those of Molodensky (1948), de Graaff-Hunter (1950), Levallois (1957) and Sir Harold Jeffreys (1952), in that I consider values of gravity at the physical

surface of the Earth and not on any internal surface, real or imaginary. On this basis, Jeffreys (1952) has given a treatment of the free-air reduction extrapolating the external field from gravity given on the actual surface so that the external field on and outside the actual surface is correctly reproduced. However for the comparison of satellite with surface data, an even more straightforward way of formulating the problem seems to be available which entirely avoids such questions as the form of equipotential surfaces, the definition of height and so on and concentrates attention entirely on observable quantities.

The observations which can be made at the surface of the Earth give values of the geopotential U (actually differences from the sea-level value) and values of the normal gradient of U, that is values of gravity, g. Values of gravity are thus known as a function of geopotential U and of positional co-ordinates such as longitude and geocentric colatitude. As has been pointed out by many authors, ordinary spirit-levelling measurements of height fundamentally yield differences of geopotential. Now from the observations of artificial satellites the external potential can be specified by, for instance, the values of the coefficients in a spherical harmonic expansion and hence again it is possible to express the value of gravity as a function of geopotential and other co-ordinates. The values so expressed may then be compared with the observed values on the surface.

3. Mathematical development

As one possible way of making the comparison between surface gravity and that derived from a "satellite" potential, I shall derive a Taylor series expansion for the latter.

Since spherical polar co-ordinates (r, θ, ϕ) are the natural ones to use in dealing with the motion of artificial satellites (but see Vinti 1960), they will be used in the working below.

Let the geopotential be expressed in the form

$$U = \frac{fM}{a}\left\{\frac{a}{r} - \frac{a}{r}\sum J_n\left(\frac{a}{r}\right)^n P_n(\cos\theta)\right\} + \tfrac{1}{2}r^2\omega^2\sin^2\theta, \qquad (1)$$

where a is the Earth's mean radius and the coefficients J_n are determined from satellite observations. J_n differs slightly from the coefficient associated with the *equatorial* radius. Terms that are functions of longitude ϕ are omitted since they cannot at present be found from satellite observations.

g, equal to $|\text{grad } U|$, may also be written as a function of r and θ. But equally g may be regarded as a function of U and θ so that near sea-level

$$g(U,\theta) = g(U_0,\theta) + \frac{\partial g}{\partial U}\delta U + \ldots \qquad (2)$$

where U_0 is the value of U at sea-level and $\partial g/\partial U$ is evaluated at sea-level. This is adequate for moderate heights above sea-level, but in general further terms of the Taylor series should be included.

Equation (2) therefore gives a value of gravity to be compared with observed values on the surface and, to evaluate it, $\partial g/\partial U$ has to be calculated for U specified by equation (1).

Now the term fM/a in equation (1) is one thousand times greater than the term $(fMa^2/r^3) \times J_2P_2(\cos\theta)$ and that itself is nearly one thousand times greater than

any subsequent term in the gravitational potential, at least so far as present information goes. We therefore ignore all these subsequent terms in calculating $\partial g/\partial U$ and take for the geopotential

$$U = \frac{fM}{a}\left\{\frac{a}{r} - \left(\frac{a}{r}\right)^3 J_2 P_2(\cos\theta)\right\} + \tfrac{1}{2}r^2\omega^2\sin^2\theta.$$

Put $m = a^3\omega^2/fM$. Then

$$U = \frac{fM}{a}\left\{\frac{a}{r} - \left(\frac{a}{r}\right)^3 J_2 P_2(\cos\theta) + \frac{1}{2}\left(\frac{r}{a}\right)^2 m\sin^2\theta\right\}.$$

If the development is restricted to first order in J_2,

$$g = -\frac{\partial U}{\partial r} = \frac{fM}{a^2}\left[\left(\frac{a}{r}\right)^2 - 3\left(\frac{a}{r}\right)^4 J_2 P_2(\cos\theta) - \frac{r}{a}m\sin^2\theta\right]. \tag{3}$$

Write g_m for the mean value of g:

$$g_m = \frac{fM}{a^2}(1 - \tfrac{3}{2}m).$$

Then

$$\frac{fM}{a} = ag_m(1 + \tfrac{3}{2}m).$$

Now U can be written in the form

$$\frac{fM}{a}\left\{\frac{a}{r} - \alpha\left(\frac{a}{r}\right)^3 + \beta\left(\frac{a}{r}\right)^{-2}\right\}$$

where $\alpha = J_2P_2(\cos\theta)$ and $\beta = \frac{1}{2}m\sin^2\theta$ are both small quantities and a/r is of the order of unity.

Then to first order in m and J_2,

$$\frac{a}{r} = \frac{Ua}{fM} + \alpha\left(\frac{Ua}{fM}\right)^3 - \beta\left(\frac{Ua}{fM}\right)^{-2}$$

or

$$\frac{a}{r} = \frac{U}{ag_m}(1 - \tfrac{3}{2}m) + \left(\frac{U}{ag_m}\right)^3 J_2 P_2(\cos\theta) - \frac{1}{2}\left(\frac{U}{ag_m}\right)^{-2} m\sin^2\theta.$$

We let $U/ag_m = u$ and write

$$\left(\frac{a}{r}\right)^n = u^n[1 - \tfrac{3}{2}nm + nu^2 J_2 P_2(\cos\theta) - \tfrac{1}{2}nu^{-3}m\sin^2\theta].$$

With the aid of this expansion, the formula for g becomes

$$\frac{g}{g_m} = (1 + \tfrac{3}{2}m)u^2\{1 - \tfrac{4}{3}m + u^2 J_2 P_2(\cos\theta) - 2mu^{-3}\sin^2\theta\}. \tag{4}$$

Hence

$$\frac{1}{g_m}\frac{\partial g}{\partial u} = 2u(1 - \tfrac{3}{2}m) + 4u^3 J_2 P_2(\cos\theta) + 2mu^{-2}\sin^2\theta. \tag{5}$$

This gives the expression for $\partial g/\partial U$ that we require to insert in equation (2). We note that since du/dh is approximately equal to $-a^{-1}$ and since u is of the order of unity, this equation is equivalent to first order to the free-air relation

$$\frac{\partial g}{\partial h} = -\frac{2g_m}{a}.$$

Further,

$$\frac{1}{g_m}\frac{\partial^2 g}{\partial u^2} = 2(1-\tfrac{2}{3}m)+12u^2J_2P_2(\cos\theta)-4mu^{-3}\sin^2\theta.$$

We may obtain a simpler expression for $\partial g/\partial u$, for now u is equal to $(U_0-\int g\,dh)/ag_m$ where the integral $\int g\,dh$ is evaluated from sea-level upwards and U_0 is the value of U at sea-level, that is $ag_m(1+\frac{1}{3}m)$. Thus u is equal to

$$1+\tfrac{1}{3}m-\frac{1}{ag_m}\int g\,dh$$

and to first order,

$$\frac{1}{g_m}\frac{\partial g}{\partial u} = 2(1-\tfrac{1}{3}m)+4J_2P_2(\cos\theta)+2m\sin^2\theta$$

or

$$\frac{1}{g_m}\frac{\partial g}{\partial u} = 2+e\tfrac{8}{3}P_2(\cos\theta)$$

where

$$e = \tfrac{3}{2}J_2+\tfrac{1}{2}m.$$

It will be remembered that in all these formulae, a is the Earth's mean radius and J_2 is $(C-A)/Ma^2$.

The difference between observed gravity and values derived from a "satellite" potential by equation (2) are gravity anomalies and numerically they will be almost identical with free-air anomalies. In principle, however, they are rather different, for with the anomalies suggested by Levallois (1957) the object is to compare observed gravity with that calculated from a formula *at the same point in space*; whereas the object here is to compare gravity at *the same values of the geopotential*, on the actual Earth and on the model as de Graaff-Hunter (1950) does. In general, these two comparisons are not the same.

I would also like to emphasize that the values of gravity calculated from the "satellite" potential are not *conventional* values like those derived from the International Gravity Formula but are just as much the results of observation as are surface gravity measurements. We are concerned with comparisons between two sets of observations, not between observation and convention.

It should be mentioned that this approach to the problem of comparing satellite results with surface gravity measurements is very similar to that of Marussi (1951) and Hotine (1957) in their discussion of geodetic problems. The essential point is that geopotential is taken as a co-ordinate instead of a length such as radius vector or height.

Acknowledgments

This paper has been prepared as part of the research programme of the National Physical Laboratory and is published with the permission of the Director of the Laboratory.

National Physical Laboratory,
Teddington, Mx.:
1960 *July* 14.

References

de Graaff-Hunter, J., 1950. *Bull. géod. int.* No. 56, 191.
Hotine, M., 1957. Geodetic co-ordinate systems. Assoc. Int. Géod., Gen. Assembly, Toronto.
Jeffreys, H., 1952. *Mon. Not. R. Astr. Soc. Geophys. Suppl.*, **6**, 316.
Lambert, W. D., 1960. *Geophys. J.*, **3**, 360.
Levallois, J.-J., 1957. *C.R. Acad. Sci.* (*Paris*), **244**, 2479.
Marussi, A., 1951. *Bull. géod. int.* No. 19, 68.
Molodensky, M. S., 1948. *Izvest. Akad. Nauk. U.S.S.R.* (*Ser. geog. geophys.*), **12**, No. 3.
Vinti, P., 1960. *J. Res. Nat. Bur. Stds.*, **63B**, 105.

The Measurement and Computation of Anisotropy of Magnetic Susceptibility of Rocks

R. W. Girdler

(Received 1960 October 1)

Summary

A method is described for the experimental determination of anisotropy of magnetic susceptibility of rock specimens using a transformer a.c. bridge. The principal susceptibilities are calculated using a least squares solution of the susceptibility tensor on an electronic computer. In the experimental design, sufficient data are obtained to enable an estimate to be made of the precision of the results. An example is given to illustrate the procedure.

1. Introduction

The magnetic moment **M**, of unit volume of rock in a weak magnetic field **H**, is given by:

$$\mathbf{M} = \mathbf{M}_r + \mathbf{M}_i \qquad (1)$$

where $\mathbf{M}_r$ is the remanent moment (assumed to be unaffected by the weak field **H**) and $\mathbf{M}_i$ is the induced moment which is practically independent of the geometrical shape of the specimen on account of the small susceptibility (much less than unity).

The development of the spinner magnetometer by Johnson & McNish (1938) and the astatic magnetometer by Blackett (1952) have led to extensive studies of the natural remanent magnetization $\mathbf{M}_r$, of rocks. Comparatively few workers have studied the induced magnetization $\mathbf{M}_i$ which may show anisotropy. Ising (1943) and Granar (1958) have made a study of the susceptibility anisotropy of varve clays using a suspended sample type magnetometer and Howell, Martinez & Statham (1958) measured the susceptibility anisotropy of some sediments using the spinner type magnetometer. Graham and others in Washington have used a Maxwell inductance bridge in which the direction of maximum susceptibility was found by rotating a specimen in a Helmholtz coil and observing the out-of-balance voltage of the bridge.

For the measurement of susceptibility anisotropy an a.c. bridge method has the advantages that it is unaffected by extraneous fields which affect many d.c. and magnetometer methods and measurements can be made in low fields. A transformer type bridge is found to be more convenient than the classical Maxwell bridge and this is described here together with a method for calculating the susceptibility anisotropy from a set of measurements on one specimen so that an estimate of the precision of the results can be obtained.

2. Description of apparatus for measuring susceptibility anistropy

The susceptibility anisotropy is measured by inserting the specimen in various orientations in an air-core coil which forms one arm of a bridge. The inductance of the coil changes, increasing if the material is paramagnetic and decreasing if it is diamagnetic. The change of inductance causes the bridge to be thrown out of balance and restoration of the balance provides a measure of the susceptibility.

(a) *The transformer bridge.*—The essential feature of this bridge is that two of its arms consist of coils wound on a single core of high permeability nickel–iron alloy so that coupling between them is almost perfect. This arrangement has the great advantage that any stray impedances such as capacities between any part of the bridge and Earth can be made to have almost negligible effect on the balance point so that no Wagner earthing device is needed.

The idea of using tightly coupled inductors was patented by A. D. Blumlein in 1928 but seems to have received little attention until 1945 when Kirke described a series of radio-frequency bridges using the transformer principle. The principle has been discussed by Clark & Vanderlyn (1949) and an application was described by Watton & Pemberton (1949).

(b) *Theory of the bridge.*—The simplest form of the bridge is shown in Figure 1. The two coils constituting the transformer have self-inductances L_1 and L_2.

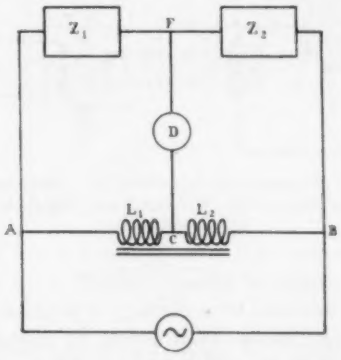

FIG. 1.—Basic transformer bridge circuit.

The impedances Z_1 and Z_2 which it is desired to compare are placed in series across the transformer and the detector D is connected between C and F.

In developing the theory of the bridge two assumptions are made: (i) the coupling between the two coils which form the ratio arms is perfect and (ii) the coils have negligible resistance. Although neither of these conditions can be accurately fulfilled, it is possible to wind transformers so that imperfections do not affect measurements made for accuracies less than 1 part in 10 000. With these assumptions, the condition for balance of the bridge is:

$$\frac{Z_1}{Z_2} = \frac{N_1}{N_2} \qquad (2)$$

where N_1 and N_2 are the number of turns of the two arms of the transformer. It can be shown that maximum sensitivity is obtained when $Z_1 = Z_2$ and $N_1 = N_2$.

In the bridge constructed Z_1 and Z_2 were two equal inductance arms and the transformer was tapped at the centre. In such a configuration thermal drift of the balance position is minimized because of symmetry of the identical arms.

(c) *Components and operating conditions.*—The inductance arms are in the form of solenoids designed to give uniform field to within 0·5 per cent for rock cylinders 3·5 cm in diameter and 3·5 cm in height (a non uniform field would cause apparent anisotropy in the case of an isotropic sample). It is desirable to wind the solenoids on rigid formers made of material such as tufnol. The coils have inductance of less than 2 mH and are arranged with axes at right angles to each other to avoid mutual inductance. Careful thermal insulation of the coils is necessary to minimize drift of the bridge balance from temperature effects.

The transformer consists of 400 turns (200 on each arm) of No. 38 S.W.G. enamel and rayon insulated copper wire wound on a Mu-metal core and screened in a metal box of dimensions 6·5 × 6·0 × 4·5 cm. The centre point of the transformer is earthed and all screening is grounded to this point.

The bridge is operated at 1 440 c/s and has an impedance of 36·5 ohms. A potential of 3 volts across the bridge is required to give a field of 1 oersted in the coils and the power consumption is 0·24 watt. The complete circuit is shown in Figure 2.

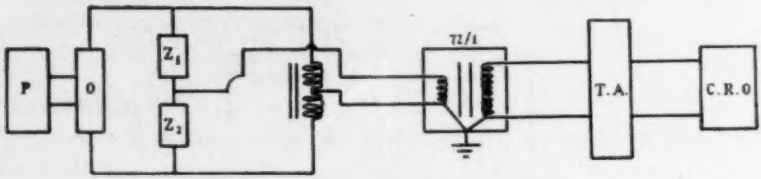

FIG. 2.—Circuit diagram of susceptibility apparatus. (P = Power supply, O = Oscillator, T.A. = Tuned amplifier, C.R.O. = Cathode ray oscilloscope).

The output of the bridge is passed through a 72 : 1 step-up transformer screened in a mu-metal box and then through a tuned amplifier. The amplified voltage is observed on a cathode ray oscilloscope. In a later modified version of the bridge the step-up transformer and tuned amplifier are replaced by a single transistorized tuned amplifier.

(d) *Methods of balancing the bridge.*—The bridge has to be balanced for differences in both resistance and inductance between the two arms. Two ways have been used for balancing the difference in resistance. The first employs a potentiometer device in parallel with the two coils as shown in Figure 3. The condition of balance for this network is given by:

$$\frac{N_1}{N_2} = \frac{L_1}{L_2} = \frac{R_1(R_3R_4 + RR_3 + RR_4 + R_2R_3)}{R_2(R_3R_4 + RR_3 + RR_4 + R_1R_4)}, \qquad (3)$$

where L_1 and L_2 are the inductances of the two coils, R_1 and R_2 are the resistances of the two coils, R_3 and R_4 are the resistances of the potentiometer arms and R is the resistance in series with the detector. In practice it was found convenient to make R = 1 000 ohms and R_3 and R_4 variable over a range of 0 to 10 000 ohms.

A second method of balancing the difference in resistance consists of moving a single loop of copper wire parallel to the axis of one of the coils. The loop has

the same effect as a small variable resistance in series with one of the coils. This method is probably preferable as the loop is external to the circuit and no extra components and soldered junctions are necessary.

The difference in inductance of the two coils was balanced by moving a small ferrite "slug" along the axis of one of them.

(e) *Advantages of the transformer bridge.*—(i) The most important advantage is the almost complete elimination of stray impedances such as capacities between any part of the bridge and earth which affect the balance. Referring to Figure 3, the self capacities of the transformer will be effectively between *A* and *C* and

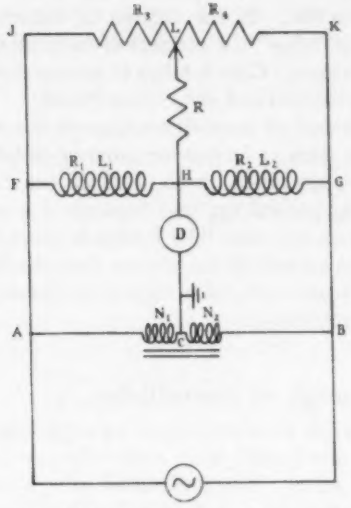

FIG. 3.—Transformer bridge network used for measuring anisotropy of susceptibility of rocks.

between *B* and *C* while any mutual capacity will be between *A* and *B*. If the mid-point of the transformer is earthed, *H* and *L* will also be at earth potential when the bridge is balanced. Hence any stray capacities between *F* and *H* and *H* and *G* and earth will appear between *A* and *C* and *B* and *C* respectively and similarly any stray capacities between *J* and *L* and *L* and *K* will also appear between *A* and *C* and between *B* and *C*. The same applies to capacities between the generator and earth. Any capacity between *A* and *B* is unimportant as it merely shunts the generator. It is easily shown that the bridge balance is not disturbed by any impedance that may be connected between *A* and *C* or *B* and *C* if there is perfect coupling between the transformer coils and they have negligible resistance. Because of the perfect coupling any current which the added impedances cause to flow in either coil produces a voltage drop across the coil and induces a corresponding e.m.f. in the other coil so that the ratio of the potential difference between *A* and *C* and between *B* and *C* remain unaltered. There is therefore very little drift of the bridge balance due to stray impedances.

(ii) The ratio of the impedances of the two arms is equal to the turns ratio of the transformer. It is relatively easy to obtain two equal arms by using a

transformer with a large number of turns, thus avoiding the difficulties associated with constructing stable, equal resistances required for other bridge networks.

(iii) The compactness of the ratio arms and the elimination of the Wagner earth reduces the size of the bridge considerably and the whole network could be shielded in an aluminium box $58 \times 38 \times 30$ cm. However, to retain symmetry it is probably better to keep the coils separate with separate shielding.

(f) *Measurement of susceptibility anisotropy of rocks.*—For the measurement of susceptibility anisotropy of rocks the bridge is first balanced by adjusting the resistance controls and by moving the "ferrite slug" in one of the coils. The rock specimen is then inserted into the other coil and the balance is restored by moving the ferrite "slug". The movement of the "slug" is measured using a dial gauge calibrated in 0·01 mm. If the change of inductance is linear over the distance travelled by the "slug" the amount of movement is proportional to the susceptibility of the specimen. Care is taken to ensure that the "slug" moves over a linear part well inside the coil and away from the edge. The instrument may be calibrated by using cylinders of same dimensions as the rock cylinders and filled with standard materials such as ferrous ammonium sulphate. Twelve measurements are made for each specimen, three of which are duplicates. Readings are taken in three sets in 0, 45, 90 and 135° positions starting with the cylinder upright and from two positions on its side. The bridge is quickly balanced and a set of twelve observations takes 15 min. In its present state the bridge measures changes of inductance of 0·00015 per cent and is capable of measuring differences of bulk susceptibility of $0{\cdot}5 \times 10^{-6}$ emu/g.

4. Calculation of anistropy of susceptibility

The theory of calculation of anisotropy of susceptibility has been discussed by Ising (1943) and by Granar (1958), both with reference to observations obtained using a torsion magnetometer. The method of calculation appropriate for a set of measurements obtained on an a.c. bridge has been developed with the aid of Nye (1957).

Throughout, it is assumed that the induced moment is a linear function of the field strength, the field strength being small. The magnetic susceptibility k for an anisotropic medium is given by:

$$\mathbf{M}_i = k_{ij}\mathbf{H}_j \qquad (k_{ij} = k_{ji}) \tag{4}$$

where $\mathbf{M}_i$ is the induced moment with direction i,

$\mathbf{H}_j$ is the effective magnetic field in the direction j,

and k_{ij} is a second order symmetric tensor.

For an isotropic medium, k has the same value in all directions and the induced moment $\mathbf{M}_i$ is in the direction of the inducing field $\mathbf{H}$. For an anisotropic medium, the susceptibility is characterized by six constants, either by the six tensor components k_{11}, k_{12}, ... k_{33} or by three principal susceptibilities k_a, k_b and k_c and three angles determining the orientation of a, b, and c. Geometrically, the relation $\mathbf{M}_i = k_{ij}\mathbf{H}_j$ is represented by an ellipsoid, the principal axes of which are parallel to a, b, and c.

The susceptibility k, in a given direction l_i referred to general axes is given by:

$$k = l_i l_j k_{ij} \tag{5}$$

and the magnitudes and directions of the principal susceptibilities are obtained

from the two equations:

$$|k_{ij} - \lambda\delta_{ij}| = 0 \tag{6}$$

$$(k_{ij} - \lambda\delta_{ij})l_j = 0 \tag{7}$$

where δ_{ij} is the Kronecker delta.

Since nothing is known about the principal axes of susceptibility of a given rock specimen, axes OX_1, OX_2, and OX_3 are chosen such that OX_1 is parallel to the orientation mark on the specimen (i.e. the strike of the sample measured with respect to present magnetic north). OX_2 and OX_3 are mutually perpendicular to OX_1 (Figure 4). Measurements along these directions give the coefficients A_1, A_2, and A_3. To solve the susceptibility tensor further measurements are required and the directions chosen are illustrated in Figure 5. The direction cosines are:

$A_1(1, 0, 0)$ $A_4(1/\sqrt{2}, 1/\sqrt{2}, 0)$ $A_7(-1/\sqrt{2}, 1/\sqrt{2}, 0)$
$A_2(0, 1, 0)$ $A_5(1/\sqrt{2}, 0, 1/\sqrt{2})$ $A_8(-1/\sqrt{2}, 0, 1/\sqrt{2})$
$A_3(0, 0, 1)$ $A_6(0, 1/\sqrt{2}, 1/\sqrt{2})$ $A_9(0, -1/\sqrt{2}, 1/\sqrt{2})$.

This is found to be a very convenient experimental design for the following reasons: (a) the directions are such that measurements are easily made by rotating the specimen on three orthogonal planes through the positions 0, 45, 90 and 135°; (b) the directions give a relatively simple matrix for the solution of the six susceptibility coefficients k_{ij} and (c) by using nine measurements, it is possible to obtain an estimate of error for the best fit of the susceptibility-ellipsoid and hence for the magnitudes and directions of the principal axes.

The best fitting ellipsoid for the nine observations (A_r) is obtained from a least squares solution of equation (5) which may be written in matrix notation as follows:

$$\mathbf{A} = \boldsymbol{\theta}\mathbf{k} \tag{5a}$$

where

$$\mathbf{A} = \begin{bmatrix} A_1 \\ A_2 \\ A_3 \\ A_4 \\ A_5 \\ A_6 \\ A_7 \\ A_8 \\ A_9 \end{bmatrix} \quad \boldsymbol{\theta} = \begin{bmatrix} 1 & 0 & 0 & 0 & 0 & 0 \\ 0 & 1 & 0 & 0 & 0 & 0 \\ 0 & 0 & 1 & 0 & 0 & 0 \\ \frac{1}{2} & \frac{1}{2} & 0 & 0 & 0 & 1 \\ \frac{1}{2} & 0 & \frac{1}{2} & 0 & 1 & 0 \\ 0 & \frac{1}{2} & \frac{1}{2} & 1 & 0 & 0 \\ \frac{1}{2} & \frac{1}{2} & 0 & 0 & 0 & -1 \\ \frac{1}{2} & 0 & \frac{1}{2} & 0 & -1 & 0 \\ 0 & \frac{1}{2} & \frac{1}{2} & -1 & 0 & 0 \end{bmatrix} \quad \mathbf{k} = \begin{bmatrix} k_{11} \\ k_{22} \\ k_{33} \\ k_{23} \\ k_{31} \\ k_{12} \end{bmatrix}$$

Since there are nine observations and only six unknowns the matrix is not square and the best value of $\mathbf{k}$ is given by the least squares solution:

$$\mathbf{k} = (\boldsymbol{\theta}_t\boldsymbol{\theta})^{-1}\boldsymbol{\theta}_t\mathbf{A} \tag{8}$$

where $\boldsymbol{\theta}_t$ is the transpose of $\boldsymbol{\theta}$ and $(\boldsymbol{\theta}_t\boldsymbol{\theta})^{-1}$ is the reciprocal of $\boldsymbol{\theta}_t\boldsymbol{\theta}$.

The final equation giving the six coefficients k_{ij} is

$$\begin{bmatrix} k_{11} \\ k_{22} \\ k_{33} \\ k_{23} \\ k_{31} \\ k_{12} \end{bmatrix} = \frac{1}{18} \begin{bmatrix} 10 & -2 & -2 & 4 & 4 & -2 & 4 & 4 & 2 \\ -2 & 10 & -2 & 4 & -2 & 4 & 4 & -2 & 4 \\ -2 & -2 & 10 & -2 & 4 & 4 & -2 & 4 & 4 \\ 0 & 0 & 0 & 0 & 0 & 9 & 0 & 0 & -9 \\ 0 & 0 & 0 & 0 & 9 & 0 & 0 & -9 & 0 \\ 0 & 0 & 0 & 9 & 0 & 0 & -9 & 0 & 0 \end{bmatrix} \begin{bmatrix} A_1 \\ A_2 \\ A_3 \\ A_4 \\ A_5 \\ A_6 \\ A_7 \\ A_8 \\ A_9 \end{bmatrix} \tag{9}$$

The magnitudes and directions of the principal susceptibilities are then obtained by substituting the six values of $\mathbf{k}_{ij}$ into equations (6) and (7).

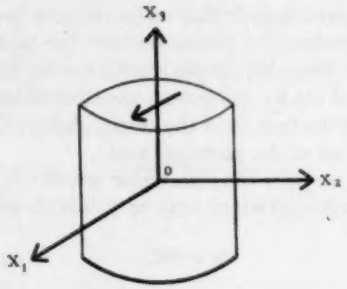

FIG. 4.—Reference axes chosen for measurement of rock cylinders.

4. The use of electronic computer for calculating susceptibility anistropy

As the solution of the above equations for the magnitudes and directions of the principal susceptibilities takes considerable time, the work was programmed for the Cambridge University Electronic Computer, EDSAC II. I am indebted to Dr D. W. Allen for preparing the programme. The nine observations A_r are fed into the computer which performs the following operations:

(a) Determines the values of $\mathbf{k}_{ij}$ from $\mathbf{k}_{ij} = \mathbf{MA}_r$ (equation (9) above).

(b) The values thus obtained for $\mathbf{k}_{ij}$ are substituted in equation (5a) to give:

$$\mathbf{A}_{\text{new}} = \boldsymbol{\theta}\mathbf{k} \tag{10}$$

and the residual values $(\mathbf{A} - \mathbf{A}_{\text{new}})$ are printed. These values immediately give some idea of the quality of the experimental data.

(c) Using the values obtained for $\mathbf{k}_{ij}$, equation (6) is solved for λ giving the three principal susceptibilities λ_1, λ_2, and λ_3.

(d) The values of λ_i and k_{ij} are used to solve the set of equations

$$(k_{ij}-\lambda\delta_{ij})l_j = 0,$$

giving the direction cosines of the principal susceptibilities.

(e) The direction cosines are converted to the (θ, ϕ) notation where θ is the angle in degrees measured clockwise from OA_1, and ϕ is the angle of inclination with reference to the A_1-A_2 plane (positive inclination downwards, negative inclination upwards). (θ, ϕ) are obtained from the equations:

$$\tan\theta = \frac{l_2}{l_1} \quad \text{and} \quad \sin\phi = l_3 \tag{11}$$

and the values of (θ, ϕ) are printed under the corresponding values of λ.

The complete operation for one set of data takes approximately 15 seconds.

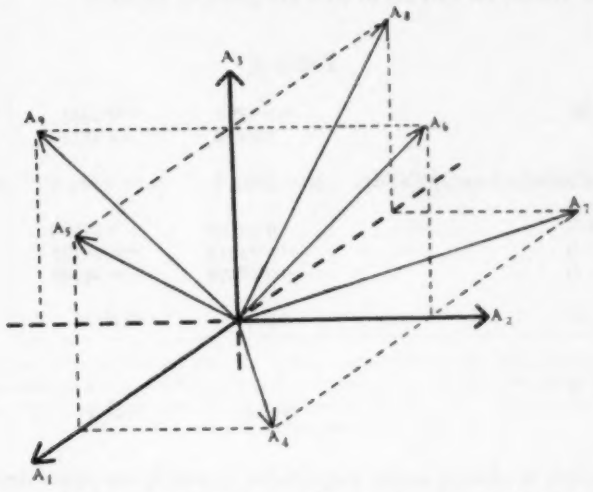

FIG. 5.—Directions A_1 ... A_9 along which measurements are obtained for the determination of susceptibility anisotropy.

5. Estimation of precision of results

The use of nine measurements on each rock specimen enables an estimate to be made of the errors for the magnitudes and directions of the principal susceptibilities.

On the assumption that the errors of measurement are small and normally distributed, Hext has derived confidence intervals for the magnitudes of the principal susceptibilities together with confidence regions on the unit sphere for their directions. The work has been generalized for the estimation of second-order tensors and is being published in detail separately (Hext 1961).

The procedure first tests for differences between specimens from the same sample. If the susceptibility tensors are not significantly different (at the 5 per cent level, say), a statistical test for isotropy is applied to the common or average tensor. For an anisotropic case the six tensor components are estimated using

equation (8) and a variance–covariance matrix is also derived. The standard errors and 95 per cent confidence intervals for the estimates of the latent roots are then obtained. The coordinate reference axes are now transformed to coincide with the estimated latent vectors and the lengths of the principal axes of the 95 per cent confidence ellipses for each principal susceptibility are calculated.

6. An example of the calculation and estimation of precision of susceptibility anistropy

The measurements on a rock specimen (3807A) from the Skaergaard layered intrusion of East Greenland are used to illustrate the procedure of calculation and estimation of precision of susceptibility anisotropy. The experimental values obtained for A_r are $A_1 = 3062$, $A_2 = 3038$, $A_3 = 2873$, $A_4 = 3035$, $A_5 = 2917$, $A_6 = 2919$, $A_7 = 3068$, $A_8 = 3014$ and $A_9 = 2989$ (the units are arbitrary). The EDSAC results for this set of data are given in Table 1.

Table 1

Residuals in A_r		−0·1111	−0·4444	1·8889
		1·2222	−1·1111	−0·7775
Magnitudes of principal susceptibilities		$\lambda_1 = 3075{\cdot}8$	$\lambda_2 = 3044{\cdot}1$	$\lambda_3 = 2851{\cdot}8$
Direct cosines	l_1	0·95107	0·20060	0·23502
	l_2	−0·24912	−0·94777	0·19918
	l_3	−0·18279	−0·24798	−0·95136
Declinition w.r.t. OX_1	θ	14°·7	281°·9	319°·7
Inclination w.r.t. X_1OX_2	ϕ	10°·5	14°·4	−72°·2

This example is chosen as the magnitudes λ_1 and λ_2 are approximately equal and λ_3 is considerably smaller than both λ_1 and λ_2, the ratios being:

$$\lambda_1 : \lambda_2 : \lambda_3 = 108 : 107 : 100.$$

We would therefore expect a small confidence region for the direction of λ_3 and approximately equal, larger regions for λ_1 and λ_2.

The errors for the magnitudes and directions of the principal susceptibilities have been computed by the method given by Hext. The confidence intervals for the magnitudes are:

$$\lambda_1 = 3075{\cdot}8 \pm 1{\cdot}5$$

$$\lambda_2 = 3044{\cdot}1 \pm 1{\cdot}5$$

$$\lambda_3 = 2851{\cdot}8 \pm 1{\cdot}7$$

and the 95 per cent confidence ellipses (i.e. regions in which we are 95 per cent confident that the true directions lie) are illustrated on a Schmidt equal area projection in Figure 6. The shaded regions are for the latent roots λ_1 and λ_2 (downwards) and the unshaded region for the latent root λ_3 (upwards). As expected, the

confidence region for λ_3 is smaller than the regions for λ_1 and λ_2 which are approximately equal. The results also show that there can be considerable error in two of the directions although the absolute magnitudes of the three axes are well determined.

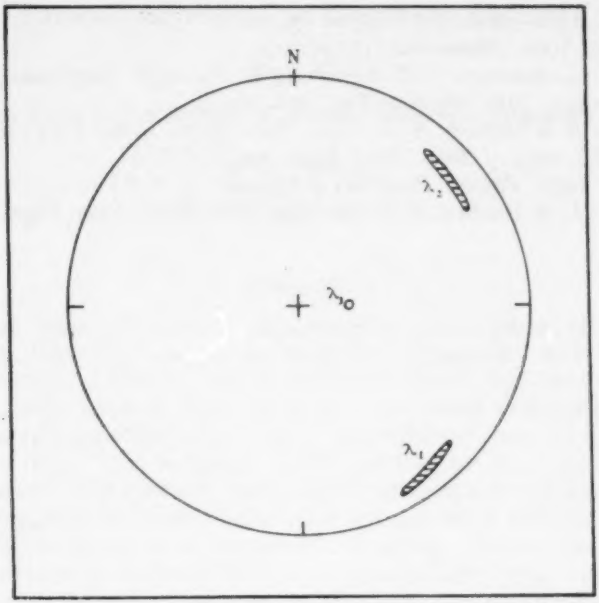

FIG. 6.—Directions of maximum (λ_1), intermediate (λ_2) and minimum susceptibilities (λ_3) with confidence ellipses at the 95 per cent level for a rock cylinder from the Skaergaard layered intrusion. (The directions have been corrected for geological field data.)

7. Acknowledgments

My grateful thanks are due to Sir Edward Bullard for his keen interest and help in all aspects of this work, to Professor C. W. Oatley of the Cambridge University Engineering Department for first suggesting the construction of a transformer bridge, to Dr D. W. Allen for his help with the EDSAC computing programme, to Mr G. R. Hext for his enthusiasm for the statistics of the subject and to Professor L. R. Wager for the loan of rock samples. My thanks are also due to Mr B. C. Browne, Dr J. C. Belshé and Dr J. A. Clegg for helpful discussions and to Mr L. H. Flavill and Mr K. Plachecki for invaluable technical assistance in the laboratory. Finally, I wish to thank the Cambridge University Mathematical Laboratory for the use of EDSAC II and the Shell Petroleum Company for a research scholarship.

Department of Geology,
Durham Colleges,
University of Durham:
1960 *September.*

References

Blackett, P. M. S., 1952. *Phil. Trans. Roy. Soc., A*, **245**, 303.
Clarke, H. A. M. & Vanderlyn, P. B., 1949. *Proc. Instn. Elect. Engrs.*, **96**, Pt. II, 365.
Granar, L., 1958. *Arkiv. för Geofysik.*, **3**, No. 1.
Hext, G. R., 1960. *Biometrika.* (In press.)
Howell, L. G., Martinez, J. D. & Statham, E. H., 1958. *Geophysics.*, **23**, 285.
Ising, G., 1943. *Ark. Mat Astr. Fys.*, **29A**, No. 5.
Johnson, E. A. & McNish, A. G., 1938. *Terr. Magn. Atmos. Elect.*, **43**, 393.
Kirke, H. C., 1945. *J. Instn. Elect. Engrs.*, **92**, Pt. III, 2.
Nye, J. F., 1957. *Physical Properties of Crystals.* (O.U.P.)
Watton, W. L. & Pemberton, M. E., 1949. *Proc. Instn. Elect. Engrs.*, **96**, Pt. II, 379.

Palaeomagnetism in Northern Ireland

Part I

The Thermal Demagnetization of Natural Magnetic Moments in Rocks

R. L. Wilson

(Received 1960 December 3)*

Summary

This paper describes a palaeomagnetic investigation of some laterites, containing hematite and maghemite, which have been baked by an overlying Tertiary lava in Northern Ireland. The laterite was magnetically unstable, but a technique of thermal demagnetization eliminated a secondary component of magnetization along the Earth's present field. This technique established that the lava and baked laterite agreed in direction, and it further allowed a determination of the strength of the Earth's field, which was apparently reversed at the time of baking, and of the temperature of baking. This determination of a geologically ancient field strength is particularly significant, since many such determinations from rocks of different ages might allow estimates of ancient latitudes for the various continents, independent of estimates derived from directions of magnetization.

1. Introduction

The rocks investigated here were collected from an unusual geological formation of Tertiary age known as the Interbasaltic Layer, which is particularly well exposed at the Giant's Causeway on the north coast of Co. Antrim, Northern Ireland. This formation consists of three or four lava flows which have undergone the following changes (Eyles, 1952):

The eruption of the lowest lava in the Interbasaltic Layer was followed by a prolonged quiescence, during which the weather conditions brought about two transformations: (a) The bulk of the flow, *in situ*, was altered to a grey bauxite or clay; (b) part but not all of the iron content of the lava was taken up in solution and redeposited within a few feet of the surface as a deep red or red-brown *laterite* containing ferric iron oxides. When this process was fairly complete, the next lava erupted, and heated the underlying laterite so as to give it a thermoremanence induced in the Earth's magnetic field. This second lava in turn underwent the same chemical alteration as the first, and then *its* red lateritic upper surface was heated by the third lava, and so on. The red laterite horizons remain now to mark the tops of these highly altered flows.

* Received in original form 1960 August 23.

Laterite is a relatively unexploited palaeomagnetic material. However, its hematite content, coupled with its natural occurrence as a baked material, make it a fruitful source of palaeomagnetic information.

Oriented samples of the underlying laterite baked by the uppermost flow of the Interbasaltic Layer were collected from between 1 and 24 inches below the contact surface, along with samples of the bauxitic remains from the interior of the flow above. The natural moments of the cores from these samples were initially found to have scattered directions of magnetization. Alternating fields failed to remove the unstable magnetizations, but thermal demagnetization was used successfully.

Other similar nearby baked contacts are now being examined.

2. The technique of thermal demagnetization

Magnetic moments were measured under an astatic magnetometer, while the specimens were manipulated inside a specially constructed furnace just below the magnetometer. The specimen is a cylinder $\frac{7}{8}$ inch in diameter and 1 inch long, and rests with its axis horizontal in a quartz V-trough rotatable about the vertical axis, inside the furnace. In this attitude only two of the vector components may be measured by rotation about a vertical axis. To allow direct measurement of the third component, a slot is cut by a hacksaw in the flat end of the rock specimen; and by means of a quartz screwdriver inserted into this slot through a 6 mm hole in the side of the furnace, the specimen, while hot, is turned through 90° about its horizontal axis. Measurements, with the specimen in four different attitudes separated by 90° intervals, allow the averaging of independently read values of each vector component, which eliminates certain systematic errors inherent in the measuring technique.

The laterite specimens tend to break easily on coring or heating, and it is therefore necessary to cast them (oriented) inside a $\frac{1}{16}$ inch thick plaster jacket, in a cylindrical mould of 1 inch internal diameter. This jacket preserves the specimen during manipulation and heating to 650 °C. However, the process of casting reduces the accuracy of orientation by an estimated 5°.

The total vector moment is measured at convenient temperature intervals, usually every 50 °C from room temperature to the Curie point. At each temperature, it is necessary to wait one to three minutes for thermal equilibrium, before readings may be taken.

The laterites usually remained unchanged chemically when heated in air.

3. Thermal demagnetization of the natural moments

To show how the magnetic vector behaves during heating, the three components of the specimen's moment are plotted directly in Cartesian coordinates, by projecting the vector on to two conveniently chosen mutually perpendicular planes. Regarding these projections for a series of temperatures, one may easily reconstruct mentally how the vector has changed with temperature.

Such a plot is shown in Figure 1 for a baked laterite specimen from $2\frac{1}{2}$ inches below the contact. This diagram immediately suggests what would be much less obvious in conventional displays; namely, that the vector observed at room temperature may be the resultant of two vectors, one lying closely parallel to the direction of the Earth's present dipole field F in Northern Ireland and being erased at

temperatures between 250 and 350 °C, the other lying about 150° away from the present dipole field direction, influenced little by low temperatures, and persisting right up to the Curie point. Both vectors lie close to the plane containing *up* and *south* directions.

Using smaller temperature intervals for a similar specimen, a more detailed investigation shown as a single projection in Figure 2 reveals an added feature, a small curved "tail" which sometimes occurs near room temperature. Eight baked

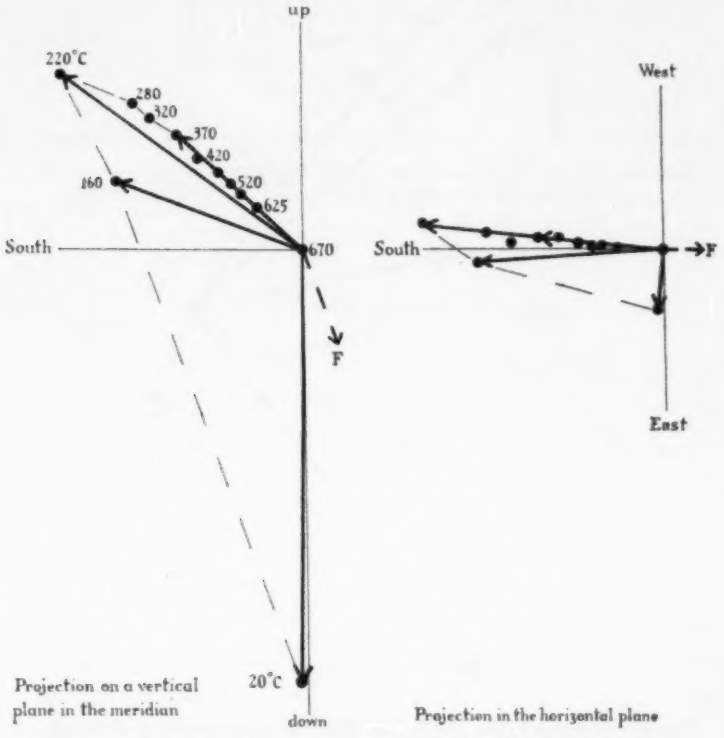

FIG. 1.—Three-dimensional representation of the effects of thermal demagnetization on a baked laterite specimen. F is the direction of the present dipole field in Northern Ireland.

laterite specimens, from between 1 and 24 inches below the contact, bore in various proportions the features demonstrated in Figures 1 and 2. In addition three specimens of bauxite from the overlying flow showed no change in direction of magnetization above 165 °C, and a change of only about 5° below this temperature (Figure 3).

Before examining more deeply the mechanisms within the rocks which have produced the observed results, we may view the results phenomenologically, and draw some conclusions at this stage.

The most important result is that during each thermal demagnetization a definite unique direction of magnetization was revealed at high temperatures. The direction is easily calculated from the slopes of the high temperature regions.

The eight baked laterite and three bauxite directions are plotted in Figure 4, where it is obvious that at high temperatures the bauxitic remains of the overlying flow agree well with the baked laterite below. The mean direction is 178° east of true north and 41° up, with a standard deviation of 8°. Much of this error is probably due to the difficulty of orienting specimens inside the plaster jackets.

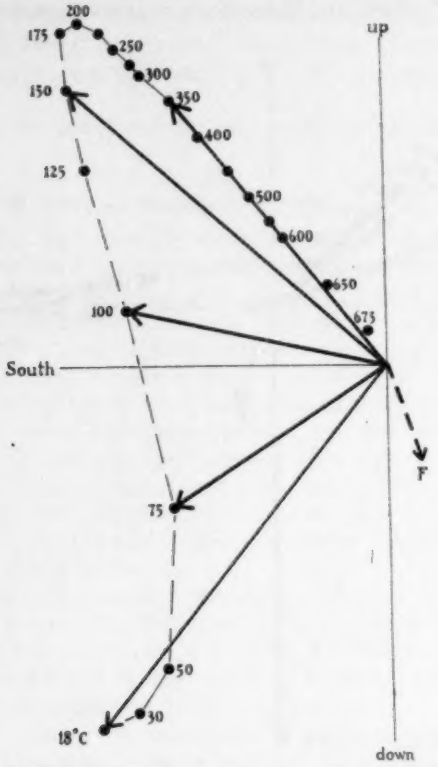

FIG. 2.—A detailed examination of a baked laterite specimen, showing a "tail" erased at temperatures below 75 °C.

This agreement supports strongly the supposition that these reversed high temperature directions do indeed represent the ancient field at the time of baking. The rocks seem therefore to have been successfully cleaned thermally. Their mean direction is 22° from the mean direction of all the Tertiary rocks measured from Northern Ireland (see Part II, Section 2). Since the scatter of all these Tertiary directions is about 20°, it is reasonable to assume that this 22° deviation from the mean reflects a rather large secular variation at the time of baking.

The second important point is that despite the drastic chemical alteration to bauxite of the overlying lava, the original direction of magnetization of this lava still remains recorded in the bauxite. It follows that even extreme weathering does not necessarily destroy the original moment of the igneous rock.

Third, it is apparent that some agency has produced a moment in the low temperature regions of Figures 1 and 2, close to the direction of the Earth's present

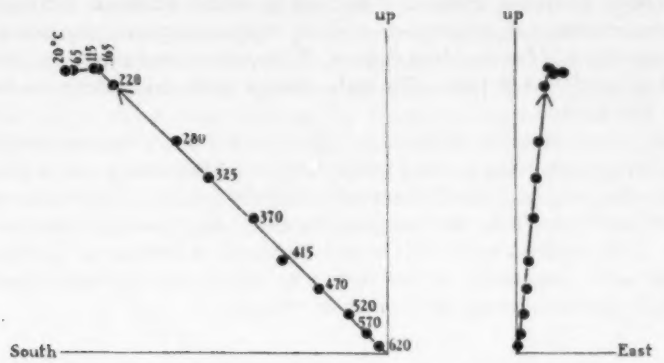

FIG. 3.—Thermal demagnetization of the overlying lava which has been weathered to bauxite. There is little change of direction on heating.

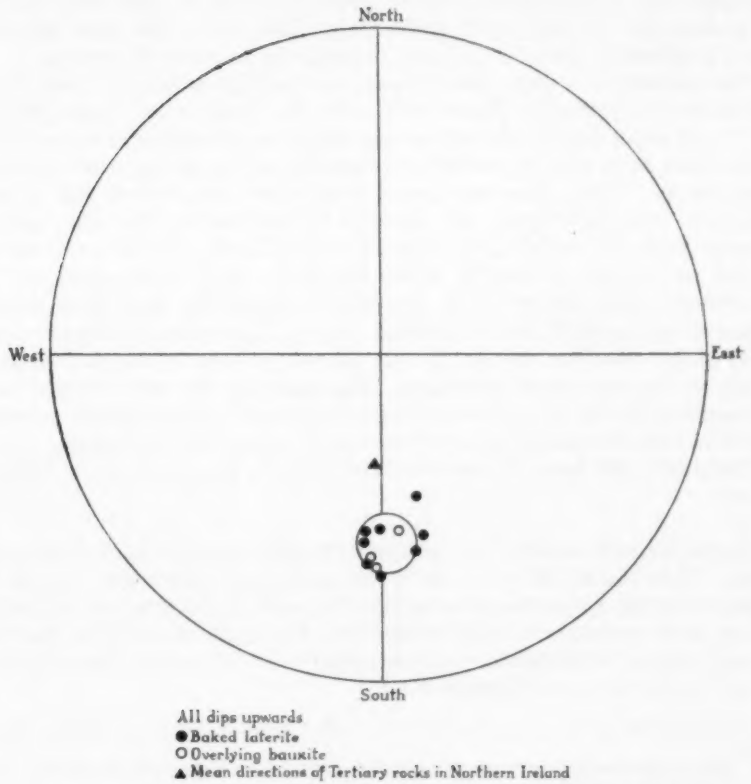

FIG. 4.—A plot of the directions found at high temperatures in eight baked laterite and three overlying bauxite specimens.

dipole field in Northern Ireland. This may be either a viscous remagnetization slowly acquired over some time past, or it may represent a partial thermoremanence due to reheating to a few hundred degrees. Temperatures of 150 °C are commonly achieved at moderate depths of burial. Partial thermoremanence is discussed again in Section 5.

Finally, the curved tail observed in Figure 2 very probably represents viscous remagnetization occurring in the Earth's field in the laboratory over a short time, since this effect can be directly observed simply by placing a specimen under the magnetometer in zero field and watching the decay of its moment even over a few minutes. The mechanism for this is also discussed in Section 5. However, this tail gives some indication of the extent to which viscous magnetization influences the natural moment over weeks or months.

4. The magnetic minerals in the laterite and their properties

Identification of the mineral content of the laterite was made using the techniques of X-ray, thermomagnetic, and electron diffraction analysis.

X-ray powder photographs* showed the lines of clay, of hematite, and also of a face-centred cubic mineral with cell dimensions $5{\cdot}31 \pm 0{\cdot}01$ Å. This cubic mineral could have been either maghemite or magnetite; for while in a pure state they have cell dimensions 5·32 and 5·38 Å respectively, either one might have been considerably altered in size by the Al and Ti impurities known to be present.

The moment of a virgin laterite specimen during heating and cooling in a 3 000 oe field is plotted in Figure 5† (Curve A). This reveals Curie points at 600 °C and about 690 °C, the higher one being less precisely determined. This higher Curie point may be attributed to hematite and hence the lower one to the cubic mineral. While magnetite cannot have a Curie point above 580 °C, maghemite can (Pouillard 1950), and therefore is indicated as this cubic mineral. However, while the 600 °C Curie point does repeat closely, the difference between this and 580 °C could conceivably be attributable to a large systematic error.

Additional confirmation of the presence of maghemite arose from electron diffraction measurements on the laterite.‡ At 113 °K, magnetite undergoes a sudden magnetic transition revealed by the altered deviation of an electron beam passing by the magnetized specimen. Maghemite on the other hand remains unchanged on cooling through this critical temperature. Since a laterite specimen showed no such change, the cubic mineral again behaves like maghemite.

Maghemite and hematite are therefore likely to be the magnetic minerals present.

Maghemite and hematite are cubic and rhombohedral forms of ferric oxide, Fe_2O_3. While the crystal structure of the hematite is very stable, that of the maghemite is only metastable so that at high temperatures it converts spontaneously without chemical change to the hematitic form. One might therefore wonder how the maghemite in the laterite survives heating to 710 °C without change, as the heating and cooling curves in Figure 5 reveal.

* I am indebted to Dr A. L. Mackay and his staff at Birkbeck College for the use of X-ray equipment.

† These measurements were made on a vibrating magnetometer designed by Professor P. M. S. Blackett and D. J. Sutton (1956), but adapted by the author for use with a furnace.

‡ Electron diffraction measurements were kindly done by Professor M. Blackman and his staff, at Imperial College.

Pouillard has shown that pure maghemite converts to hematite near the comparatively low temperature of 400 °C, but that small amounts of aluminium or titanium filling unoccupied sites in the maghemite lattice raise the conversion temperature considerably. Seven per cent of aluminium, for example, raises this temperature above 700 °C, and incidentally lowers the Curie point to about the observed value of 600 °C. Since aluminium abounds in this bauxite region, and also since spectroscopic tests show that both aluminium and titanium are present (about 5–10 per cent), it seems likely that one or both of these elements affect the observed stability of the maghemite against heating to 710 °C.

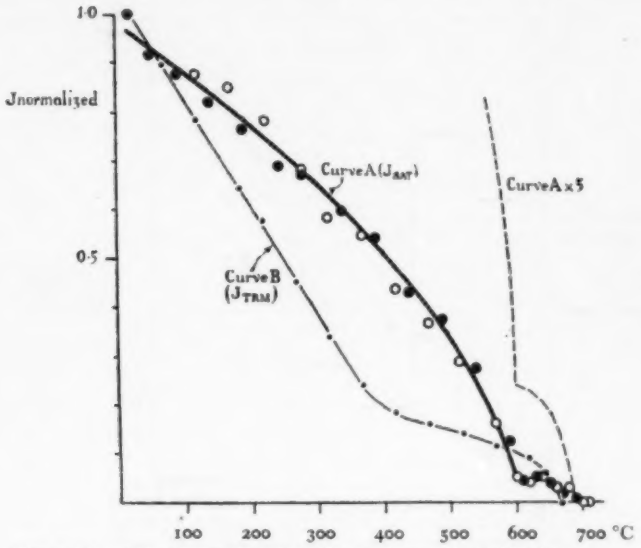

FIG. 5 (A).—The moment of a laterite specimen in a field of 3 000 oersteds, as a function of temperature. The shape and amplitude remain unchanged after heating to 710 °C. Two Curie points are present.

○ heating. ● cooling.

(B).—Thermal demagnetization in zero field of a thermoremanence induced in 0·4 oersteds. The 600 °C Curie point is absent.

An unusual property of the laterite is revealed by contrasting the thermal demagnetization in a 3 000 oe field with thermal demagnetization in zero field of a thermoremanence previously acquired in 0·4 oe (Figure 5). The former curve, which is the same during heating and cooling, shows that a virgin specimen is not changed by heating to 710 °C. It is therefore surprising that the 600 °C Curie point, so evident from the saturation moment, does not appear during demagnetization of the thermoremanence in zero field.

The reason is seen in the distribution of partial thermoremanences which may be acquired in each 100 °C interval from room temperature to 700 °C (Figure 6). There are two concentrations in this distribution. That at higher temperatures lies almost entirely above 600 °C, and must therefore be associated with the hematite. The concentration below 400 °C is very likely due to the maghemite, and shows that in zero field the maghemite was almost completely demagnetized above 400 °C, 200 °C below its Curie point! This is a most unusual phenomenon, and it

is fortunate in that it allows measurement of the natural moment of the apparently stable hematite at any temperature above 400 °C, rather than only above the Curie point of the maghemite, 600 °C.

The association of the maghemite with the low temperature concentration of Figure 6 is strengthened by the behaviour of the laterite after heating to 850 °C. Figure 7 gives the thermal demagnetization curves done in zero field on thermoremanences acquired in 0·4 oe, (A) on cooling from only 700 °C, and (B) on cooling from 850 °C. The steep initial slope of curve A corresponds to the low temperature partial thermoremanences attributed to maghemite in Figure 6. Heating

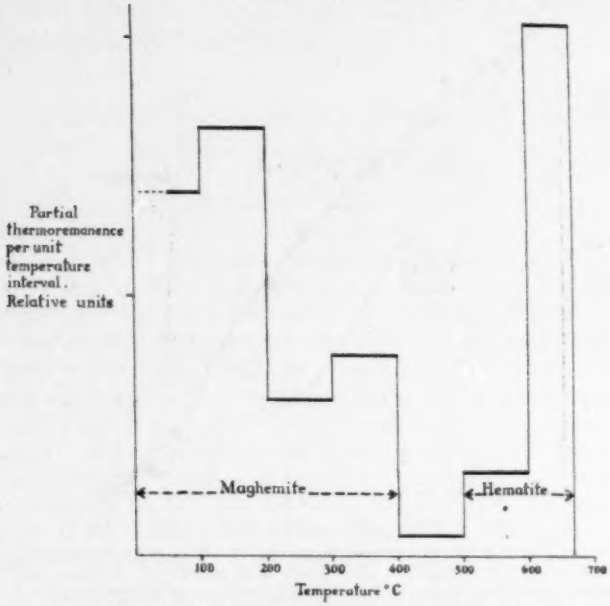

FIG. 6.—The partial thermoremanences acquired by a laterite specimen cooled through various temperature intervals in 0·4 oersteds. All measurements were made at 70 °C, except the lowest range, which was measured at 20 °C.

to 850 °C has destroyed this steep initial slope and has increased the moment at higher temperatures. This may be explained by postulating the conversion of maghemite to hematite at some temperature between 700 °C and 850 °C. These results are consistent with Pouillard's interpretation of different experiments on artificially produced aluminium-stabilized maghemite.

5. The contributions by the maghemite and hematite to the natural moment

An interpretation of the high and low temperature moments demonstrated in Figures 1 and 2 may now be attempted in terms of the minerals present. The hematite undoubtedly contributes to the stable high temperature component of magnetization, since its moment lies entirely in the partial thermoremanence region above 600 °C (Figure 6). The upper region of the broad maghemite distribution

in Figure 6 may also contribute something to this high temperature stable component; but some of the maghemite seems to be contributing to the secondary vector in Figures 1 and 2, since only the maghemite occupies that partial thermoremanence region below 400 °C where the secondary vector is found. Further, the maghemite probably is also the source of the "tail" observed near room temperature in Figure 2.

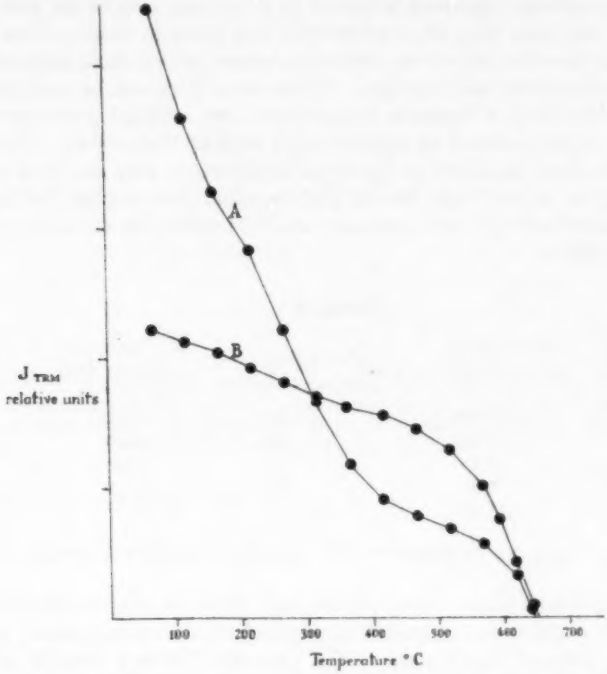

FIG. 7.—Thermoremanence vs. temperature for the same specimen, (A) after cooling from 700 °C, and (B) after cooling from 850 °C, in 0·4 oersteds.

The hematite has therefore been completely stable. The maghemite has either been partly unstable, acquiring over a long time in the present field a large viscous moment which is erased by heating to between 250 °C and 350 °C, or else it has been given a partial thermoremanence by the elevated temperatures to which it may have been heated during burial.

6. The magnitude of the ancient field

Koenigsberger (1938) originally envisaged measurement of the magnitude of the ancient field by considering the ratio of the natural thermoremanence of a rock to the artificial thermoremanence induced by cooling it from above its Curie point in a known field. The general applicability of this procedure is limited by the fact that most rocks change their magnetic behaviour on heating. However, Figure 5 shows that the hematite in the measured laterites does not change on heating, and it appears from Section 4 that it has been stable over geological times.

We may therefore hope to use Koenigsberger's method to find the ancient field

strength, with the proviso that our measurements be restricted to those temperatures embracing only the *stable* part of the natural moment; that is, to temperatures above about 350 °C. To be more certain, 400 °C has been chosen as the lower limit of acceptable measurement.

The intensity of the natural thermoremanence, J_{nat}, of a specimen from 1 inch below the contact is plotted in Figure 8 as a function of temperature above 400 °C. The artificial thermoremancences acquired in 0·13, 0·40, 0·82 oe are also plotted, and it can be seen that they all resemble the J_{nat} curve in shape. This is additional confirmation that there is no magnetic change (except for a slight lowering of the Curie point after each heating). These same data can be replotted as in Figure 9 to show that at constant temperature, the artificial thermoremanence (open circles) is proportional to applied fields smaller than 0·8 oe. The natural intensity (black dots) measured at the same temperatures may therefore be interpolated linearly on these straight lines to find the value of the ancient field strength. The five values deduced for this specimen, and four values for a second specimen, are given in Table 1.

Table 1

	1st specimen		2nd specimen
T °C	Ancient field (oersted)	T	Ancient field
420	0·38$_5$	400	0·43$_5$
470	0·40	450	0·41$_5$
520	0·42	500	0·41
570	0·43	550	0·43
595	0·47		
Mean	0·42 ± 0·03 oersteds	Mean	0·42 ± 0·01 oersteds

These confirm each other within the accuracy of the measurements, and agree fairly closely with the present dipole field strength in Northern Ireland, which is 0·535 oe. The present dipole field at the apparent Tertiary latitude of 43° N (Wilson 1959) is 0·48 oe, so that without many further measurements the small difference between the two dipole field strengths would be indistinguishable because of the secular variation, even if we assume that the field has always had the same dipole strength. It should be emphasized, however, that the *sign* of this derived ancient field strength is *reversed* (see Part II), so that the apparent agreement of the ancient and modern field strengths is not one of sense, but of magnitude only.

7. The ancient temperature of baking

Since the natural moments of the laterite specimens appear to be total thermoremanences (see Figure 8), the lava must have heated the laterite above the hematite Curie point, near 670 °C. This is therefore a lower limit to the temperature of baking. An upper limit is set by the fact (Section 5) that the maghemite converts to hematite between 700 °C and 850 °C. Since the maghemite still is present in the natural state, the overlying lava cannot have raised the temperature high enough to convert it.

The temperature of the baked laterite due to the lava above must therefore have risen to between 670 °C and 850 °C.

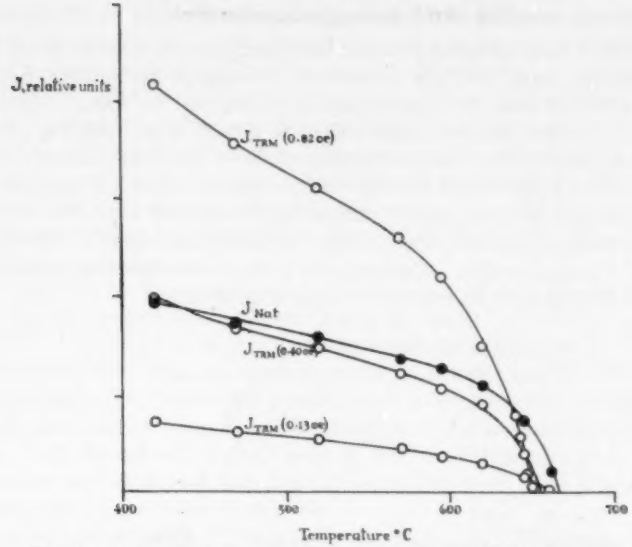

FIG. 8.—Intensity vs. temperature curves for natural remanence and for thermoremanences induced in the same laterite specimen in fields of 0·13, 0·40 and 0·82 oersteds. Temperatures are restricted to the range where the natural moment is stable, above 400 °C.

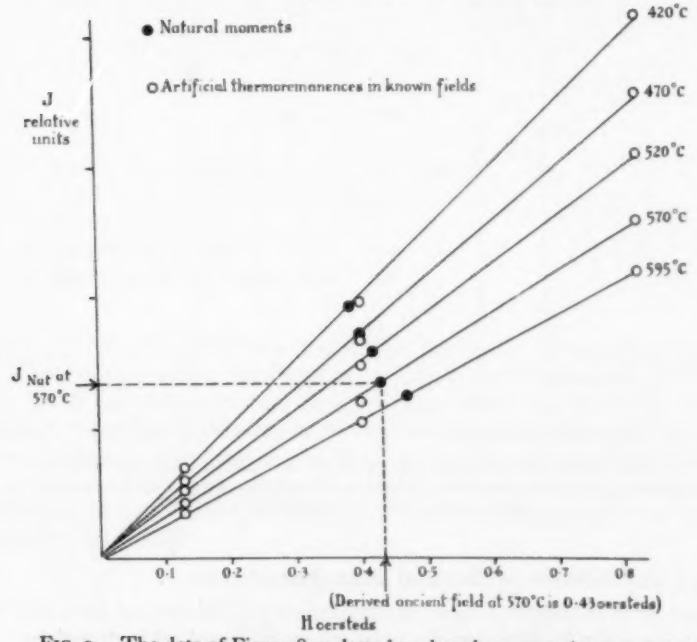

FIG. 9.—The data of Figure 8 replotted to show how, at a given temperature, the natural moment may be compared with thermoremanences acquired in known fields, so as to deduce the ancient field strength. The thermoremanence is proportional to applied field at any fixed temperature for fields up to 0·8 oersteds.

8. Attempts at alternating field demagnetization

If one were able to clean these unstable laterites by means of alternating fields, then this technique could perhaps be used to investigate the ancient magnetic field strength of the Earth, the temperature of baking, or the stable direction of magnetization. However, despite careful efforts to do this, it was found impossible. Figure 10 demonstrates the contrasting results from the two methods of demagnetization, for laterites from another baked contact above the one just described. Alternating fields and heating started to produce the same result for low fields and temperatures, but only the heating eventually resulted in a well-defined, final direction of magnetization. Alternating fields have therefore been abandoned, as far as these laterites are concerned, in favour of heating.

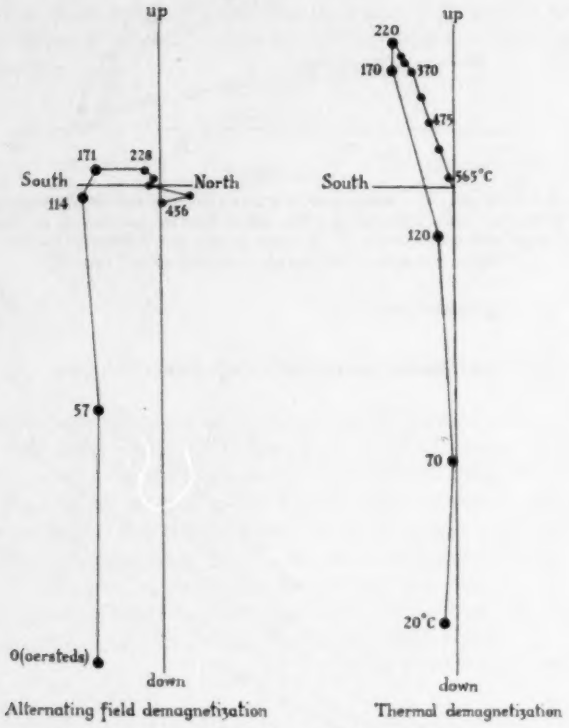

FIG. 10.—Contrast between the effects of alternating field and thermal demagnetization on similar specimens of laterite. Only heating gives a unique direction of magnetization.

9. Future possibilities of thermal demagnetization

Several lavas of different ages investigated in this laboratory have had small scatter, being fairly homogeneously magnetized in inexplicable directions. It is difficult to justify the rejection of these data, although the directions of magnetization of such rocks do not fit into the general pattern formed by the majority of rocks for a given place and period. The reason for these deviations is unknown.

In rejecting these rocks, not knowing what else to do with them, we may be ignoring data which are highly relevant to, say, the movement of continents, or perhaps to the history of the Earth's magnetic field itself.

A powerful and general method of experimental (not statistical) analysis is therefore needed to provide a convincing *criterion of acceptability* for rocks. The author believes that the technique of thermal analysis outlined in this paper may be one such method. Highly unstable Carboniferous lavas have already responded very satisfactorily to thermal cleaning, as have also some of the apparently stable but strangely directed magnetizations mentioned above, and this will be reported in a subsequent paper.

Perhaps just as important is the opportunity this thermal analysis affords of measuring the *strength* of the ancient field of the Earth. Thellier (1959) has already shown how hematite-bearing artefacts can reveal the magnitude of the Earth's field over historic times. But whenever hematite of any age has been baked by a lava or an intrusion, there exists the possibility of a determination of the Earth's field strength as it was at that time. Not only do other hematite-bearing formations similar to the Interbasaltic Layer exist in diverse parts of the world, but also red sandstones may be found, baked by igneous bodies of various ages, though the moments in these cases are quite weak.

If we should indeed find that the Earth's field has always been a dipole field of about the same magnitude as at present, then there is the possibility of deducing the ancient latitudes of the land masses from the field strength, as well as *independently* from the magnetic dip of the rocks, using the relations:

$$H = \frac{P}{r^3}\sqrt{(4-3\cos^2\lambda)} = 0{\cdot}31\sqrt{(4-3\cos^2\lambda)}$$

and

$$\tan I = 2\tan\lambda$$

H = field strength at the surface of the earth
P = mean dipole moment of the Earth
r = radius of the Earth
λ = geographic latitude
I = dip of Earth's magnetic field.

Such a double check is extremely desirable in any field of physics, and especially in an historical field where the object of enquiry cannot be measured directly. A further advantage of field strength determination would be that the correlation of the ancient magnetic dip with the ancient field strength could be made on a single diagram, independently of the ages of the rocks or their present geographical position. In this way, data from all over the world could contribute to one single plot relating dip and field strength, which could then be compared with the curve for the present dipole field

$$H = \frac{2P}{r^3\sqrt{(1+3\cos^2 I)}} = \frac{0{\cdot}62}{\sqrt{(1+3\cos^2 I)}}$$

to decide whether the field has remained essentially constant or not over geological times.

Finally, any quantitative information about ancient field strengths, both in magnitude and sign, must contribute to theories of the generation of the Earth's magnetic field.

Department of Physics,
Imperial College of Science and Technology,
London S.W.7:
1960 *August* 16.

References

Blackett, P. M. S. & Sutton, D. J., 1956. *Lectures on Rock Magnetism* (Weizmann Science Press of Israel).
Blundell, D., 1957. Thesis, Imperial College, London.
Brynjolfson, A., 1956. *Naturwiss.*, **7**, 154.
Brynjolfson, A., 1957. *Advances in Physics*, **6**, 23, 247.
Cox, A. 1957. *Nature* (*London*), **179**, 4561, 685.
Creer, K., 1958. *Ann. Geophys.* (*Paris*), **14**, 3 (July–Sept.).
Creer, K.. 1959. *Geophys. J.*, **2**, 261–275.
Eyles, V. A., 1952. *Mem. Geol. Survey—Composition and Origin of the Antrim Laterites and Bauxites.*
Koenigsberger, J., 1938. *Terr. Mag. and Atm. Electricity*, **43**, 119–130 and 299–320.
Leng, J., 1955. Thesis, Imperial College, London.
Pouillard, E., 1950. *Ann. Chem.* (*Phys.*), **5**, 164–214.
Rimbert, F., 1959. *Revue de l'Inst. Fr. du Petrole et Annales des Combustible Liquides XIV*, **1** and **2** (Jan. and Feb.).
Thellier, E., 1941. *C.R. Acad. Sci.* (*Paris*), **213**, 59–61.
Thellier, E., 1946. *C.R. Acad. Sci.* (*Paris*), **222**, 905–907.
Thellier, E., 1959. *Ann. Geophys.* (*Paris*), **15**, 3.

Palaeomagnetism in Northern Ireland

Part II

On the Reality of a Reversal of the Earth's Magnetic Field

R. L. Wilson

(Received 1960 December 3)*

Summary

A large variety of evidence is presented concerning reversal of the Earth's magnetic field during the Tertiary igneous activity in Northern Ireland. Different magnetic minerals, which acquired their natural moments in different ways, all support the reality of a field reversal, as opposed to self-reversal of the rocks in a normal field.

1. Introduction

In a recent paper (Wilson 1959), the author published the results of palaeomagnetic measurements on sixty-five different Tertiary lavas, dykes and sills covering a wide area of North-eastern Ireland. This work included and extended the work of Hospers & Charlesworth (1954) in the same area. All these rocks were magnetized in a direction opposite to that of the present magnetic field, the mean direction being 187° east of true North, and 62°·4 up. This suggested that the Earth's field might actually have been reversed during the period when these igneous rocks were formed. The question of the reality of such apparent field reversals, though often discussed, is still open to doubt. It could be, for example, that all sixty-five of these igneous bodies are in fact self-reversed, due to some physico-chemical mechanism which is so subtle that it escaped our notice.

One method of attacking this problem is to carry out for the case of *one particular apparent reversal* a great variety of independent experimental examinations of widely differing rock types which have also become magnetized by different mechanisms, such as thermoremanence or chemical remanence. The purpose of this paper is to present such a variety of evidence concerning the Tertiary reversed rocks in Northern Ireland.

The experiments, besides comprising straightforward measurements on igneous rocks, leaned heavily on baked contacts as evidence of reversal. Thermal demagnetization was used both to remove secondary moments from some of these rocks and, in one case, to reveal the partial thermoremanence in laterite near a particular "cool" contact.

* Received in original form 1960 August 23.

2. The various evidences

Subsections 2.1 to 2.4 discuss rocks which were magnetically stable and required measurement only at room temperature.

(2.1) *The Tertiary lavas and intrusive rocks of Northern Ireland*

The first evidence is the directions of natural remanence found in the Tertiary igneous rocks themselves. Sixty-five basalt lavas, dykes and sills consisting of

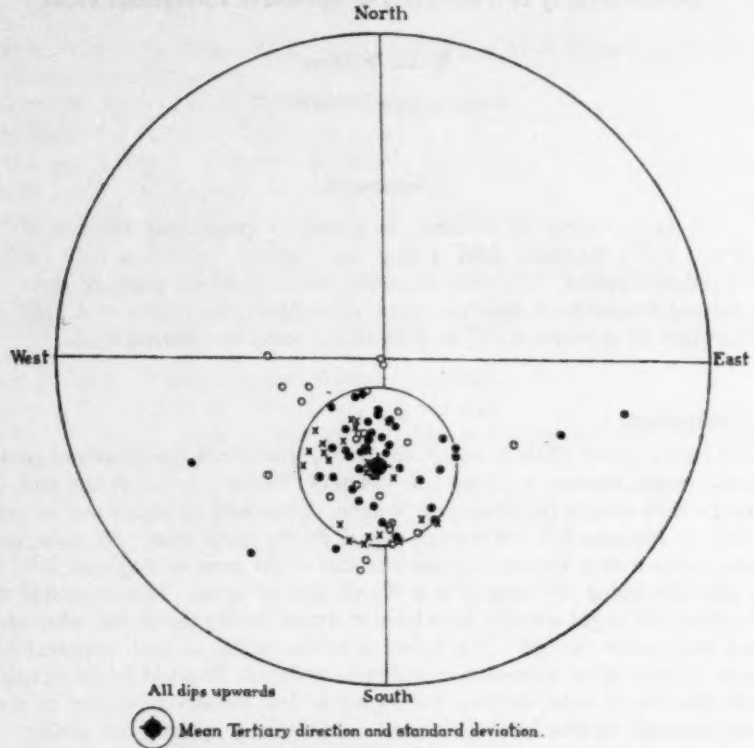

FIG. 1.—Directions of magnetization of all the Tertiary rocks from Northern Ireland.

various types of basic rock, particularly olivine and tholeiitic basalts, were *all* reversely magnetized (Figure 1 and Table 1). These were collected over a continuous range of about seventy miles, and their time span includes all the remaining Tertiary igneous rocks in Northern Ireland. Even those few samples, which were rejected because the standard deviation of several specimens from the samples exceeded 10°, showed reverse directions.

Table 1

Rock group	Mean Declination East of North	Mean Dip	$\mathcal{N}$	N	n	R	$\delta°$	$\epsilon°$
Hosper's lower basalts	194	−60·2 (up)	24	72	120	23·253	14	2·9
Lower basalts	173	−64·6	19	35	70	17·599	22	5·5
Upper basalts	206	−62·2	6	7	14	5·723	17	7·1
Intrusions	184	−63·3	16	25	49	15·268	17	4·4
Non-igneous	191	−62·3	24	—	—	22·282	22	4·5
Combined results	188	−62·8	89	173	277	83·938	19	2·0
Reverse of present dipole field	180	−70·8					15*	

$\mathcal{N}$ = Total number of measured distinct igneous bodies in group
N = number of separate samples from the $\mathcal{N}$ bodies
n = number of independent specimens measured
R = resultant of $\mathcal{N}$ unit vectors
δ = standard deviation for a single reading = $\cos^{-1}(R/\mathcal{N})$
ϵ = standard deviation of the mean of $\mathcal{N}$ vectors = $\delta/\sqrt{\mathcal{N}}$.

* Vestine (1947) has noted that the present Earth's field, if measured at a large number of places on the Earth's surface, varies in direction from the ideal dipole field with a standard deviation of about 15°.

(2.2) *Non-igneous rocks of Northern Ireland*

The top few inches or feet of many of the flows all over this area have been laterized prior to the deposition of the subsequent flow, as was described in Part I, Section 1. That is, they now consist essentially of ferric oxides in clay. Close to the contacts this has been baked and consequently has a thermoremanence. Farther away it has not been so strongly heated and has a remanence perhaps similar to that found in unbaked chemically magnetized red sandstones. Twenty-four such non-igneous samples were accepted because their directions lay within two standard deviations (44°) of their own mean direction. These data are included as hollow circles in Figure 1, and are also in Table 1. They were all reversed, and their mean direction agreed with that of the igneous rocks to within *two degrees*.

(2.3) *Baked limestone from near Portrush*

A large volume of limestone near the pier at Portrush has been strongly heated by a nearby intrusion of Tertiary dolerite. The Curie point of the magnetic mineral in the limestone is 590 ± 15 °C, so that it is probably fairly pure magnetite. Five specimens cut from three separately oriented samples had directions of natural remanence shown in Figure 2 as black dots. Not only is the mean direction of the limestones consistent with the directions of the Tertiary rocks discussed in (1), but the scatter of the limestone directions is much smaller than the standard deviation for those rocks as a whole. This is an indication that the scatter of the limestone directions is due only to experimental error, and therefore that they represent fairly well the direction of the field at the time of baking; at least its axis if not its sense. The limestones themselves are reversely magnetized.

(2.4) *A multiple baked contact from Scrabo Hill*

An especially useful case of baking was found at a sandstone quarry at Scrabo Hill, near Belfast. Here, a sill is intruded into Triassic sandstone. This sill has in turn been cut by a dyke. All three, the sill, the dyke, and the sandstone have been baked strongly by a large Tertiary intrusion which now forms the top of Scrabo Hill. Further, the original hematite in the Triassic sandstone has been

reduced to magnetite (presumably by the intrusion) over a large region, and so is strongly magnetic. Directions of specimens from the sill, dyke and sandstone, are plotted in Figure 2 as hollow circles, and they all agree, again with a small enough scatter to be attributable to experimental error only. This agreement is again good

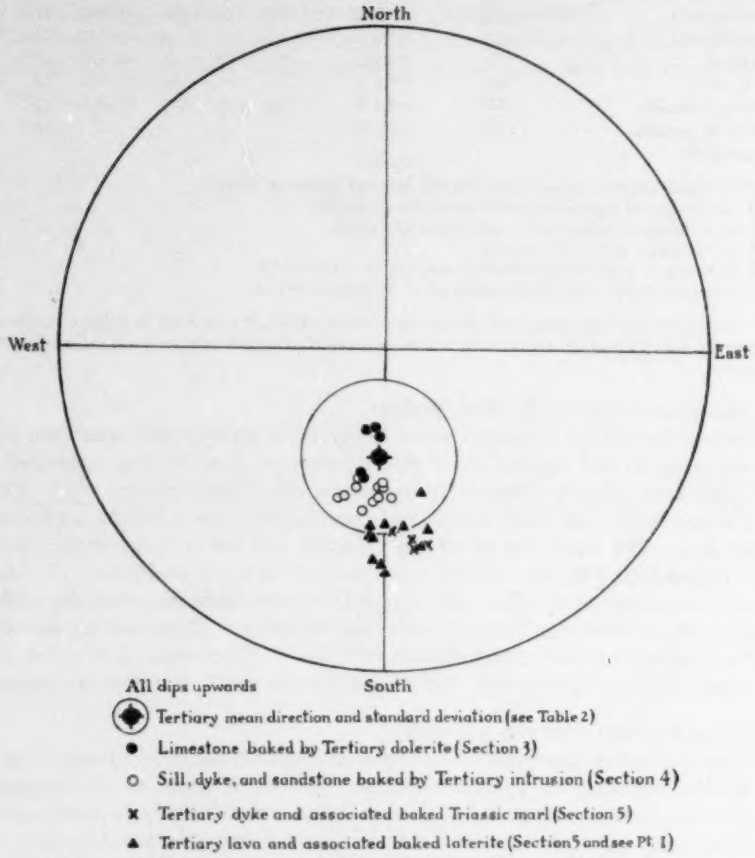
North
West
East
South
All dips upwards
Tertiary mean direction and standard deviation (see Table 2)
Limestone baked by Tertiary dolerite (Section 3)
Sill, dyke, and sandstone baked by Tertiary intrusion (Section 4)
Tertiary dyke and associated baked Triassic marl (Section 5)
Tertiary lava and associated baked laterite (Section 5 and see Pt. I)

FIG. 2.—Plot of directions of magnetization mentioned in Sections 3, 4 and 5.

evidence that the direction is that of the ancient field at the time of baking. All three formations have reversed directions and in addition no sign of self-reversal was found during heating of the natural moment of the sandstone.

We now consider in subsections 2.5 to 2.8 some more specialized results, which are derived from magnetic measurements made on rocks at high temperatures as described in Part I.

(2.5) *Two baked contacts requiring thermal "cleaning"*

The agreement of the direction of magnetization of an igneous body with that of the associated baked material provides quite strong evidence for the direction

and sense of the applied field during baking. With this in mind, two further baked contacts were investigated; one a Tertiary dyke baking Triassic marl, the other the basalt baking laterite, which was the subject of Part I. The dyke, the baked Triassic marl, and the baked laterite had all badly scattered directions of magnetization, their standard deviations being in excess of 25°. The high weathered basalt lava was not so badly scattered. The *high temperature* directions of magnetization of all these rocks were not badly scattered, however, and these are plotted in Figure 2, crosses representing the dyke and associated baked marl, triangles representing the basalt lava and associated baked laterite. All these directions were reversed, and the scatters in both cases have been reduced to the experimental error one would expect from the technique of measurement.

During these heatings, no specimen at any temperature showed the slightest tendency towards self-reversal, such as has sometimes been found in reversely magnetized rocks. In fact, it was shown that the natural thermoremanence of the baked laterite could be reproduced in the laboratory to establish the magnitude of the ancient field. This reproducibility could hardly be expected of a specimen which was somehow self-reversed, without that self-reversal manifesting itself.

(2.6) *An attempt to produce self-reversal in the laboratory*

In only one instance was any indication of self-reversal observed. A core was measured from the unweathered lava which heated the laterite to be discussed in 2.7 and 2.8. Thermal demagnetization of the *natural* moment showed no hint of self-reversal, and revealed a natural Curie point at about 350 °C. A much smaller component in precisely the same direction persisted up to about 570 °C. After heating to 600 °C, a thermoremanence was produced by cooling in 0·4 oe, and reheating showed that a large quantity of mineral with a Curie point at 565 °C had been formed during the heating. Further, during the reheating, this thermoremanence *increased* by 8 per cent at 150 °C, and then decreased regularly to zero at 565 °C, indicating a partial reversal at low temperatures. By an application, during cooling, of 0·4 oe at high temperatures and zero field below 400 °C, this partial reversal could be increased to 23 per cent of the maximum intensity. A full reversal of sign could not be accomplished.

It is clear that the rock after heating to 600 °C in the laboratory was no longer the same as before, but the hint of reversal nevertheless introduces a note of caution.

(2.7) *Partial thermoremanence in a baked laterite*

The purpose of this section is to present what appears to be a case of partial thermoremanence as a point in favour of a reversal of the Earth's field. The investigation concerns the baked contact immediately above the contact described in Part I. Again, laterite is the baked material, but the overlying lava is this time in an unweathered state.

The first question to be discussed is that of the temperature of baking of the laterite near the contact. Two phenomena besides the partial thermoremanence indicate a lower temperature of baking than was found for the contact below.

First, the baked material has not at all been disrupted, as other contacts often have been by the gushing lava. The position of the contact between the lava and an underlying thin layer of blackened plant remains can be determined to within less than one mm. This possibly indicates that the lava was cool enough to flow slowly and viscously. It is 70 ft thick here as opposed to 30 ft thick two miles

away, where the same contact is very disrupted and indeterminate. It may therefore have piled up so thick here as a result of high viscosity at low temperature.

Second, the laterite below this contact, in contrast with other baked laterites at lower levels, is a dark brown colour; but when heated in the laboratory to only 550 °C it becomes an orange-red precisely like the lower baked laterites. It therefore seems probable that 550 °C was never reached near this contact.

With these observations in mind, the magnetic evidence for a low temperature of baking will be discussed.

Maghemite and hematite are present in this laterite, but the maghemite is in such relative abundance and is so strongly magnetic that it outweighs magnetically the hematite. The Curie point of the maghemite is slightly above 600 °C, and investigations in both low and high fields show that no other Curie point is observable. It was found experimentally that by heating the laterite to any temperature between 20 °C and 600 °C, a corresponding portion of the initial remanence could be erased. Cooling in some field substituted a new partial thermoremanence in place of the erased moment. Reheating then revealed the superposition of the partial thermoremanence on the older remanence. Hence if the lava above did heat this laterite to such an intermediate temperature, one would expect to find a partial thermoremanence in the natural moment.

Accordingly, the natural moments of specimens from various distances below the contact were observed during thermal demagnetization. As with laterites in Part I, the natural moment had always a low temperature component closely parallel to the Earth's present field, which was practically erased by heating to 220 °C.

Figure 3 shows the behaviour of a specimen from 9 inches below the contact at temperatures above 220 °C. The change of natural moment with temperature has a sharp discontinuity of direction or an elbow at about 450 °C. Several other specimens from various distances below the contact showed similar elbows, the temperatures of which are plotted in Figure 4, as a function of distance from the contact, along with the estimated errors. It must be emphasized that while the five specimens closest to the contact have well-defined elbows and large low temperature branches as shown in Figure 3, the specimens farther than 10 in. away showed progressively smaller effects until, about 2 ft away, the elbow was practically indistinguishable from experimental error. Indeed, not all of the distant specimens showed convincing elbows, and only the data from those which did has been plotted in Figure 4. An elbow in a specimen 17 in from this contact is evident in the right-hand plot of Figure 10 of Part I.

The directions of the high temperature branches for fifteen different laterite specimens are plotted in Figure 5. They are quite widely scattered (see 2.8), yet despite this the low temperature branches all point South and upwards in qualitative agreement with the direction of magnetization of the flow above (177° East of North, 62° up). The more distant specimens showed this as a small but usually observable tendency of the moment to swing South and up. It follows that the low temperature directions are independent of the high temperature directions.

The only hypothesis which has been found to explain these phenomena is the following:

The upper lava, perhaps being cool enough to have practically come to rest, was gently deposited upon the laterite. The maximum temperature reached at the contact interface was about 475 °C, and this decreased regularly to 375 °C 20 inches from the contact (Figure 4); the gradient being about 5 °C per inch. The

laterite, which previously bore a reversed, but somewhat scattered natural moment, had this partly removed by the heating, and then gained a partial thermoremanence along the ambient field as it cooled. This can now be erased by reheating to the maximum temperature originally reached at any point in the laterite. We know this to be physically possible because the partial thermoremanence mechanism can be directly demonstrated in the laboratory.

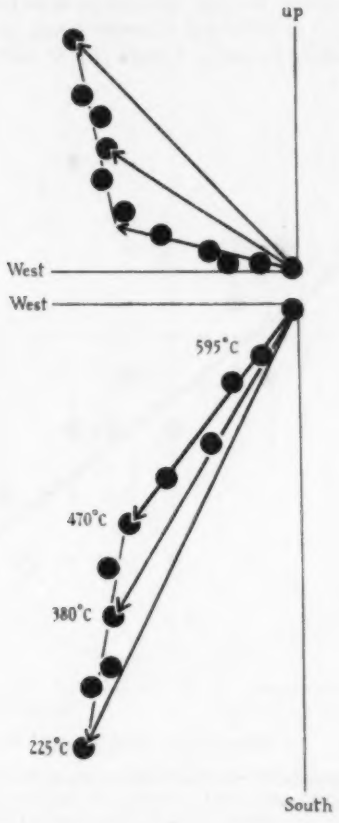

FIG. 3.—The thermal demagnetization of a laterite specimen from 9 inches below a "cool" lava. Two vector directions are separated by the heating.

If this hypothesis be accepted, then the essential feature concerning our main problem of field reversal is that all the partial thermoremanences are directed opposite to the present Earth's field, regardless of the maximum temperature at which they become completely erased.

Further arguments concerning reversal, based on the above evidence and interpretation, may now be discussed:

(a) The natural moment of the lava above and the partial thermoremanences it induced in the laterite below are both reversed, a point which has already been used to support field reversal, without reference to laboratory tests.

(b) All laboratory tests indicate that the impure maghemite in the laterite is at the present time a single and simple substance with a unique Curie point and with no tendency to self reversal. In opposition to this, it may then be argued that some reversal mechanism has been lost without trace.

Néel (1951) has postulated several two-component reversal mechanisms. Ion exchange could also cause self-reversal (Gorter 1954), as could Graham's (1953) oxidation mechanism. More recently, Uyeda (1958) and Carmichael (1960) have

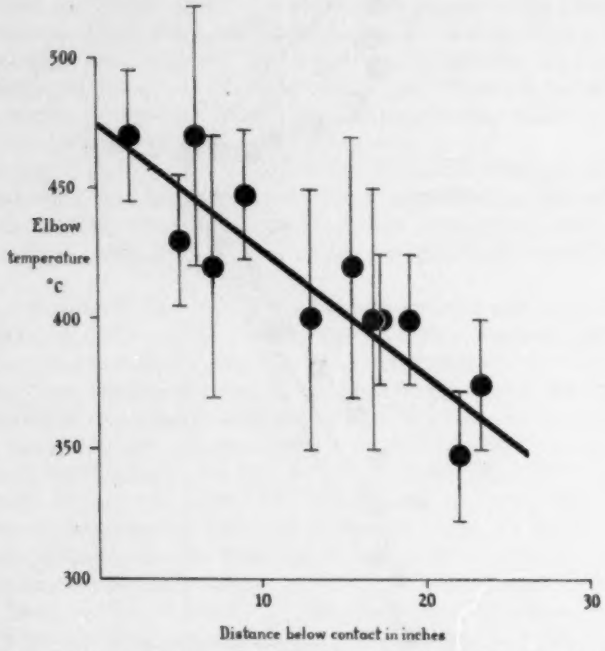

FIG. 4.—The temperatures at which elbows occur in the natural remanences of laterite specimens, as a function of distance from the contact.

demonstrated complete or partial self-reversals probably involving exchange coupling in members of the ilmenite–hematite series $x\mathrm{FeTiO_3} \cdot (1-x)\mathrm{Fe_2O_3}$, for values of x near to 0·6 and 0·1.

It is practically impossible to establish that no such reversal mechanism has operated, and subsequently has been obliterated by some magnetic or chemical change. But the continued survival of the partial thermoremanences and elbows (Figure 3) argues rather strongly that no such drastic change can have taken place at all, and that the maghemite is now as it was just after baking. Since we cannot observe any reversal properties now, it follows that the hypothesis of the Earth's field reversal is supported by the reversed partial thermoremanences.

(2.8) *Reversal in the pre-baking high temperature moments of* (2.7)

Turning to the high temperature branches of the partially baked laterite specimens discussed in 2.7 (see Figure 3), we may examine the bearing their mode of origin has on the issue of reversal. Fifteen cores of laterite were measured at high temperature, and the directions of their pre-baking moments are plotted in Figure 5. Although scattered, these directions certainly are reversed, for only one of them is closer to the Earth's present field direction than to its reverse.

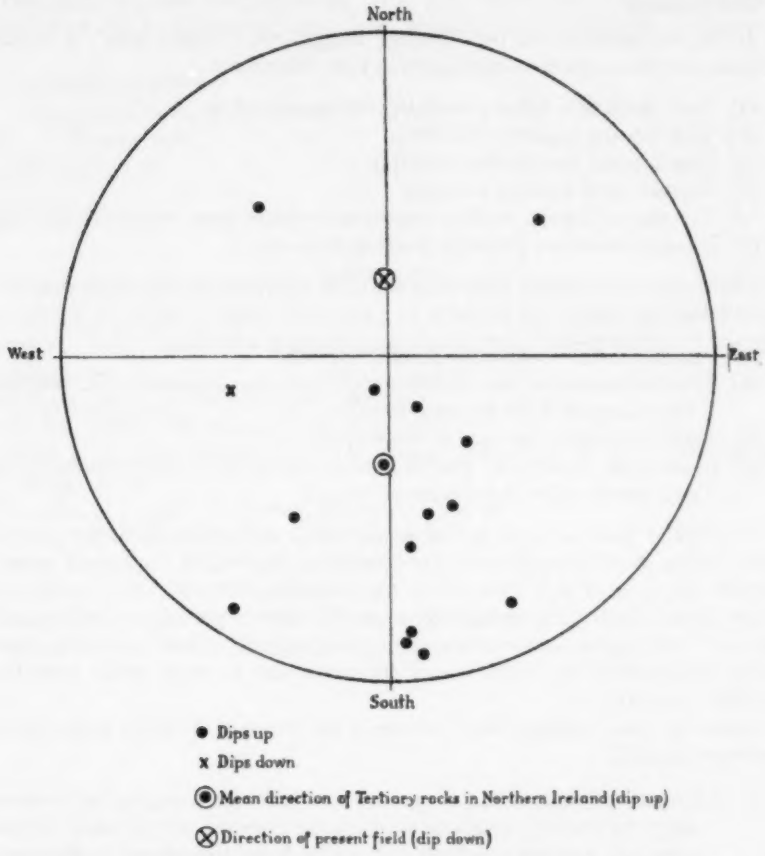

FIG. 5.—High temperature remanence directions for fifteen cores of laterite.

These high temperature moments cannot be thermoremanences; for the maghemite is a secondary mineral and was not present when the hot lava from which the maghemite derives was deposited; nor was the maghemite heated enough by the overlying lava to produce these high temperature moments (Section 2.7); and since we may still observe the partial thermoremanences in the laterite, no significant subsequent heating can have occurred. The mode of origin must therefore be other than thermoremanent, perhaps chemical (Haigh 1958, Kobayashi 1959).

However, the essential idea is that the low temperature remanence in the maghemite is a partial thermoremanence, while the high temperature remanence *in the same material* is necessarily of entirely different origin, whatever that may have been. The fact that both modes of magnetization in the same material have led separately to reversed moments contributes further to that variety of evidence we are seeking, and strongly supports field reversal.

3. Conclusions

In this investigation of the reversely magnetized Tertiary rocks of Northern Ireland, several magnetic materials have been examined:

(a) Basic lavas and dykes containing titanomagnetites.
(b) Clay bearing hematite (laterite).
(c) Clay bearing maghemite (laterite).
(d) Triassic marl bearing hematite.
(e) Triassic sandstone bearing magnetite (reduced from original hematite).
(f) Jurassic limestone probably bearing magnetite.

These various materials have been found in different combinations magnetized in the following ways:

(a) Original thermoremanence in igneous rocks.
(b) Thermoremanence due to baking of: hematite, magnetite (in sandstone), titanomagnetite (in igneous rocks).
(c) *Partial* thermoremanence in maghemite.
(d) Remanence in unbaked laterite, which may be chemical remanence but in any case is not a thermoremanence.

The baked rocks always agreed in direction and sense with the associated baking rocks, even in complicated combinations. Heating of the natural moments revealed no signs of self reversal in any material, although one lava specimen having altered chemically on heating to 600 °C, showed partial reversal on cooling in 0·4 oe. The natural remanence of every rock here described was opposed to the present direction of the Earth's magnetic field, and no other rocks were found normally magnetized.

There are three possible explanations of the reversed Tertiary rocks found in Northern Ireland:

(a) All these different rocks, magnetized in different ways, are self-reversed, while the Tertiary magnetic field was then normal as it is today. The self-reversing properties of all the rocks have subsequently disappeared completely.
(b) Some of these rocks are self-reversed, and others not, while the Tertiary magnetic field was alternately reversed and normal in such a way that all of the rocks ended by being reversely magnetized. It may be argued that a correlation could exist between the sign of the Earth's field and the type of rock (self-reversing or not) extruded. However, this cannot explain the reversed magnetization of baked rocks which have been formed at any time prior to the baking.
(c) None of the rocks are self-reversing, and the Tertiary magnetic field was reversed during the entire time span investigated.

In view of the variety of evidence presented, the first and second interpretations seem highly improbable, while the second and third both support the reality of reversal of the Earth's magnetic field in Tertiary times. It is reasonably certain that the Earth's field was reversed during the long period of Tertiary igneous activity in Northern Ireland.

Acknowledgments

The author is grateful to Professor P. M. S. Blackett, Dr J. A. Clegg, Dr C. W. F. Everitt, Dr P. H. S. Stubbs and Mr G. W. Massé for their help with this work.

Department of Physics,
Imperial College of Science and Technology,
London S.W.7:
1960 *August* 16.

References

Carmichael, C., 1960. Thesis, University of Western Ontario.
Gorter, C., 1954. *Saturation Magnetization and Crystal Chemistry of Ferrimagnetic Oxides.*
Graham, J., 1953. *J. Geophys. Res.*, **58**, 243.
Haigh, G., 1958. *Phil. Mag.*, **3**, 27, 267 (March).
Hospers, J. & Charlesworth, H. A. K., 1954. *Mon. Not. R. Astr. Soc. Geophys. Suppl.*, **7**, 32.
Kobayashi, K., 1959. *J. Geomag. Geoelect.*, X, **3**, 99.
Néel, L., 1951. *Ann. Geophys.* (*Paris*), **7**, 90.
Thellier, E., 1959. *Ann. Geophys.* (*Paris*), **15**, 3.
Uyeda, S., 1958. *Jap. J. Geophys.*, II, **1**.
Vestine, E. & others, 1947. *Publ. Carnegie Inst.*, No. 576.
Wilson, R., 1959. *Phil. Mag.*, **4**, 42, 750 (June).

Report on Progress in Geophysics

Palaeomagnetic Directions and Pole Positions, Part III

Pole numbers 3/1 to 3/87

Compiled by E. Irving

(Received 1960 December 28)

The results are presented as a table with 20 columns. The detail given in originals is not always sufficient to allow entries in all columns. The first 10 columns give geological information and information about sampling, columns 13–16 give the results of a statistical analysis of the observed directions of magnetization, and columns 17–19 give an interpretation of the results of this analysis in terms of an assumed model of the Earth's field.

Columns, 2, 3 and 4. Identification numbers are entered in column 2. The letter (m 1), (m 2), etc. following a number indicates that the result is a modification of a previous result. Information about the rock unit from which the pole determination has been made is given in columns 3 and 4. Its geological age is specified by these period symbols: Quaternary Q, Tertiary T, Cretaceous K, Jurassic J, Triassic $\mathfrak{T}_R$, Permian P, Carboniferous C, Devonian D, Silurian S, Ordovician O, Cambrian ϵ, and Pre-Cambrian Pϵ. Subdivisions of periods from Cambrian to Cretaceous, where recognized, are denoted by u, m or l. Epochs within the Tertiary (Palaeocene, Eocene, etc.) are denoted by Tpa, To, Tm and Tp. The Quaternary is divided into Recent Qr, and Pleistocene Qp. Subdivision of the Pre-Cambrian is not attempted. The symbols given in column 3 refer to the *geological* age of the rock unit studied and not necessarily to the period at which the magnetization was acquired, unless evidence (noted in particular in column 9) is described in the original which allow it to be reasonably supposed that the directions of magnetization were acquired at the time the rock unit was formed. Many rock units have acquired their magnetization long after the time of their formation and where authors have estimated the probable "magnetic age" this is entered in brackets after the geological age. Where possible, a distinction is made between a collecting *site* which is thought of as the particular place (say a quarry) from which a sample is collected, and a collecting *locality* which refers to a more general area (for example, a canyon section) which may comprise several sites at different stratigraphic levels. The variation in sampling schemes used by different workers does not always allow this distinction to be made.

Columns 5, 6, 7 and 8. The thickness of the rock unit which has been sampled is given in column 5 and in column 6 the spread of sampling localities (or sites) is indicated either as an area, or as a distance between extreme localities in those cases where the localities are few or are distributed along a zone rather than over an area. Pieces of rock, separately oriented, are referred to as samples, and from

them one or more specimens are usually cut. The numbers of these samples and specimens are entered in columns 7 and 8. The distinction between samples and specimens has not always been made in originals, and in cases of doubt the entry is made in column 7.

Column 9. Stability tests, where made, are noted in column 9. The tests are of six main types which are identified by these abbreviations; conglomerate *cg*, fold *fd* and igneous contact work *ct*, and thermal demagnetization *th*, alternating field demagnetization *ac*, and steady field demagnetization *dc*. The presence of reversals in the same rock sequence is a strong argument in favour of stability and this information is recorded in columns 11 and 12. Remeasurements of specimens after storage, and deviation tests (deviations from the present Earth's field) are less critical and are not mentioned. Presumptive evidence relevant to stability is obtained from studies of the variation of saturation magnetization with temperature and of certain ratios such as the Koenigsberger ratio, but although important in other respects this evidence is indirect and is not mentioned here.

Column 10. In most cases, denoted by *nt* in column 10, results have been obtained from measurements of the direction of the natural remanent magnetization. Sometimes the specimens have been partially demagnetized to remove the secondary components and these cases are denoted by *ac* (alternating field demagnetization) or *th* (thermal demagnetization).

Columns 11 and 12 give the percentage of positive and negative polarizations recorded. The convention is to regard the field as negative (positive) when the pole towards which the north (south) seeking magnetization points is in the present-day northern hemisphere. This convention leads to ambiguities in the Pre-Cambrian but is generally suitable for comparative purposes in younger rocks. These "polarity ratios" are approximate only.

Columns 13 and 14 contain estimates of the mean direction of magnetization. The declination D_m is reckoned clockwise east from geographic north, and I_m, the inclination, is regarded as negative if the direction is upwards and positive when below the horizontal. For rock units in which the beds are undisturbed the horizontal is the present day horizontal, but if the beds have been tilted the horizontal is assumed to be the bedding plane which, in the case of igneous rocks, is obtained from adjacent sediments. The D_m and I_m values are in parenthesis for those cases in which it is considered in the original that the magnetization post-dated considerably the time of formation; the directions in these cases are given relative to the present day horizontal plane and irrespective of deformation of the beds. The absence of parenthesis must not, of itself, be taken to imply that the magnetization originated at the time of deposition.

Columns 15 and 16. These columns contain estimates of the precision of the observations and the error in the mean. Unless otherwise stated in footnotes these values have been obtained using Fisher's Analysis (Fisher 1953); the precision is an estimate, k, of Fisher's κ and describes the distribution of points about the mean direction (D_m, I_m). The error angle, a, is the half-angle of the cone whose axis is the direction (D_m, I_m) and within which the true mean lies with a probability of 95 per cent. The precision and error are not always comparable as between different entries, since they have been calculated using differing schemes for weighting according to the number of specimens, samples and collecting sites and according to variation in the within-sample k_s, within-site k_w, and between-site k_b precision. The procedures used are indicated in footnotes where adequate information is available in the original.

In *columns 17 and 18* the northern hemisphere co-ordinates of the palaeomagnetic poles are given. The errors $d\phi$ and $d\chi$ are the semi-axes of the elliptical error area round the pole at a probability of 95 per cent, $d\phi$ in the co-latitude direction and $d\chi$ perpendicular to it. Pole positions are given only in those cases where they are given in the original, or, in those cases where results have been obtained from a large body of data for which the sample stability and coverage is adequate. Pole positions are not given where there is evidence for supposing that the magnetization occurred after deposition (at some known or unknown time) unless the original author chose to interpret his results in this way. If for any reason pole positions are required for these latter entries the data necessary for calculating them are in the list.

Notes on the interpretation of palaeomagnetic directions. It has been common practice in the past six years to interpret palaeomagnetic results from a rock formation in a particular region in terms of the position of the Earth's dipole axis relative to that place at the time the formation was laid down. One procedure is to assume that the region in which the rock formation is found is fixed relative to the present geographic coordinates and to obtain the palaeomagnetic poles (or points at which the axis cuts the Earth's surface) of the geocentric dipole axis in these coordinates. This may be done by calculation (Creer & others 1957) or graphically (Graham 1955). An alternative procedure is to consider the Earth's dipole field as fixed and to calculate the position, relative to this, of the region in which the rock formation is found (Clegg & others 1954, Irving 1957, Creer & others 1958, Blackett & others 1960). The past position of the region is defined by the ancient latitude and longitude and by an angle defining the rotation relative to the present meridian. Only the colatitude and rotation are obtained directly from any single mean direction (D_m, I_m), the longitude being indeterminate; however using many results from different continents and with certain restrictions (the most important one being a limitation of the movements to a minimum) an approach to the problem of determining ancient relative longitudes can be made (Creer & others 1958, Irving 1958). The ancient colatitude, λ, is given from the relationship $\cot \lambda = \frac{1}{2} \tan I_m$ and may be readily obtained from column 14. The rotation is measured by the angle between the horizontal component of the mean direction and the present meridian and may be obtained from column 13. Whichever procedure is used the same three basic assumptions are necessary:

(1) that the directions of magnetization observed in the rock formation are the directions of the Earth's magnetic field at the time the rock was laid down,

(2) that throughout geological time the Earth's main field (after averaging out the secular variation) has approximated to a geocentric dipole, and

(3) that in the samples studied the secular variation has been averaged out. (The time needed to achieve this is not known with certainty but under present conditions it is not less than about 10^3 years and is not likely to be more than about 10^5 years.)

The palaeomagnetic pole obtained in this way must not be confused with the palaeogeographic pole; predictions about the position of the latter can be made from palaeomagnetism only if the further assumption is made that the geocentric dipole field has always been *axial* being coupled to the Earth's spin axis.

References

1. Angenhiester, G., 1956. *Akad. Wiss. Gottingen Nacht., Maths.-Phys. Kl.*, **9**, 187.
2. Blackett, P. M. S., Clegg, J. A. & Stubbs, P. H. S., 1960. *Proc. Roy Soc. A.*, **256**, 291.
3. Clegg, J. A., Almond, M. & Stubbs, P. H. S. *Phil. Mag.*, **45**, 583.
4. Collinson, D. W. & Runcorn, S. K., 1960. *Bull. Geol. Soc. Amer.*, **71**, 915.
5. Cook, R. M. & Belshé, J. C., 1958. *Antiquity*, **32**, 167.
6. Cox, A. V. & Doell, R. R., 1960. *Bull. Geol. Soc. Amer.*, **71**, 645.
7. Creer, K. M., 1955. Thesis, Univ. Cambridge.
8. Creer, K. M., Irving, E. & Runcorn, S. K., 1957. *Phil. Trans. Roy. Soc. A*, **250**, 144.
9. Creer, K. M., Irving, E., Nairn, A. E. M. & Runcorn, S. K., 1958. *Ann. Geophys.*, **14**, 492.
10. Deutsch, E. R. & Watkins, N. D., 1961. *Nature (Lond.)*, **189**, 543.
11. Domen, H., 1960. *Bull. Fac. of Educ., Yamaguchi Univ.*, **9**, 31.
12. Doell, R. R., 1955. Thesis Univ. Calif. Berkeley.
13. Doell, R. R., 1956. *Trans. Amer. Geophys. Union*, **37**, 156.
14. Fisher, R. A., 1953. *Proc. Roy. Soc. A*, **217**, 295.
15. Goldich, S. S., Baadsgaard, H., Edwards, G. & Weaver, C. E., 1959. *Bull. Am. Assoc. Petroleum Geologists*, **43**, 654.
16. Graham, J. W., 1954. *J. Geophys. Res.*, **59**, 215.
17. Graham, J. W., 1955. *J. Geophys. Res.*, **60**, 329.
18. Graham, J. W., 1956. *J. Geophys. Res.*, **61**, 735.
19. Green, R., 1959. Thesis, Austr. Nat. Univ.
20. Gusev, B. V., 1959. *Inf. Bull. Inst. Geol. Arkitiki, Leningrad*, **4**, (30).
21. Hospers, J., 1954. *Kon. Nederl. Akad. Wetenschappen (B)*, **57**, 112.
22. Irving, E., 1957. *Adv. in Physics*, **6**, 194.
23. Irving, E., 1958. *Geophys. J.*, **1**, 224.
24. Kato, Y. & Nagata, T., 1953. *Proc. 7th Pacific Sci. Congr.*, **2**, 562.
25. Kintzinger, P. R., 1957. *Bull. Geol. Soc. Amer.*, **68**, 931.
26. Komarov, A. G., 1959. *Akad. Nauk SSSR Izv. ser geofiz*, 1219.
27. Kumagai, N., Kawai, N. & Nagata, T., 1950. *J. Geomagn. Geoelec.*, **2**, 61.
28. Makarova, Z. V., 1959. *Akad. Nauk SSSR Izv. ser. geofiz*, 1520.
29. Nagata, T., 1953. *Bull. Earthq. Res. Inst.*, **21**, 1.
30. Pospelova, G. A., 1959. *Akad. Nauk SSSR Izv. ser. geofiz*, 1591.
31. Roche, A., 1958. *C.R. Acad. Sci., Paris*, **246**, 3364.
32. Roche, A., 1960. *C.R. Acad. Sci., Paris*, **250**, 377.
33. Runcorn, S. K., 1956. *Bull. Geol. Soc. Amer.*, **67**, 301.
34. Thellier, E. & O., 1951. *C.R. Acad. Sci., Paris*, **233**, 147.
35. Torreson, O. W., Murphy, T. & Graham, J. W., 1949. *J. Geophys. Res.*, **54**, 111.
36. Watanabe, N., 1959. *J. Fac. Sci., Univ. Tokyo*, **2**, 1.
37. Watson, G. S. & Irving, E., 1957. *Mon. Not. R. Astr. Soc. Geophys. Suppl.*, **7**, 289.
38. Wilson, R. L., 1959. *Phil. Mag.*, **4**, 750.

Country	No.	Age	Rock unit	Sampling: Thickness in m	Sampling: Lateral spread
U.S.S.R.	1	Qr	Sheveluch Volcanic Domes, Kamchatka, 19th-20th cent. (57 N, 161 E)	—	≃ 100 km
	2	Q	Tuffs and lavas, Armenia (40 N, 45 E)	—	≃ 100 km
	3	Tp–Qp	Lavas, Armenia (40 N, 45 E)	—	≃ 100 km
	4	Q	Lavas, Kurile Islands (49 N, 154 E)*(6)	—	≃ 100 km
Japan	5	Qr	Archaeological baked clays, Honshu*(7)	—	1 000 km
	6	Qr	Recent lavas, Honshu*(8)	—	—
	7	Qp–r	Lavas, 11 flows*(5) (36 N, 138 E)	—	—
	8	Qp	Yamaguchi Basalt, 85 sites*(3)*(9) (34·5 N, 131·5 E)	—	90 km
France	9	Qp	Chaine de Puy, 10 flows (45·5 N, 3 E)	—	—
	10	Qp	Basaltes des Plateaux, 8 flows (45·5 N, 3 E)	—	—
England	11	Qr	Archaeological baked clays, 14 sites*(3)*(10)	—	360 km
Tunisia	12	Qr	Archaeological baked clays, 3 kilns, 146 B.C.–A.D. 300 (37 N, 10 E)	—	—
U.S.A.	13	Tm(Q)	Neroly Fm., sediment, 3 localities (37 N, 122 W)	—	80 km
	14	Tm–p	Payette Fm., sediments, Idaho, 1 site (43 N, 115 W)	25	500 m
	15	Tm–p	Ellensburg Fm., sediments, Wash., 1 site (46 N, 120 W)	25	75 m
	16	Tm	Arikee Fm., sediments, S. Dak., 1 site (44 N, 103 W)	20	200 m
	17	Te	Green River Fm. sediments: 1 site, Colo (39·5 N, 108 W)	10	30 m
	18		Green River Fm. sediments: Laney Sh., 1 site, Wo. (41·5 N, 108·5 W)	30	360 m
	19	Te	Wasatch Fm., Wo., 1 site (44·5 N, 109 W)*(13)	15	25 m
	20	T	Duchesne River Fm., Utah, sediments (40 N, 110 W)	15	—
France	21	Tm	Cantal, 3 flows*(5)	—	—
	22	Tm	Limagne, 2 flows*(5)*(14)	—	—
Germany	23	Tm	Vogelsberg Basalts, 42 flows*(5) (50·5 N, 9·5 E)	—	—
U.S.S.R.	24	Tp	Lava flows, Armenia (40 N, 44 E)	—	≃ 100 km
England	25	Kl	Wealden sediments, Isle of Wight (50·5 N, 1·5 W)*(15)	—	6 km
U.S.A.	26	J	Carmel Fm., sediments, Moab, Utah (39 N, 109 W)	15	—
	27	Jl	Kayenta Fm., Glen Canyon Group, (sediments): Kanab, Utah (37 N, 113 W)	30	—
	28		Kayenta Fm., Glen Canyon Group, (sediments): Navajo Nat. Mon. (37 N, 111 W)	61	—
	29		Kayenta Fm., Glen Canyon Group, (sediments): Echo Cliffs, Ariz. (37 N, 112 W)	42	—
	30		Kayenta Fm., Glen Canyon Group, (sediments): Kayenta, Ariz. (37 N, 110 W)	15	—
U.S.S.R.	31	l–m	Siberian Traps, Lr. Tunguska Region: 6 sites (66 N, 88 E)	—	≃ 100 km²
	32		Siberian Traps, Lr. Tunguska Region: 4 sites (67·0 N, 88·8 E)	—	370 km
U.S.A.	33	Ku	Chinle Fm.: Moab, Utah, 2 sites (39 N, 109 W)*(16)	42	—
	34		Chinle Fm.: Moab, Utah, 2 sites (39 N, 109 W)*(16)	67	—
	35		Chinle Fm.: Colorado Nat. Mon., 2 sites (39 N, 109 W)	15	—
	36		Chinle Fm.: Colorado Nat. Mon., 2 sites (39 N, 109 W)	30	—

Sampling				Polarity		Directions of magnetization				Palaeomagnetic pole position			
No. of samples	No. of specimens	Stability	Treatment	+	−	D_m	I_m	Precision	Error	Lat.	Long.	Error $d\phi$, dx	Reference
≃ 17	—	ac, dc, th	nt	—	100	4	+62	—	6	77	20 W	7, 9	30
≃ 50	—			—	100	0	+58	—	3	88	135 W	3, 4	30
≃ 60	—			100	—	192	−45	—	2	76	166 W	2, 3	30
≃ 7	—			—	100	345	+65	—	5	80	115 W	7, 8	30
≃ 1350	≃ 1350	—	—	—	100	356	+53	17	3	86	19 W	3, 4	36
25	—	—	nt	—	100	356	+47	119	7	—	—	— —	29, 24, 36
—	—	—	nt	—	100	359	+47·5	18	11	82·5	35 W	10, 14	27, 6
≃ 300	≃ 650	ac	nt	9	91	0	+57	18	4	87	132 E	—	11
—	—	—	nt	—	100	353	+62	—	—	84·5	106 W	—	31, 6
—	—	—	nt	100	—	206	−63·5	—	—	72	84 E	—	31, 6
73	—	—	nt	—	100	0	+66·5	242	2·5	—	—	—	5, 6
18	—	—	nt	—	100	359	+54·5	—	—	—	—	—	34, 6
29*(3)	—	th, fd*(12)	nt	—	100	(7)	(+58)	89	3	—	—	—	13, 12, 6
13*(3)	13	—	nt	—	100	0	+62	240	3	*(27)	—	—	35
23*(2)	25	cg	nt	4	96	0·5	+68·5	12	9	*(27)	—	—	35, 6
21*(3)	40	—	nt	5	95	66	+69	3	26	*(27)	—	—	35, 6
7*(2)	9	—	nt	—	100	345·5	+65	168	4·5	*(27)	—	—	35, 6
19*(2)	19	—	nt	—	100	355	+63	28	6	*(27)	—	—	35
4*(2)	5	—	nt	—	100	351·5	+63·5	—	—	*(27)	—	—	35, 6
24	85*(1)	—	nt	—	100	2	+65	14	5	83	99 W	6, 8	4
—	—	th	nt	—	100	329	+41	—	—	57	119 W	—	32
—	—	th	nt, th	100	—	158	−35	—	—	57	133 W	—	32
200	—	—	nt	31	69	8·5	+57·5	13	6	76·5	160 E	7, 9	1, 6
30	—	ac, dc, th (nt)		—	100	15	+43	—	5	67	174 W	4, 6	30
19*(2)	97	fd, ac	nt	—	—	2	+59	8·5	2	—	—	—	38
9	—	31*(1)	nt	—	100	349	+63	10	9	80	160 W	11, 14	4
10	—	33*(1)	nt	—	100	4	+53	12	9	85	23 E	9, 13	4
7	—	27*(1)	nt	—	100	335	+50	7	11	*(28)	—	—	4
14	—	43*(1)	nt	—	100	14	+43	14	6	73	19 E	5, 7	4
8	—	43*(1)	nt	—	100	20	+50	14	6	72	6 W	6, 8	4
≃ 54	≃ 130	—	nt	—	100	90	+71	—	4	48	148 E	8, 10	28
26	67	—	nt	—	100	62	+76	—	8·5	65	156 E	15, 16	10
10	60	—	nt	—	—	59	+73	—	—	48	66 W	—	4
				100	—	160	−10	—	—	50	114 E	—	4
14	39	—	nt	—	—	160	+44	—	—	23	90 W	—	4
				100	—	156	− 7	—	—	49	109 E	—	4
7	31*(1)	—	nt	—	100	34	+60	14	7	*(28)	—	—	4
6	29*(1)	—	nt	—	100	356	+66	25	5	*(28)	—	—	4

Country	No.	Age	Rock unit	Sampling: Thickness in m	Sampling: Lateral spread
U.S.A.	37	T_R	Moenkopi Fm. (red sediments): Zion Nat. Park, Utah (36 N, 112 W)	—	400 km
	38		Marble Canyon (37 N, 111 W)	70	1·5 km
	39		Capitol Reef, Utah (38 N, 111 W)*(16)	21	—
	40		Sand Canyon, Colo. (40 N, 109 W)	30	—
	41		Split Mt., Colo. (40 N, 109 W)	30	—
	42		Vernal, Utah (41 N, 109 W)	15	—
	43		Poverty Tank, Ariz. (36 N, 111 W)	36	—
	44		Echo Cliffs, Ariz. (37 N, 112 W)	97	—
U.S.A.	45	T_R–P	Chugwater Fm. (red sediments): Red Mt., Colo. (41 N, 106 W)	48	—
	46		Rawlins, Wo. (42 N, 107 W)	27	—
	47		Thermopolis, Wo. (44 N, 108 W)	120	—
	48		Lander, Wo. (43 N, 109 W)	105	—
	49		Dinwoody Lake, Wo. (43 N, 109 W)	72	—
	50		Fort Washakie, Wo. (43 N, 109 W)	40	—
	51		Shell, Wo. (45 N, 108 W)	30	—
	52		Sheep Mt., Wo. (45 N, 108 W)	20	—
	53		Alcova Resvr., Wo. (43 N, 107 W)	27	—
	54		Troublesome Creek, Wo. (42 N, 107 W)	27	—
U.S.S.R.	55	Cu–Pl	Ultrabasic rocks of Maymecha-Kotuy (72 N, 102 E)*(29)	—	—
U.S.A.	56	P	Supai Fm. (red sediments): Hunter's Pt., Ariz. (36 N, 109 W)	30	—
	57		Oak Creek Canyon, Ariz. (35 N, 112 W): Upper	140	—
	58		Lower	106	—
U.S.A.	1/105 (m1)	Cu	Naco Fm.: Carizzo Creek, ss. (36 N, 113 W)*(11)	60	—
	59		Fossil Creek, Lst. (34 N, 112 W)	45	—
U.S.A.	60	Dl–m	Onondaga Lst., 2 localities, N.Y. (42·5 N, 74 W)	—	—
Australia	61	Du–Cl	Victorian Red Beds, 8 sites (37 S, 147 E)*(18)	550	160 km
Australia	62	Du(Q)	Catombal Fm., N.S.W., 16 sites (33 S, 149 E)*(4)*(19)	460	110 km
Australia	63	Du(Q)	Yalwal Stage, N.S.W. (37 S, 150 E): Sediments *(4)*(20)	—	2 km
	64	Du	Nethercote basalts, 7 sites*(4)	180	5 km
Australia	65	Dm	Red beds in Murrumbidgee Series, 1 site, Alum Creek, N.S.W. (34·7 S, 148·8 E)	30	—
Australia	66	Su–Dl	Igneous rocks in A.C.T. (35.2 S, 149·0 E)*(4)*(21)	—	—
Australia	67	Sm	Duro Porphyry, 2 sites, N.S.W. (34·7 S, 148·9 E)	—	200 m
Wales	68	Su	Ludlow Series, 1 site (52 N, 5 W)	22	—
U.S.S.R.	69	S	Ural Peridotites, 1 quarry (67 N, 66 E)	—	—
	70	O	Ukrainian Basalts (51 N, 26 E): 2 quarries	—	—
	71		1 quarry	—	—

Sampling				Polarity		Directions of magnetization				Palaeomagnetic pole position			
No. of samples	No. of specimens	Stability	Treatment	+	−	D_m	I_m	Precision	Error	Lat.	Long.	Error $d\psi$, $d\chi$	Reference
16	—	—	nt	—	100	0	+27	—	—	—	—	—	33
11	—	—	nt	—	100	325	+35	—	—	—	—	—	35
10	39	—	nt	100	—	139	+24	—	—	26	114 E	—	4
				100	—	151	− 6	—	—	46	114 E	—	4
8	27*(1)	—	nt	100	—	148	− 7	11	9	43	118 E	5, 9	4
5	23*(1)	—	nt	100	—	156	− 4	28	6	46	105 E	3, 6	4
9	38*(1)	—	nt	100	—	158	− 4	18	6	46	104 E	3, 6	4
11	27*(1)	—	nt	—	100	337	+36	22	7	64	127 E	5, 8	4
22	42*(1)	—	nt	—	100	349	+28	17	6	66	95 E	4, 6	4
18	16*(1), 52*(1)	—	nt	77	23	335	+15	30	6	47	116 E	3, 5	4
						151	− 6	12	6				
9	12*(1), 21*(1)	—	nt	64	36	328	+12	43	4	46	121 E	3, 5	4
						149	−19	25	6				
6	18*(1), 15*(1)	—	nt	46	54	332	+16	56	5	52	103 E	4, 7	4
						170	−19	13	11				
10	12*(1), 37*(1)	—	nt	76	24	344	+27	55	4	47	100 E	4, 8	4
						157	+15	8	9				
10	20*(1), 22*(1)	—	nt	52	48	339	+25	30	6	52	111 E	3, 5	4
						154	−20	17	7				
11	25*(1), 28*(1)	—	nt	53	47	346	+14	23	6	44	105 E	3, 5	4
						146	+ 6	34	5				
5	5*(1), 16*(1)	—	nt	76	24	340	+36	—	—	56	113 E	4, 8	4
						155	−23	16	7				
9	35*(1)	—	nt	100	—	148	− 6	58	3	40	115 E	2, 3	4
10	48*(1)	—	nt	100	—	152	−18	10	8	49	118 E	4, 8	4
9	43*(1)	—	nt	100	—	134	−12	10	7	36	135 E	4, 7	4
388	—	—	nt	100	—	295	−68	—	5	40	150 E	7, 8	20
7	24*(1)	—	nt	100	—	164	+ 5	32	5	49	96 E	3, 5	4
14	32*(1)	—	nt	100	—	161	+10	13	8	46	96 E	4, 8	4
16	55*(1)	—	nt	100	—	141	+18	25	4	33	116 E	2, 4	4
8	31*(1)	—	nt	100	—	150	− 3	40	4	46	113 E	—	4
9	20*(1)	—	nt	100	—	125	+16	22	7	23	130 E	4, 7	4
65*(2)	—	cg*(17)	nt	—	100	177	+79	19	4	—	—	—	18, 6
≃40	113	—	nt	—	100	(17)	(−65)	—	—	—	—	—	19
≃80	150	fd*(19)	nt	—	100	(1)	(−67)	75	5	—	—	—	19
14	45	cg*(20)	nt	—	100	(15)	(−64)	10	13	—	—	—	19
19	45	ac*(24)	nt	29	71	5	−23	29	14	65	160 E	8, 15	19
11	21	—	nt	—	100	40	−29	10	10	58	151 W	5, 11	19
≃40	80	fd	nt	13	87	12	−37	6	21	71	172 W	14, 24	19
7	14	—	nt	—	100	306	−11	—	—	—	—	—	19
5*(2)	33	—	nt	100	—	205	−36	33	14	—	—	—	7
6	—	—	nt	—	100	89	+38	—	—	16	140 E	—	26
8	—	—	nt	—	100	255	+58	—	—	21	27 W	—	26
6	—	—	nt	—	100	140	+75	—	—	28	46 E	—	26

Country	No.	Age	Rock unit	Sampling: Thickness in m	Sampling: Lateral spread
U.S.A.	72	Om	Trenton Lst., N.Y. — Conglomerate (42·5 N, 75 W)*(22)	—	—
	73		Flat-lying beds and distorted zone (43·5 N, 75 W)*(23)	—	—
	74	O	Juniata Fm., Bedford, Penn. (40 N, 79 W)	425	—
U.S.A.	75	€*(25)	Deadwood Fm., Rawlins, Wo. (42 N, 107 W)	15	—
U.S.A.	76	€	Lodore Fm., Vernal, Utah (41 N, 110 W)	60	—
U.S.A.	77	P€*(26)	Beltian of Montana (sediments) — McNamara Fm., Blackfoot Canyon (47 N, 114 W)	25	—
	78		Miller Peak Fm., Donovan Cr. (47 N, 114 W)	20	—
	79		Spokane Shl. — Prickly Pear Canyon (47 N, 112 W)	120	—
	80		Spokane Shl. — McDonald Cr. (49 N, 114 W)	15	—
	81		Grinnel Argillite, Glacier Nat. Pk. (49 N, 114 W)	21	—
	82		Appekunny Argillite, Glacier Nat. Pk. (49 N, 114 W)	33	—
U.S.A.	83	P€	Grand Canyon Series, Ariz. (36 N, 112 W) — Shinumo Quartzite*(16)	30	—
	84		Hakatai Sh.*(16)	10	—
	85		Hakatai Sh. and Bass Lst.	140	—
	86		Bass Lst.*(16)	92	—
U.S.A.	87	P€	Bonito Canyon Quartzite, Ft. Defiance, Ariz. (36 N, 109 W)	30	—

(1) Statistics for this entry calculated giving each *specimen* unit weight.
(2) Statistics for this entry calculated giving each *sample* unit weight.
(3) Statistics for this entry calculated giving each *site* unit weight.
(4) Statistics calculated using a two-tier analysis (**37**); the between-site precision, k_b, is given.
(5) Statistics for this entry calculated giving unit weight to each lava flow.
(6) Results from T*p*–Q*p* lavas of the Kuriles also reported (**30**). The directions are reversed but highly scattered and no mean direction is given.
(7) Directions and pole calculated from data (**36**), corrected to Tokyo (35° 40′ N, 139° 48′ E). There are 174 sets of observations distributed amongst 55 sites. They represent archaeological units usually of varying age within each site. The ages range from 4000 B.C. to A.D. 1600. The statistics are calculated giving each set unit weight.
(8) Calculated from data, corrected to Tokyo (35° 40′ N, 139° 48′ E), from 5 flows ranging from A.D. 864 to A.D. 1779. Each flow given unit weight.
(9) Statistics calculated from data in **11**, giving each site unit weight.
(10) Directions corrected to Cambridge (52 N, 0 E). Ages range from 1st to 16th century.
(11) Pole calculated in list I (**1/105**) and is corrected here.
(12) Magnetization post-dates the Early Pleistocene folding, so pole is not given.
(13) Five other samples from Wasatch of Colorado gave random directions.
(14) Specimens from one flow heated to 300° C before measurement.
(15) Correction of directions to bedding increases scatter suggesting instability, furthermore treatment in a.c. fields suggest presence of an unstable component; therefore no pole is given. The entries in columns 15 and 16 are the r.m.s. deviation of the observations and in the mean (**38**).
(16) The directions have a planar distribution being strung out along a great circle between the stable direction and the present (or dipole) field. The entries in the first row from column **11** onwards are an average of these directions; the second row gives an estimate of this stable direction obtained by choosing a point on the great circle near the end of the planar distribution farthest from the present field.

Sampling				Polarity		Directions of magnetization				Palaeomagnetic pole position			
No. of samples	No. of specimens	Stability	Treatment	+	−	D_m	I_m	Precision	Error	Lat.	Long.	Error $d\phi$, dx	Reference
28*(2)	—	cg	nt	—	100	(177·5)	(+71)	23	5·5	—	—	—	18, 6
45*(2)	—	cg	nt	—	100	179	+82	23	5	—	—	—	16, 6
12	56*(1)	—	nt	100	—	131	+26	6	8	20	153 E	5, 9	4
7	34*(1)	—	nt	100	—	151	−14	16	7	47	117 E	4, 7	4
11	26*(1) 7*(1)	—	nt	21	79	59 234	+ 4 +13	14 25	8 13	23	6 E	4, 7	4
20	53*(1)	—	nt	—	100	26	−43	30	4	14	42 E	3, 5	4
14	23*(1)	—	nt	100	—	234	+30	20	7	11	14 E	4, 8	4
39	71*(1)	—	nt	—	100	232	+55	18	4	5	152 W	4, 6	4
5	19*(1)	—	nt	100	—	206	+39	10	8	16	41 E	6, 10	4
16	44*(2)	—	nt	100	—	225	+48	15	6	2	28 E	5, 8	4
15	38*(1)	—	nt	100	—	223	+29	15	6	15	24 E	4, 7	4
14	61*(1)	—	nt	— 100	100 —	288 246	+65 +33	— —	— —	37 7	166 W 7 E	— —	4 4
14	41*(1)	—	nt	— 100	100 —	291 245	+58 +31	— —	— —	36 9	177 W 6 E	— —	4 4
10*(2)	—	—	nt	100	—	205	+65	6	21	4	52 E	—	6
14	43*(1)	—	nt	100 100	— —	232 225	+52 +34	23 —	5 —	6 21	26 E 22 E	3, 6 —	4 4
16	74*(1)	—	nt	—	100	31	−25	19	4	33	34 E	2, 4	4

(17) Directions in some deformed beds not appreciably scattered suggesting post-depositional magnetization; no pole is therefore given.

(18) The directions *in situ* are close to the present field; the magnetization is considered (**19**) to be post-depositional and no pole is given.

(19) These sedimentary beds are steeply-folded. The mean direction (given here) with the beds *in situ* is along the present field, and the between-site precision, $k_b = 75$; after correction for folding $k_b = 4$. The magnetization is therefore Recent not Devonian and no pole is given (**19**).

(20) With the beds *in situ* the mean direction (given here) is along the present field. Directions in 14 pebbles of similar rock type in overlying Devonian beds not random. The magnetization is Recent not Devonian in age and no pole is given (**19**).

(21) Eight volcanic and intrusive units (each given unit weight) covering a long time span. Two units, the Ainslie Volcanics (**1/116**) and the Mugga Porphyry (**1/120**) for which results have already been reported are included. Correction to "bedding" decreases scatter.

(22) Directions in different conglomerate blocks not scattered, no pole is given.

(23) Directions in flat-lying and deformed beds have similar directions; moreover directions in blocks in the distorted zones are less scattered than the bedding poles of these blocks (**18**). The magnetization of the distorted zone and probably that also of the flat-lying beds is post-depositional. No pole is given.

(24) A.C. field of 900 (peak) oersted do not alter the magnetization either in direction or intensity (P. M. Stott personal communication to the compiler).

(25) Cited as Mississippian in **4**.

(26) Illite shale in Beltian dated at 750 million years (**15**).

(27) Poles not given (a) because these data were not interpreted in this fashion in the originals, (b) because the thickness and lateral extent are small, and (c) because except in entry **3/15** there is not substantial stability evidence (see discussion in **21**, p. 114).

(28) Pole is not given in the original.

(29) Detailed sampling from 6 igneous bodies. A total of 1600 samples collected but most were unstable. Radiogenic age from one intrusive gave 250 million years.

Report of Geophysical Discussion

A geophysical discussion entitled **The Structure of the Ocean Floor** was held under the Chairmanship of *Dr T. F. Gaskell*, on 1960 November 25. He opened the meeting by stressing the importance of knowledge of the difference between oceanic and continental structure and by drawing attention to the development of new techniques which made a variety of observations possible.

The first speaker was *Mr B. C. Browne*, who gave an outline of recent developments in gravity measurements at sea. He first described how gravity measurements should be most useful in elucidating the structure of the ocean floor providing that almost continuous observations of sufficient accuracy could be made. Until recently the only way in which the required accuracy could be achieved was to make the observations in a submarine whilst it was submerged. However, during the last few years two firms, LaCoste–Romberg and the Askania Werke, have both developed special gravity meters which can be used in surface ships. The design of such instruments is difficult. The basic problem is to measure the mean value of the acceleration due to gravity to within, say, 1 in 10^6 on board a vessel which is subject to both horizontal and vertical accelerations which may be as great as $\pm 0{\cdot}1$ g. Experience has shown that, by using an instrument with a time constant of several hundred seconds, the effects of vertical accelerations can certainly be eliminated. The effects of horizontal acceleration are less easy to remove. The resultant acceleration will be systematically greater than the acceleration due to gravity and hence the long time constant will only reduce the fluctuations and not the systematic effect, which may amount to some thousands of milligals. To overcome this serious difficulty, LaCoste–Romberg have designed and constructed a special accelerometer which automatically computes the correction which must be applied to the gravity meter. Askania, however, have devised a method by which their gravity meter only responds to the component of the acceleration along a particular axis. By mounting their instrument on a gyrostabilized platform, this axis is maintained in the direction of the true vertical and hence horizontal accelerations do not affect its reading. In practice, both instruments suffer from various other types of error and modifications and improvements are being made to overcome these. Perhaps the most outstanding difficulty is navigation. In order to interpret the gravity meter records, one must know not only the ship's position but also its east–west velocity relative to the Earth. At present no satisfactory world-wide system of navigation has been devised, possessing the requisite precision but it is hoped that inertial navigation, combined with observation of satellites or radio signals may provide a solution.

After Mr Browne's paper had been read, *the Chairman* asked *Mr B. D. Loncarevic* to describe some of the measurements made on the summer cruise of the *Discovery II* using an Askania gravity meter mounted on a gyrostabilized platform. Continuous readings were obtained over large sections of the track. It has been possible to study the repeatability of observations at the intersections of tracks and provisional gravity values have been calculated for eighteen such intersections.

The agreement of values on different courses is as follows: five were within 5 mgal, nine between 5 and 10 mgal and four were over 10 mgal. The maximum disagreement was 16 mgal. The local field over that part of the Mid-Atlantic ridge where these intersections were obtained, had gravity gradients of up to 30 mgal per mile, so that a small error in position or time of the observations could account for most of the disagreement. Thus it was tentatively concluded that under reasonably calm conditions at sea (wind force 3–4) the errors due to horizontal accelerations are no larger than the uncertainties due to navigation.

Dr A. H. Cook commented that Transit satellites, combined with an inertial navigation system, might solve the problems of navigation for geophysical purposes. With quite simple ship equipment and measurements it should be possible to get positions correct to a few hundred metres at every passage of the satellite, while with more complex equipment and measurements, positions should be obtained to better than 100 m. Oceanographers should consider what accuracy they require in relation to the complexity and expense of the equipment they are prepared to operate and the time they are prepared to wait for results.

Dr M. N. Hill then gave his paper on magnetic measurements in the Western Approaches of the English Channel. He described how recent investigations with a proton precession magnetometer towed astern of ships in this area have revealed four structural lines in the total magnetic field anomaly running in approximately ENE to WSW directions. These lines are in pairs with low anomalies to the north: a type of anomaly which could be produced by elongate projections in the basement rocks. These projections would have to be of higher susceptibility than the surrounding material and might take the form of overthrusts. In the region of these two pairs of structural lines there is a marked absence of small steep anomalies such as exist in many places to the north and to the south. This suggests the existence of a relatively thick layer of uniform material infilling a basin running roughly parallel with the French and English coastlines. The structural trends and the position of the basin obtained by the magnetic measurements are in close agreement with those obtained by seismic methods and previously reported by Day & others (1956). The seismic methods showed that sedimentary rocks filled the basin to a thickness of between 3 000 and 4 000 ft. It was postulated that this basin was formed during the Armorican Earth movements. An extension of the area of survey is planned which should show whether or not these magnetic trends continue out beyond the continental shelf.

In the discussion which followed this paper, *Professor O. T. Jones* remarked that the results Dr Hill had described demonstrated that continental structures continued further to sea than had been previously thought. *Dr Gaskell* asked what information was available beyond the 1 000 fathom line and if the increased depth of water would make observations more difficult. The Speaker replied that although there was nothing known yet there should not be any difficulty in extending the work. *Dr R. W. Girdler* asked what intensity of magnetization had been considered in the interpretation of the anomalies. As this aspect of the work had not been considered in detail, the Chairman asked *Dr R. G. Mason* to comment in the light of his work at La Jolla. *Dr Mason* said that one needed to assume rather higher intensities than commonly encountered on land. However the dredged material did have a high susceptibility, the median value being 0·03 emu/cm^3. *Mr Loncarevic* in reply to a question about the gravity anomalies in the region described by Dr Hill, stated that in a crossing near Ushant a free air anomaly of +30 mgal was observed and −5 mgal over the trough.

The third speaker, *Dr A. S. Laughton*, reviewed the evidence for a Mid-Atlantic ridge valley. The presence of a continuous valley running down the centre part of the Mid-Atlantic ridge can have very critical implications on the interpretation of the forces acting on the Earth's crust here, so that it is important to review critically the evidence for it. During the IGY sixteen transatlantic profiles of topography were obtained with precision echosounders at approximately 8° intervals from 32° S to 48° N (Fuglister 1960). Five of these profiles were shown, some having clear evidence of a unique valley in the centre of the ridge and others containing a number of features any of which could be selected as the valley. *Dr Laughton* mentioned that the detection of adiabatic warming down in the prominent valley at 36° N demonstrated the existence there of an enclosed basin. Twenty-five profiles in the north Atlantic, published by Heezen, Tharp & Ewing (1959) show that a unique feature does exist on many sections, although the sections are too short to exclude the possibility of other features on the flanks of the ridge. Sixty-four sections at eight-mile intervals between 58° N and Iceland by the *Anton Dohrn* and *Gauss* show that no valley exists between 58° N and 64° N (Ulrich 1960). Detailed surveys carried out by *Discovery II* since 1954 in the region of 47° N indicate that over at least 75 miles the valley is a continuous feature (Hill 1960) and that with certain interruptions it can be traced for 150 miles. One discontinuity was examined in detail in 1960 and found to be the result of lava flows from two volcanic peaks facing each other on either side of the valley, which had partially filled the valley. It appears then to be misleading to infer a single continuous valley from the widely spaced profiles available at the present and that surveys should be made with a sufficiently small interval so that correlation is unambiguous. Other features on the ridge should also be examined to see if they are elongate. In 1960 one small peak 100 miles west of the valley was shown to be elongated parallel to the valley.

After thanking Dr Laughton for his contribution *the Chairman* commented that in the light of our knowledge of, for example, the African rift system the speaker's picture of a more or less continuous feature which varies its strike as traced from north to south was far more likely than a perfectly straight continuous feature. In reply to *Dr Lowes's* question, whether the magnetic contrast was good enough to say anything about the nature of the rocks which had blocked the valley, Dr Laughton said that the magnetic anomaly with the associated gravity pattern and the dredging of basaltic material was the evidence upon which the conclusion had been based. *Miss Botley* asked if the specimens were recent and if there were grounds for connecting the ridge with the Alpine or present orogeny. The speaker answered that the region was seismically active and that not only does the seismic belt follow the ridge, but that the presence of the ridge was actually predicted in some places because of the seismic activity and only later demonstrated. *Dr A. H. Cook* asked whether the method of Byerly and Hodgson could be applied to determine the direction of movement in the earthquakes on the ridge. *Dr L. Knopoff* answered that the use of the method would be marginal because of the small number of stations reporting these shallow earthquakes. *Mr B. C. Browne* enquired about the sensitivity of water bottle work and whether the technique might be used more extensively. The speaker thought that such a development might be fruitful, whereupon *Dr Carruthers* drew attention to the discovery of the Hirondelle deep which was made long ago with this technique. That basin was shown to be separated from the ocean on all sides by ridges rising

to within 1 800 m of the surface because its potential bottom temperature equated with that very much deeper down outside.

Finally, *Mr D. H. Matthews* spoke on contrasting seamounts in the N.E. Atlantic. The distinction which he developed was that, whereas seamounts in the deep ocean are individual volcanoes and are associated with steep magnetic gradients and relatively large anomalies, some seamounts at the continental margin are certainly not volcanoes and are either non-magnetic or are associated with anomalies having relatively low gradients. Caryn Peak (Miller & Ewing 1956) is an ideally simple oceanic seamount—a circular magnetized cone, but others investigated by *Discovery II* have been elongate structures. The anomaly associated with an isolated seamount north of Madeira (Laughton, Hill & Allan 1960) has been interpreted in terms of the reversed magnetization of olivine basalts like those dredged from there. However, the anomalies in the Iberian Abyssal Plain are better accounted for in terms of dykes reaching to the sea floor. Elongated ridges and the associated anomalies on the flanks of the Mid-Atlantic Ridge also suggest fissure eruptions but in the areas mapped near the Median valley, the build-up of central volcanoes has obscured any magnetic lineation due to underlying fissures which may be present. Three large flat-topped seamounts rise from the continental slope off Portugal. A single crossing of the southernmost revealed no magnetic anomaly. Detailed surveys have been made of the other two: Vigo Seamount and the northernmost Galicia Rock. The magnetic anomalies observed were only slightly smaller than those over the volcanic seamounts, but the gradients were very much smaller, especially when allowance is made for the differences in depth of water present. Dredging from the tops of the banks has produced widely assorted rocks (50 per cent crystalline: gneisses and plutonics) some of which must be erratic. The flanks of the banks have yielded collections rich in limestones which can only be matched among the Mesozoic rocks of the Mediterranean region. These seamounts may be capped by the limestones. *Mr Browne* asked if the structure of the continental slope seamounts might be elucidated from seismic observations, to which the speaker replied that velocities of approximately 4 and 5·5 km/s had been observed on the top and flanks respectively. *The Chairman* then pointed out that the velocity recorded for the top is too low for solid lava, but that the range of values is comparable with that from the Hawaiian lavas. *Dr Laughton* added that, although the Pacific guyots are capped with limestone, they have strong magnetic anomalies with steep gradients. Finally he remarked that the steepness of the slopes on the sides of Galicia Bank contrasted with the smooth circular outline of Vigo seamount and that possibly they were fault scarps. *Mr Matthews* felt that the difficulty with this hypothesis was that, unless the faults were low angled, the scarps would be rapidly eroded.

The Chairman thanked all the contributors for a most interesting review of recent developments in oceanography and adjourned the meeting at 18.00 hr.

References

Day, A. A., Hill, M. N., Laughton, A. S. & Swallow, J. C. (1956). *Quart. J. Geol. Soc.*, **112**, 15–44.

Fuglister, F. C. (1960). *Atlantic Ocean Atlas* (Woods Hole Oceanographic Institution, Mass.).

Heezen, B. C., Tharp, M. & Ewing, M. (1959). The floors of the oceans. I The north Atlantic. *Spec. Pap. Geol. Soc. Amer.*, **65**, 122 pp.

Hill, M. N. (1960). A median valley of the Mid-Atlantic Ridge. *Deep Sea Res.*, **6**, 193–205.

Laughton, A. S., Hill, M. N. & Allan, T. D. (1960). Geophysical investigations of a seamount 150 miles north of Madeira. *Deep Sea Res.*, **7**, 117.

Miller, E. T. & Ewing, M. (1956). Geomagnetic measurements in the Gulf of Mexico and in the vicinity of Caryn Peak. *Geophys.*, **21**, 406.

Ulrich, J. (1960). New results on the topography of the Reykjanes Ridge. *Abstract Int. Ass. Phys. Ocean.* (U.G.G.I., Helsinki 1960), **16**.

Book Reviews

Petrology for Students: an introduction to the study of rocks under the microscope

Alfred Harker

(Eighth Edition, revised by C. E. Tilley, S. R. Nockolds, and M. Black, Cambridge, University Press. 1960. 15s.; $1.95)

When a textbook was first published in 1895, reached its eighth, revised, edition in 1954, and was reprinted in 1956 and 1960, there is little for the reviewer to do other than welcome the continued vigour of an old friend. He may wonder if it is the conservatism of teaching in British universities which has fostered this longevity, for "Harker" stands back from the line of modern petrology. The book has little chemistry; it is not quantitative; it says practically nothing of the origin and descent of igneous rocks; it devotes no great space to sediments and metamorphics; and yet it still meets the needs of students (and some seniors) as a guide to the identification of all but the most exotic rocks.

It is because of its clarity of expression and wealth of example that the book has remained serviceable for so long, and the revisers have wisely left its character unchanged. Little is omitted, and the new matter added carries references to published work up to about 1952. The line drawings, which bring out the essential features of rock-sections in a way that photomicrographs, with their redundant detail, often fail to do, have been reduced in number from 100 to 99.

The book will introduce the study of rocks under the microscope to many more geological students, and not only to those who, in the modest words of the Preface to the Seventh Edition, "do not aspire to specialize in Petrology." It is exceedingly good value for its price.

R. WALLS.

Mathematical Tables for the Approximation of Geophysical Anomalies and Reductions by Interpolation Polynomials

V. A. Kazinskii

(English translation by D. E. Brown)

(1960, 94 pp., Pergamon Press)

This compilation mainly comprises eleven numerical tables which take up 69 pages, and these are preceded by 25 pages of explanatory text including a "worked

example" of each type of calculation for which the tables have been computed. Basically these computations fall into two groups, though the adopted sequence of tables does not make this division. One group deals with the calculation of anomalies produced by a body, given its shape. The second group deals with quantitative assessment of gravity contour maps. In all cases an integral is approximated by a second degree interpolation formula and the application procedure is inherently simple. After choosing an interpolation interval to suit the problem in hand, contributions read from the tables are multiplied by the appropriate interpolation coefficients and then summed.

Anomaly calculations presented deal with gravity and magnetic anomalies, irregular shapes, and internal variations of density, the irregular inhomogeneous body being divided into slabs defined by interpolation interval and co-ordinates of the corresponding nodes. Eötvös gradient and curvature effects due to irregularities in mine workings are also derived. From the worked examples it appears probable that the methods were developed in connexion with very detailed surface and underground surveys for mining purposes by gravity meter and torsion balance. This may well be their most suitable field of application for, though the tables are approximate and the neglected remainder integral occasionally may be appreciable where the convenient interpolation interval bears an undesirable phase relationship to the shape of the natural body, the system can be used for both reduction and interpretation. Thus the tables provide a simple process whereby detailed underground information can be incorporated to correct observations for the effects of nearby excavations or known deposits before assessing the residual anomalies as to future exploration. On the other hand, those concerned with regional problems and more generalized data will probably prefer to employ standard curves based on simple geometrical forms.

Examinations of anomaly contour maps are restricted to the gravitational field, templates being used to define the interpolation intervals and outline the zones for which corresponding gravity anomaly values are read from the map. Commencing from the anomaly map, the given templates and tables can be applied to compute vertical gradient of gravity, deviation of the vertical, separation of the geoid from the spheroid, and total mass of a body from the anomaly it produces. These methods are basically similar to, and in some cases more approximate than, others previously published but the tables are relatively short, the procedure is unified, and it is convenient to have them together in one volume. A single example, the anomaly due to a spherical body, is utilized throughout. Use of a more elaborate model would have been more instructive and convincing.

The textual material has both the virtues and the defects of extreme condensation. Main principles are stated clearly, but some stages in the development are omitted as, on occasion, are specific indications as to units. A publisher's notice on the fly-leaf apologizes for poor reproduction of text by non-letterpress setting and photolithography in the interest of speedy publication. It is nevertheless reasonably satisfactory except for a few symbols and indices. Print and layout of the tables are adequate.

W. BULLERWELL.

Tables Related to Radiation Emerging from a Planetary Atmosphere with Rayleigh Scattering

K. L. Coulson, J. V. Dave & Z. Sekera

(8½ in. × 11 in., xii + 548 pp., University of California Press, 1960)

This substantial volume consists of 12 pages of reading matter and 548 pages of tabulation and is designed to provide the following information. Given the flux of solar radiation at any wavelength incident normally on the outside of the Earth's atmosphere, the total intensity I in that wavelength of Rayleigh-scattered light (a) downward and (b) upward from an optical depth τ of clear unabsorbent atmosphere is given as a function of the zenith distances of the Sun and of the diffuse radiation, azimuth and surface reflectivity. The degree of polarization P, the angle between the plane of polarization and the vertical plane in the appropriate azimuth, and the Stokes parameters Q and U of the scattered radiation are also given for each combination of the independent variables. I, P, Q and U are tabulated to five places after the decimal point.

The volume is appropriately introduced by a preface from Professor S. Chandrasekhar who modestly states that the exact solution of the Rayleigh problem was immediately available given the tools of the Stokes parameters. In fact of course Chandrasekhar's famous text *Radiative Transfer* (1950) materially helped to pave the way to the present volume and for its realization a great debt of gratitude is owed to Professor Z. Sekera and his colleagues who have made themselves experts in this field over the last decade or so. One must also thank the electronic computer for turning formulae into numbers.

The tables are clearly set out and printed and the introductory explanation is adequate but would have benefited from some expansion to make it more self-contained. For example, the optical depth τ is only given for an atmosphere above sea level at seven wavelengths and it is not explicitly stated that the solution provides for multiple scattering. There are many prospective users of these tables who will not themselves be expert in the theory of radiative transfer.

P. A. Sheppard.

Geophysical Journal

RECOMMENDATIONS TO AUTHORS

1. Authors are advised to follow the general suggestions for the preparation of scientific papers given in *Notes on the preparation of papers to be communicated to the Royal Society* and in *The printing of mathematics* by T. W. Chaundy, P. R. Barrett and C. Batey (Oxford University Press, 1954). In particular the abbreviations for the names of periodicals used in the *Geophysical Journal* are those given in *Notes on the preparation of papers* . . . and the symbols, signs and abbreviations are those recommended for British scientific publications by the Symbols Committee of the Royal Society.

2. Papers should be typewritten with double spacing and on one side of the paper only. Two copies, one of them the top copy, should be submitted. All papers must be accompanied by a summary; summaries are not required for *Letters to the Editors*.

3. Tables are printed without rules. They should be numbered serially with Arabic numerals. Table headings should be brief. Units should be placed at the head of the column. Tables should be typed on separate sheets and their positions in the text indicated on the copy.

4. Illustrations, especially photographs, should be kept to a minimum, and the same information should not in general be given in both tables and illustrations. Line drawings should be in dense black ink on smooth white board or transparent tracing film. Original drawings must not be lettered; lettering should be indicated on copies or photoprints which must be supplied in addition to the originals. Wherever possible, lettering should be kept outside the diagram so that it may be set in type. Diagrams should be drawn at twice to three times the size at which they will be printed. The maximum dimensions for diagrams, when reduced and with their lettering and captions, are 8 in by 5 in. A wide variety of flat tints of dots, lines and shadings can be applied to line drawings by the blockmaker. Photographs for reproduction should be unmounted glossy prints and should be accompanied by lettered prints.

5. References should be quoted in the form recommended by the Royal Society but authors may also quote titles of papers if they wish. References in the text are made in the form (Smith 1940).

6. Authors whose work involves much mathematics should follow carefully the recommendations in *The Printing of Mathematics*.

7. The Editors will be glad to advise authors on any special points of difficulty arising in the preparation of papers for the *Journal*.

Contents

PAGE

T. Rikitake, The effect of the ocean on rapid geomagnetic changes 1

K. M. Creer, Superparamagnetism in red sandstones 16

A. H. Cook, The comparison of the Earth's gravitational potential derived from satellite observations with gravity observations on the surface 29

R. W. Girdler, The measurement and computation of anisotropy of magnetic susceptibility of rocks 34

R. L. Wilson, Palaeomagnetism in Northern Ireland:

I, The thermal demagnetization of natural magnetic moments in rocks 45

II, On the reality of a reversal of the Earth's magnetic field 59

Report on Progress in Geophysics

E. Irving, Palaeomagnetic directions and pole positions, Part III. Pole numbers 3/1 to 3/87 70

Report of Meeting

Geophysical Discussion of the Royal Astronomical Society, 1960 November 25 80

Book Reviews 85

Printed in Great Britain by J. W. Arrowsmith Ltd., Bristol